Free Radical Research, January 2010, 44(1): 1–46

informa
healthcare

Role of oxidative damage in toxicity of particulates

PETER MØLLER[1], NICKLAS R. JACOBSEN[2], JANNE K. FOLKMANN[1], PERNILLE H. DANIELSEN[1], LONE MIKKELSEN[1], JETTE G. HEMMINGSEN[1], LISE K. VESTERDAL[1], LYKKE FORCHHAMMER[1], HÅKAN WALLIN[2] & STEFFEN LOFT[1]

[1]*Department of Public Health, Section of Environment Health, University of Copenhagen, Copenhagen, Denmark, and* [2]*National Research Centre for the Working Environment, Denmark*

(*Received: 9 June 2009; revised: 27 August 2009*)

Abstract
Particulates are small particles of solid or liquid suspended in liquid or air. *In vitro* studies show that particles generate reactive oxygen species, deplete endogenous antioxidants, alter mitochondrial function and produce oxidative damage to lipids and DNA. Surface area, reactivity and chemical composition play important roles in the oxidative potential of particulates. Studies in animal models indicate that particles from combustion processes (generated by combustion of wood or diesel oil), silicate, titanium dioxide and nanoparticles (C_{60} fullerenes and carbon nanotubes) produce elevated levels of lipid peroxidation products and oxidatively damaged DNA. Biomonitoring studies in humans have shown associations between exposure to air pollution and wood smoke particulates and oxidative damage to DNA, deoxynucleotides and lipids measured in leukocytes, plasma, urine and/or exhaled breath. The results indicate that oxidative stress and elevated levels of oxidatively altered biomolecules are important intermediate endpoints that may be useful markers in hazard characterization of particulates.

Keywords: *Biomonitoring, DCFH, DNA damage, lipid peroxidation, nanoparticle, oxidative stress*

Introduction

Particulates or particulate matter (PM) are small particles of solid or liquid suspended in liquid or air. Mainly insoluble particles are considered hazardous. Humans are generally exposed to particles by inhalation of air and by ingestion, although absorption through the skin and parenteral exposure may also occur naturally or as part of medical therapy. Natural sources of particulates encompass ashes from volcanoes, dust storms, forest and grassland fires, living vegetation and sea spray. Human activities may increase the concentration of particulates in the air, such as cigarette smoke, the burning of fossil fuels in vehicles, power plants, wood stoves and industrial processes. New technologies such as production and use of engineered nanomaterials may also increase the level of exposure. The gastrointestinal tract can be exposed to particulates that can be ingested as additives or contaminants of foods. In addition, the presence of particulates in the gastrointestinal tract is an inevitable consequence of the pulmonary clearance of inhaled particles because of the retrograde transport by the mucociliary escalator and subsequent swallowing of material.

Historically, the health effects associated with exposure to particulates have mainly been linked to the pulmonary route of exposure, especially occupational exposures such as coal miner's pneumoconiosis and quartz associated silicosis and lung cancer [1]. However, the large air pollution exposure episodes in the 20th century such as the Meuse Valley fog in 1930 and the London fog in 1952 brought attention to the

Correspondence: Peter Møller, Øster Farimagsgade 5A, Postbox 2099, DK-1014 Copenhagen K, Denmark. Tel: +45 35 32 76 54. Email: p.moller@pubhealth.ku.dk

ISSN 1071-5762 print/ISSN 1029-2470 online
DOI: 10.3109/10715760903300691

hazard of inhalable particulates in environmental settings [2,3]. The most common exposure situation in large cities of the developed countries is characterized by low concentrations affecting large populations. Large-scale epidemiological studies from such locations have shown that exposure to urban air pollution is associated with increased risk of cardiovascular and respiratory diseases, including lung cancer, bronchitis and asthma [4]. In addition, particulates that previously were considered to be inert particles, such as carbon black and titanium dioxide (TiO_2), are now classified as possible human carcinogens (group 2B) by the International Agency of Research on Cancer, which is partly based on mechanistic understanding of particle-elicited chronic inflammation in tumourigenesis in rat inhalation studies [5–8]. Exposure to carbon nanotubes (CNT), used in nanotechnology, also seems to be associated with granulomas and neoplasia [9,10] and both exposure to C_{60} fullerenes and CNT is associated with intermediate events in cardiovascular diseases in animal experimental models [11,12].

Oxidative stress, defined as a situation of an imbalance between production of reactive oxygen species (ROS) or reactive nitrogen species (RNS) and antioxidant defenses, is considered to be an important mechanism of particle-induced health effects [13]. This is evidenced by reports from workshops devoted to the development of screening test systems based on biomarkers of oxidative stress, which are being considered used in the regulation of nanomaterials [14]. It is relatively easy to measure the production of ROS and RNS, as well as the concentration of free radical scavengers and antioxidant enzyme activity, in acellular conditions and cultured cells. Lipid peroxidation products and oxidatively generated DNA lesions are often used as biomarkers of oxidative stress in humans and animal experimental models because it is difficult to measure the production of ROS or RNS in multicellular organisms. Investigations of oxidative stress in humans mainly use surrogate tissue such as leukocytes, plasma and urine, which imply that PM or leaked constituents are translocated systemically or indirect effects caused by inflammatory mediators. Translocation across the air–blood barrier is mainly a phenomenon observed for nanosized particles, which may be because of their distribution pattern in the lung, resistance to phagocytosis and small size enabling passage [15]. Studies of nanosized carbon black particles suggest that the translocation across the air–blood barrier occurs via a gap-fenestration pathway [16]. This observation is in keeping with that of a study on translocation of TiO_2 nanoparticles, which showed that particles did not move between different pulmonary compartments without restrain and part of the applied dose was located in the connective tissue and capillary lumen [17]. It has been shown that whole-body inhalation exposure to ultrafine carbon particles was associated with deposition in the liver, which was speculated to originate from gastrointestinal exposure and uptake from the gut [18]. The extent of gastrointestinal uptake of particles appears to be ~ 1% of the applied dose, based on studies of C_{60} fullerenes and polystyrene latex microspheres [19,20]. The uptake of polystyrene microspheres appears to be predominantly by the villous route, whereas regions of Peyer's patches are not hotspots of uptake [21]. Interestingly it has also been shown that large carbon black particles ($<$ 44 μm) were taken up in Peyer's patches [22]. Probably less than 1% of particulates translocates from the alveoli to the circulation of humans [23–25]. This estimate is in keeping with recent studies in rats exposed to iridium (20 nm or 80 nm) or composite carbon-iridium nanoparticles (25 nm) showing a very small fraction of translocation, but the smallest particles did translocate slightly more than the larger particles [26]. However, very small particles such as 1.4 nm gold particles translocate systematically (8.5% of the instilled dose), indicating that substantial passage across the air–blood barrier is possible [27].

Here we describe the association between the exposure to particles and oxidative stress with special focus on the relationship to cardiovascular effects and cancer. Figure 1 depicts the relationship between these events; some of the mechanisms of action have vicious circles. Particle-induced oxidative stress affects cell signalling described by Nel et al. [13] in three tiers with enhanced transcription of defence genes through the transcription factor *nrf2* at low levels of oxidative stress, activation of inflammation signalling through NFκB at higher levels and activation of apoptotic pathways and necrosis at the highest level of oxidative stress. Alteration of the cell activation signalling is also considered to be an important feature of the carcinogenesis of particulates such as silica, carbon black and CNT [28,29]. We have structured the manuscript as a line of events from acellular oxidation potential of particulates, cellular uptake, effects of particulates in cells including ROS generation, depletion of intracellular antioxidants and mitochondrial dysfunction, to effects observed in animals and humans. We focus on representative types of particulates, encompassing particles in ambient air (air pollution particles, diesel exhaust particles (DEP) and wood smoke particles), silicium-containing particles (quartz or silicon dioxide), reference materials (TiO_2) and engineered carbon based nanomaterials (carbon black, CNT and C_{60} fullerenes). These are particulates that have been investigated in studies of acellular ROS generation and oxidation of biomolecules, intracellular generation of ROS and oxidatively damaged biomolecules, as well as animal experimental models. The array of particles included in our survey provides the possibility to assess differences in ability to provoke oxidative stress, but it should be emphasized that the list of particles is not exhaustive. Especially, types of

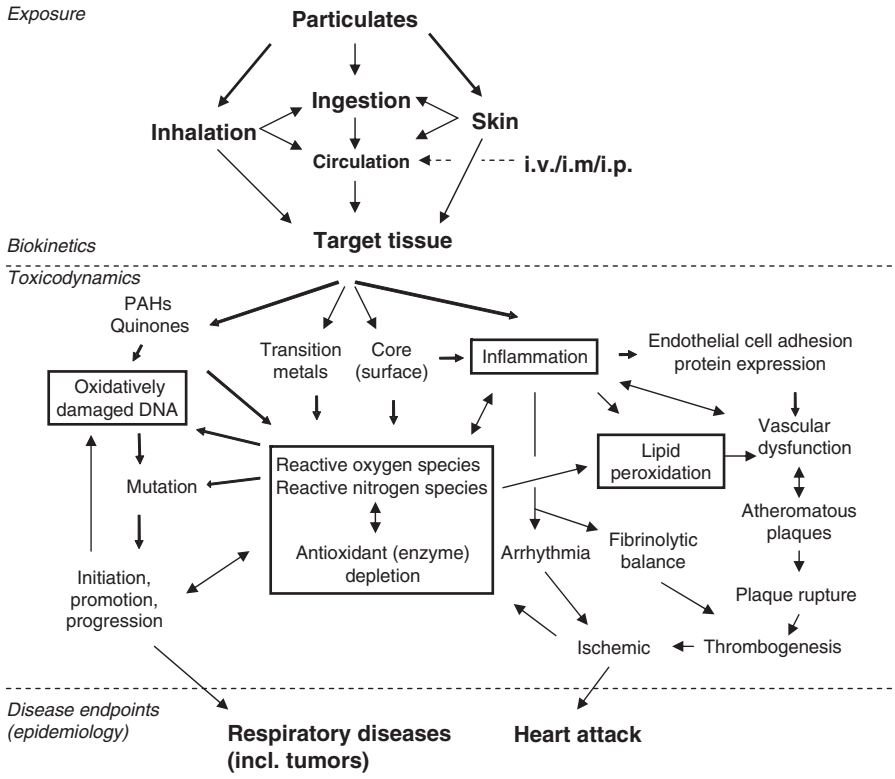

Figure 1. Hypothetical pathway for particle-induced oxidative stress and death or hospitalization of cancer and cardiovascular diseases.

asbestos fibres have not been included in the assessment, despite the fact that considerable knowledge about the fibre toxicology, including oxidative stress and the concept of frustrated phagocytosis, has been obtained from studies of asbestos fibres [28]. However, there are several types of asbestos fibres and especially of crocidolite has been associated with toxicity. It is our impression that investigations have focused on this type of asbestos fibre, which is a sound approach from a toxicological point of view, but it would possibly give rise to bias in the analysis.

Types of particulates

Particles can be classified according to the chemical composition, size and shape. The commonly used size stratification of airborne particulates encompasses particles with an aerodynamic diameter below 0.1 μm (ultrafine or nanoparticles), 2.5 μm ($PM_{2.5}$), 10 μm (PM_{10}) and total suspended particles (TSP). Usually, this is measured as mass of all particles below that size cut-off. Otherwise, the exposure can be assessed as the number concentration and size distribution of ultrafine particles. The same stratification is commonly used for PM suspended in solution, although it can be troublesome to obtain suspensions of small size particles in solution without using detergents or chemical compounds that may be harmful to living cells. Table I summarizes descriptions of the types of particles that are discussed in this manuscript. These particulates differ in size and composition; consequently they are expected to cause different levels of oxidative damage to biomolecules, cells and animals. Silica comprises a number of mineral particulates containing the element silicon, including quartz that is the most abundant type of crystalline silicon dioxide. TiO_2 and carbon black have traditionally been considered as being particulates with low toxicity and have often been used as inert particles. Carbon black and TiO_2 are almost pure preparations that can be obtained in different size modes, such as Printex 90 with a primary diameter of 14 nm. In aerosol or fluid particles agglomerate to form particles of larger size. The agglomeration increases with time and concentration of the primary particles. This has a strong importance for the toxicity of nanoparticles as shown by a study of freshly generated carbon nanoparticles (10–15 nm) that generated marked pulmonary inflammation in mice, whereas aged (agglomerated) particles with a diameter of 150–250 nm was associated with markedly lower inflammation following inhalation [30].

Particulates generated by combustion processes are often complex mixtures of organic compounds and metals adhering to a carbon core (Figure 1). This type of PM is composed of poorly soluble particles as well as soluble particulate material. Air pollution particles belong to the class of poorly soluble particles of low toxicity that also encompass carbon black and TiO_2. The organic compounds include quinones, which may generate ROS by redox-cycling, volatile organic compounds

Table I. Description of selected type of particulates that are discussed in the paper.

Particulate	Types[a]	Description
Historically hazardous particulates		
Silica	DQ12 Min-U-Sil 5 SRM1878	Silicon dioxide (quartz) is the most important type of silicate minerals. Quartz is crystalline silicate (SiO_2), which is most active when it is freshly grinded. Humans are exposed by inhalation. In the occupational setting, humans can be exposed to freshly fractured quartz, whereas the environmental exposure is considered to consist of mainly aged quartz particles. The grinded quartz usually generates particles in the form of respirable dust.
Low toxicity particulates		
Titanium dioxide	Preparations available from Sigma (ultrafine) or as pigment grade materials	TiO_2 is the naturally occurring oxide of titanium. In nature, it occurs as rutile, anatase and brookite minerals. TiO_2 is used as white pigment for food colouring, paint, sunscreens, medicines and toothpaste. TiO_2 has UV resistant properties because of its ability to absorb UV.
Carbon black	Printex 90 Printex 25 Flammruss 101 Sterling V	Carbon black is produced by incomplete combustion of heavy petroleum products. It is an amorphous form of carbon with high surface area-to-volume ratio. It is similar to soot but with a much higher surface area-to-volume ratio. Carbon black is used as a pigment and reinforcement in rubber and plastic products.
Combustion particulates		
Air pollution particles	Authentic preparations[a] SRM1648 SRM1649 EHC-93	The SRM1648 and SRM1649 are preparations of urban dust that were collected in the late 1970s in St. Louis and Washington DC, respectively. The EHC-93 preparation originates from Ottawa, Canada.
Wood smoke particles	Only authentic preparations	To the best of our knowledge there exists no commercially available preparation of wood smoke particles.
Diesel exhaust particles	Authentic preparations SRM1650 SRM2975 A-DEP[b]	Several preparations of diesel exhaust particles have been available. SRM1650 was commercially available and was issued in 1985, but is now replaced by SRM2975. These preparations were collected from a heavy-duty diesel engine and diesel-powered industrial forklift, respectively. The A-DEP preparation was collected from the exhaust of a light-duty diesel engine.
Engineered nanomaterials		
C_{60} fullerenes	Well-characterized preparations are nowadays commercially available (e.g. from Sigma), whereas earlier materials must be characterized as being authentic preparations	C_{60} fullerenes consist of 60 carbon atoms arranged in a spherical structure (truncated icosahedron) resembling a soccer ball.
Carbon nanotubes	Well-characterized preparations are nowadays commercially available	The types of carbon nanotubes include SWCNT and MWCN, which have been used in most of the studies in nanotoxicology of carbon nanotubes.

[a]We define an authentic preparation of particulates as materials that has been collected or manufactured for a specific study. These samples are usually not available to other researchers because very little of the particles have been collected. The authentic particulates may or may not have been well-characterized. This definition applies well to various particulates derived from combustion processes (e.g. authentic air pollution particulates). In addition, some pioneer publications on oxidative stress of nanomaterials have used samples that may not have been fully characterized in regard to impurities and dispersion procedures and thus identical experimental conditions are difficult to reconstitute. Thus, these preparations are regarded as being authentic particulates.
[b]Numerous papers have used DEP obtained from Masaru Sagai, National Institute of Environmental Studies (described here as A-DEP).

(e.g. benzene) and polycyclic aromatic hydrocarbons (PAH). The size distribution of air pollution particles typically depends on the local immission sources, long-range transport of particles and meteorological variables. Therefore, air pollution particles are best regarded as authentic particulates of obvious toxicological importance since they originate from the real world, but they are also unique because particulates sampled from one location may not be identical to samples from other locations or samples obtained on the same location at a different time of the year. In order to overcome this problem, particulates are available from different sources such as the National Institute of Standards and Technology (Gaithersburg, MD) that provide well-characterized standard reference material (SRM) of both urban dust and diesel exhaust particles (DEP). The A-DEP preparation from Japan is another type of particulate that has been used extensively in particle toxicology. It appears that the majority of the studies on pulmonary inflammation and allergic airway disease have used A-DEP, whereas studies on mutagenicity have been carried out on SRM1650 and SRM2975 preparations from the National Institute of Standards and Technology. Only recently there has been investigations comparing these reference materials in the same study showing that the A-DEP was more mutagenic on mass basis and resulted mainly in macrophage influx and activation, whereas SRM2975 enhanced polymorphnuclear cell inflammation [31,32].

With the emergence of nanotechnology, new types of particulates are manufactured with desirable properties such as high mechanical strength, unique drug delivering properties and resistance of biofilms adhering to surfaces. C_{60} fullerenes and CNT belong to this class of engineered nanoparticles; the latter group encompasses single-walled carbon nanotubes (SWCNT) and multi-walled carbon nanotubes (MWCNT). Although some of the exposure is delivered as agglomerates that are larger than 100 nm, they are referred to as nanoparticles due to the primary particle size.

Role of the surface reactivity for oxidative stress

The ratio between the surface area and mass is an important determinant for the toxicity of particles because chemical reactions and leakage of constituents occur from the surface of particles. The percentage of surface molecules increases exponentially when the particle diameter decreases in the nanosize range and at very small distances quantum phenomena can occur [33,34]. It is therefore the reactivity of the surface that may be the most important feature of particulates. The surface reactivity depends on the chemical composition, shape, size, solubility and surface area of particles [35,36]. However, it is most often the surface area that is reported in toxicological studies; this is probably because it is relatively easy to measure.

The large surface area of small particles is an important characteristic when determining biological effects for carbon black and TiO_2 where the inflammogenicity, depletion of glutathione and oxidative damage potential correlate remarkably well with the surface area [37–39]. The level of oxidatively damaged DNA, assessed as 8-oxo-2'-deoxyguanosine (8-oxodG), in the lung following inhalation also correlated well with primary particle surface area [40]. However, it should be emphasized that some endpoints of oxidative stress may not be closely linked with particle surface area. For instance, the heme oxygenase-1, which contains the antioxidant response element, is upregulated by oxidative stress. However, it has been shown that carbon blacks of different sizes induced similar levels of heme oxygenase-1 in cultured cells, although the oxidizing potential was directly proportional to the surface area [41]. Possibly this is because heme oxygenase-1 is a stress response gene product. In addition, the particle surface area alone is not a suitable predictor of cellular toxicity to nanosize TiO_2 particles of different crystal structure and silica where the surface properties appear important too [42–44].

The inflammogenic potential and depletion of glutathione by quartz also display linearity with respect to the size of the surface area, but the induction is much steeper than that observed for the low-toxicity particulates such as carbon black and TiO_2 [38]. In fact, the tumour response in rats exposed to various particulates by pulmonary route correlates very well with the administered surface area of a range of particulates such as carbon black and TiO_2 but not for quartz. This is attributed to the higher surface reactivity of the latter [45,46]. Freshly fractured dusts of quartz have free silicon radicals or silicon oxide-centred radicals present on the surface that can react with molecular oxygen [47,48]. Traces of iron at the surface of quartz may also facilitate ROS generation [47]. The importance of the surface reactivity for the generation of oxidatively damaged DNA has been documented in studies showing that coating the surface of quartz with either polyvinylpyridine-*N*-oxide or aluminium lactate was associated with lower generation of strand breaks and 8-oxodG in cell cultures [49,50]. In rats exposed to quartz by intratracheal (i.t.) instillation, there was a lower level of strand breaks in epithelial cells isolated from animals exposed to surface coated quartz particles [51]. Similar results have been obtained with freshly generated ultrafine particles of elemental carbon, which had higher oxidative potential and resulted in higher levels of lipid peroxidation products in canine alveolar macrophages than aged particles that had been suspended in distilled water for 24 h [52].

Cellular uptake of particulates

Particles can cross cell membranes through a passive (diffusion) or active transport. Regardless of the type of transport, it has been argued that the physicochemical properties of particles (including chemical composition,

size, shape and agglomeration status), type of exposed cells (professional phagocytes vs non-professional phagocytes), serum components and surfactant are important characteristics describing the transmembrane passage of particles [53]. The active transport (endocytosis) of particles can occur by either phagocytosis or pinocytosis. The purpose of endocytosis is to internalize macromolecules and particulates into transport vesicles derived from the plasma membrane. It is a cellular mechanism controlling entry of material into cells, which is tightly coordinated and coupled with the overall cell physiology [54]. It is especially neutrophils, macrophages and dendritic cells that possess this type of phagocytic activity, encompassing receptor-mediated and actin-based uptake of insoluble material in the size range of 1–3 μm. On the other hand, pinocytosis is characterized by ingestion of fluid and solutes via vesicles [54].

Oxidative stress studies on cultured cells exposed to particulates appear to use mainly immortalized immune cells (e.g. THP-1 and RAW264.7) or cell cultures originating from target tissue (e.g. A549 and BEAS-2B), whereas other types of cultured cells such as fibroblasts have been used less frequently. Especially the human A549 cell line, which is considered to represent type II lung cells of the pulmonary epithelium, has been used in particle toxicology. This cell line has phagocytic activity toward ultrafine (50 nm) TiO_2 particles, which appear to be internalized in cytosolic, membrane-bound vacuoles as aggregates and enmeshed lamellar bodies of particulates ~ 400 nm in size, whereas no aggregates were detected in the nucleus [55]. Another study showed that A549 cells had rapid, but similar, uptake of both fine (40–300 nm) and ultrafine TiO_2 particles (20–80 nm); the particles were predominantly located in membrane-bound vacuoles, whereas the nucleus, Golgi apparatus, rough endoplasmatic reticulum and mitochondria did not contain particles [56]. A study on luminescent silica nanoparticles concluded that particles were not present in the nucleus of A549 cells [57]. Using renal cell lines it was shown that TiO_2 (15 nm) and carbon black (13 nm) particles were located in cytoplasmatic vesicles of the cells [58]. Similar observations have been reported for SWCNT, which were not detected in the nucleus [59]. Investigations of air pollution particles have shown that ultrafine particles were located in mitochondria of RAW 264.7 cells, whereas fine particles were present in large cytoplasmatic vacuoles [60]. It is striking that most studies did not find particles in the nuclei. The nucleus is connected to the cytoplasm by the nuclear pore complex, which provides a highly regulated way of transport of biomolecules and only allows free diffusion of molecules that are less than 8 nm in diameter [61]. The observation of particle-devoid nuclei could be explained by the inability to detect small molecules due to low resolution in e.g. electron microscopy. However, an alternative interpretation could be that very few particles have a diameter less than 8 nm in biological fluids and for this reason there are no particles reaching the nucleus after cellular uptake. This is clearly a puzzle that needs to be solved by further experiments, although it is possible that ultrafine particles cross cellular membranes by passive mechanisms. It is worthwhile noting that results obtained from studies of cultured macrophages and inhalation experiments in animals have shown that ultrafine TiO_2 particles crossed cellular membranes by non-phagocytic mechanisms, whereas larger particles were phagocytosed [62].

Measurement of particle-induced ROS in acellular conditions and within cells

Analysis of the oxidation potential of particulates in acellular conditions is a fast and easy way of assessing oxidative stress, although it does not mimic the reducing environment in cells or extracellular fluid. Table II outlines an overview of studies reporting ROS production by particulates in acellular assays. The predominant assays have been electron spin resonance/electron paramagnetic resonance (ESR) with spin traps such as 5,5-dimethylpyrroline-*N*-oxide (DMPO) and oxidation of 2',7'-dichlorofluorescin (DCFH), although other assays such as consumption of dithiothreitol (DTT), dihydroethidium oxidation assay (DHE) and reduction of nitroblue tetrazolium (NBT) have been used as well. The DTT assay, based on the ability of redox active compounds to transfer electrons from DTT to oxygen, is regarded to measure ROS generation by quinone catalysis [14]. The DCFH assay is one of the most used assays for detection of ROS; it is based on the principle that DCFH reacts with ROS and RNS and generates a fluorescent product (Figure 2). In cellular assays, the cells are loaded with the parent compound 2',7'-dichlorofluorescin diacetate (DCFH-DA), which is hydrolysed intracellularly by endogenous esterases, whereas chemical deacetylation is required in acellular assays. The DCFH probe is regarded as a measurement of hydroxyl radicals, peroxynitrite, nitric oxide and more, whereas singlet oxygen, hydrogen peroxide and superoxide anions have limited capacity for oxidizing DCFH [63,64].

Oxidation potential of particulates in acellular condition

It has been shown that ultrafine carbon black particles generate ROS in a concentration-dependent manner [41,65–68], although one study using a single high concentration of Printex 90 (100 μg/ml) and ESR without spin trap did not show signs of ROS generation [52]. This suggests there were no carbon-centred radicals or that no electrons were moving freely within

Table II. *In vitro* acellular exposure to particulates and ROS generation.

Particulate	Size	Co-oxidant	Concentration	Method	Effect	Reference
Silica						
Quartz[a]	PM_{10}	H_2O_2	20 mg/ml	ESR with DMPO as spin trap and deoxyribose assay	Slightly increased ROS production (ESR: 1.2-fold, deoxyribose assay: 1.1-fold)	[79]
Crystalline silica	0.2–0.5 mm	No	Not reported	ESR with DMPO as spin trap	Increased ROS production	[80]
Coarse (Sil-O-Sil 259), amorphous quartz	45 and 40 μm	No	Not reported	ESR with DMPO as spin trap	Freshly ground coarse quartz generated ROS, whereas surface modification by heating reduced the ROS generation. Amorphous quartz did not generate ROS	[48]
Cap-O-Sil M-5	0.2–0.3 μm	No	Not reported	ESR	Unaltered ROS generation	[81]
DQ12	3.2 m^2/g	H_2O_2	Not reported	ESR with DMPO as spin trap	Increased ROS production	[74]
DQ12	Not reported	H_2O_2	20 mg/ml and 100 mg/ml	ESR with DMPO as spin trap	Detection of ROS with and without coincubation with H_2O_2, but the concentration of DQ12 needed to be 5-fold higher to obtain a similar signal in incubations without the presence of H_2O_2	[49]
DQ12	Not reported	H_2O_2	80 mg/ml and 200 mg/ml	ESR with DMPO as spin trap	Unaltered ESR signal by DQ12, whereas presence of H_2O_2 increased the signal by 3.6-fold	[75]
DQ12	Not reported	H_2O_2	5 mg/ml	ESR with DMPO as spin trap	Increased ROS generation, whereas surface modification of the quartz reduced the ROS production to 36% (PVNO-treated quartz) and 44% (aluminium lactate-treated quartz) compared to unmodified DQ12	[50]
DQ12	0.91 μm	H_2O_2	1.25 mg/ml	ESR with DMPO as spin trap	Increased ROS production that was diminished by surface modification with aluminium lactate	[76]
Min-U-Sil 5	5.2 m^2/g	No	Not reported	ESR with DMPO as spin trap	Increased ROS generation	[78]
Min-U-Sil 5	5.8 m^2/g	H_2O_2	1 and 400 cm^2	Deoxyribose assay	Increased ROS production at the highest dose	[77]
Titanium dioxide						
Fine, ultrafine	40–300 nm and 20–80 nm	No	400 $\mu g/cm^2$	ESR with DMPO or TEMPOL as spin traps	Unaltered ROS generation	[56]
Anatase	30–50 nm (20–120 m^2/g)	H_2O_2	80 mg/ml	ESR with DMPO as spin trap	Increased ESR signal (5-fold)	[69]
Nanosized	Not reported	No	> 20 cm^2	DCFH (with horseradish peroxidase)	Slightly increased ROS production (statistics not reported)	[70]
Anatase	0.45 μm	UV-A	100 μg/ml	ESR with DMPO as spin trap	No ESP signal in the absence of UV-A light	[72]
TiO_2	Not reported	H_2O_2	4.4 mg/ml	Deoxyribose assay	Unaltered ROS production	[73]
TiO_2	20–75 nm	No	30 μg/ml	DTT	Increased ROS production (2-fold)	[71]
Carbon black						
Printex 90	14 nm (300 m^2/g)	No	100 μg/ml	ESR	No detectable ESR signal, indicating no carbon-centered radicals or single electrons moving freely within the carbonaceous matrix	[52]
Printex 90	14 nm	No	10 μg/ml	DCFH	Increased ROS production (4.8-fold)	[67]
Printex 90	14 nm (338 m^2/g)	No	≤ 100 μg/ml	DCFH	Concentration-dependent increased ROS production (max: 66-fold)	[66]
Printex 90	14 nm (338 m^2/g)	No	≤ 10 μg/ml	DCFH	Increased at the highest concentration (7.6-fold)	[68]
Printex 90, Huber 990	14 nm (253.9 m^2/g) and 260 nm (7.9 m^2/g)	No	≤ 120 μg/ml	DCFH	Increased by Printex 90 (high concentrations appear to decrease the fluorescence signal). No ROS production by Huber 990 particles	[65]

(Continued)

Table II. (*continued*)

Particulate	Size	Co-oxidant	Concentration	Method	Effect	Reference
Printex 90, Printex 25, Flammruss 101)	14 nm (300 m^2/g), 56 nm (45 m^2/g), 95 nm (20 m^2/g)	No	≤ 100 μg/ml	DTT	DTT consumption is directly proportional to the surface area	[41]
Air pollution particles						
SRM1648, SRM1649	Not reported	No	40, 80, 160 μg/ml	Deoxyribose assay	Dose-dependent increase in ROS production of both SRM1648 and SRM1649	[97]
Duisburg (heavy industry) and Borken (rural site) Germany	Fine/coarse	H_2O_2	178 μg/ml	ESR with DMPO as spin trap	Fine and coarse particles generated the same level of ROS (7.5-fold), whereas the coarse particles from Duisburg generated more ROS than the fine particles (12.6-fold vs 10.3-fold)	[82]
Urban air particulates at 20 different sites (19 European cities)	$PM_{2.5}$	H_2O_2	50 μg/ml	ESR with DMPO as spin trap	Increased ROS production, but differences between sites and temporal within sites	[89]
Duisburg, Germany	Fine	H_2O_2	500 μg/ml	ESR with DMPO as spin trap	Dose-dependent increase in ROS production (DMPO-OH signal, max 1.9-fold), which was inhibited by deferoxamine and catalase	[90]
Düsseldorf, Germany Collected at different times of the year	Fine/coarse	H_2O_2	≤ 2.5 mg/ml	ESR with DMPO as spin trap	Coarse PM generated more ROS (DMPO-OH signal) than fine PM when compared at equal mass	[86]
Various cities in Germany	Fine/coarse	H_2O_2	320/380 μg/ml	ESR with DMPO as spin trap	Coarse particulates generated higher level of ROS than fine particulates. Samples collected from industrial area (Dortmund and Duisburg) generated higher level of ROS than particulates from a rural site (Borken)	[87]
Maastricht, The Netherlands	$PM_{2.5}/PM_{10}$	No	Not reported	ESR with DMPO as spin trap	No difference in ROS generating ability between $PM_{2.5}$ and PM_{10} samples. Season-dependent variation in the ROS generating ability of outdoor PM_{10} samples. Radical signals were inhibited by deferoxamine and catalase, whereas SOD had small inhibitory effect.	[83]
Maastricht, The Netherlands	$PM_{2.5}/PM_{10}$/TSP	No	Not reported	ESR with DMPO as spin trap	Differences in ROS generation in samples collected at different locations, but no clear difference between different size modes	[84]
Maastricht, The Netherlands	$PM_{2.5}/PM_{10}$/TSP	No	Not reported	ESR with DMPO as spin trap	Differences in ROS generation in samples collected at different locations, but no clear difference between different size modes	[94]
Maastricht, The Netherlands	PM_{10}	No	Not reported	ESR with DMPO as spin trap	Particulates collected in a street with high traffic intensity indicated presence of oxygen radicals, but no carbon-centred radicals	[92]
Urban street particles Stockholm, Sweden	PM_{10}	No	10–100 μg/ml	DTT	Concentration-dependent increase in oxidations that is slightly inhibited by deferoxamine	[93]
Athens, Greece	TSP	H_2O_2	Not reported	ESR with and without DMPO	Broad ESR signals, suggesting carbon-centred and semiquinone radicals. Addition of H_2O_2 increased the DMPO-OH signal	[98]
Athens, Greece	TSP, PM_{10}, $PM_{2.5}$	H_2O_2	4 and 8 mg/ml	ESR with and without DMPO	Detection of DMPO-OH signals. No difference between TSP, PM_{10} and $PM_{2.5}$	[85]

Edinburgh, Scotland	PM_{10}	No	Not reported	2.3-dihydroxybenzoic acid production	Increased ROS production	[96]
Los Angeles basin, USA	Coarse, fine and ultrafine	No	5–40 mg/ml	DTT	Ultrafine particles generated higher DTT oxidation than fine and coarse particles	[88]
Los Angeles basin, USA	Coarse, fine and ultrafine	No	≤ 50 mg/ml	DTT	Ultrafine particles generated higher DDT oxidation than coarse (21.7-fold) and fine particles (8.6-fold)	[60]
Provo, Utah	TSP	H_2O_2	Not reported	Deoxyribose assay	Increased ROS production	[91]
Five US cities	$PM_{2.5}$	No	Not reported	ESR	Similar ESR spectra of samples collected in different cities, whereas no ESR signal was observed in blank filters	[81]
Southern California	$PM_{2.5}$	No	Not reported	DTT	Increased ROS production	[140]
Wood smoke particles						
Wood smoke	Thermolysis of western bark (pine and fir)	H_2O_2	Not reported	ESR with DMPO as spin trap	Increased ROS generation in the presence of H_2O_2 that is observed in the early phase (3 min) of the incubation, whereas carbon-centred radicals predominate in the late phase of the incubation (90 min)	[103]
Wildfire, Alaska		H_2O_2	Not reported	ESR with DMPO as spin trap	Detection of carbon-centred radicals in samples with large particles, without treatment with H_2O_2. Smaller particles generate ROS in the presence of H_2O_2	[104]
Domestic chimney	Not reported	H_2O_2	Not reported	ESR with and without DMPO	Broad ESR signals, suggesting carbon-centred and semiquinone radicals. Addition of H_2O_2 increased the DMPO-OH spin adduct signal	[98]
Domestic chimney	Not reported	H_2O_2	4 and 8 mg/ml	ESR with and without DMPO	Detection of ESR signals (DMPO-OH spin adduct signal); the magnitude was similar to that obtained with urban air pollution particulates	[85]
Diesel exhaust particles						
SRM1650a	20–40 nm (108 m^2/g	No	100 μg/ml	ESR	No detectable ESR signal, indicating no carbon-centred radicals or single electrons moving freely within the carbonaceous matrix	[52]
SRM1650a	18–30 nm (108 m^2/g)	No	2.08–18.75 μg/ml	DCFH	Increased ROS production (4–5-fold)	[102]
SRM1650, SRM2975	Not reported	No	40, 80, 160 μg/ml	Deoxyribose assay	Dose-dependent increase in ROS production of both SRM1650 and SRM2975	[97]
SRM2975, DEP from a bus	Not reported	H_2O_2	4.4 mg/ml	Deoxyribose assay	Increased ROS production by SRM2975 (3-fold), but no additional effect of H_2O_2 exposure. Increased ROS production by DEP collected from a diesel engine (2.3-fold), which was further increased by co-incubation with H_2O_2 (statistical interaction was not analysed)	[73]
SRM2975	Not reported	No	≤ 10 μg/ml	DCFH	Increased ROS production at the highest dose (4.4-fold)	[68]
A-DEP	Not reported	H_2O_2	≤ 500 μg/ml	Cytochrome c reduction (superoxide anion radical) and ESR with DMPO as spin trap	Increased ROS generation and the presence of H_2O_2 enhanced the generation of DMPO-OH signals	[100]
DEP	Not reported	H_2O_2	Not reported	ESR with and without DMPO	Broad ESR signals, suggesting carbon-centered and semiquinone radicals in incubations without the presence of H_2O_2. Addition of H_2O_2 increased the DMPO spin trap signal	[98]

(Continued)

Table II. (*continued*)

Particulate	Size	Co-oxidant	Concentration	Method	Effect	Reference
DEP	Not reported	H_2O_2	4 and 8 mg/ml	ESR with and without DMPO	Concentration-dependent ESR signal intensity	[85]
DEP	PM_{10}	No	Not reported	ESR with and without DMPO	PM_{10} from gasoline or diesel exhaust generated more ROS (DMPO-OH signal) than indoor and outdoor PM_{10} samples	[83]
Engineered nanomaterials						
C_{60} fullerenes	Nanosize	No	10 μg/ml	DCFH	Increased (3.5-fold), but evidence that it is direct oxidation of the probe	[109]
C_{60} fullerenes	Nanosize	No	62.5–500 ng/ml	ESR and DCFH	No ROS production of C_{60} fullerenes suspended in aqueous solution, whereas suspension in THF was associated with increased ROS production by DCFH oxidation (10-fold) and ESR (5-fold)	[106]
C_{60} fullerenes	< 20 m^2/g	No	≤ 100 μg/ml	DCFH	Increased ROS production, without concentration-dependent relationship (max: 5-fold)	[66]
C_{60} fullerenes	< 20 m^2/g	No	≤ 10 μg/ml	DCFH	Marginally increased at the highest concentration (1.6-fold)	[68]
C_{60} fullerenes	86.2 nm	UV light	5 and 10 mg/ml	NBT and furfuryl alcohol consumption	No ROS production (indicator of singlet oxygen and superoxide anion radicals production) in aqueous solution	[110]
C_{60} fullerenes	100 nm	No	0.25 and 1 μg/ml	Dihydrorhodamine 123	Concentration-dependent increased ROS production	[107]
C_{60} fullerenes	160 nm	No	5 and 450 μg/ml	ESR	Concentration-dependent increased ROS production with ESR signal only at the high concentration	[108]
C_{60} fullerenes	Not reported	No	3 μg/ml	Indigo dye	Unaltered ROS production by water-suspended C_{60} fullerenes did not generate ROS. C_{60} fullerenes suspended in tetrahydrofuran generated ROS, whereas washed tetrahydrofuran-suspended particles did not generate ROS	[105]
C_{60} fullerenes	514.5 nm	No		DCFH dihydrorhodamine 123 and ESR	Unaltered ROS by C60 fullerenes suspended in water, whereas tetrahydrofuran suspended particles generated ROS	[106]
SWCNT	731 m^2/g	No	≤ 100 μg/ml	DCFH	Bell-shaped concentration-response relationship with maximum at 8.33 μg/ml (32-fold)	[66]
SWCNT	731 m^2/g	No	≤ 10 μg/ml	DCFH	Increased ROS production at 1 μg/ml (3.3-fold) and 10 μg/ml (7.6-fold)	[68]
SWCNT (containing 0.23% or 26% iron)	1040 and 950 m^2/g	No	120 μg/ml	ESR	Sample with 26% iron generated ROS, whereas the sample with 0.23% iron did not give rise to ESR signals	[11]
MWCNT	378 m^2/g (5.9 μm long)	Yes	9 mg/ml	ESR	No ROS generation (particulates act as scavengers)	[78]

[a]The preparation of quartz (SINTEF) was available from University of Trondheim, Norway.

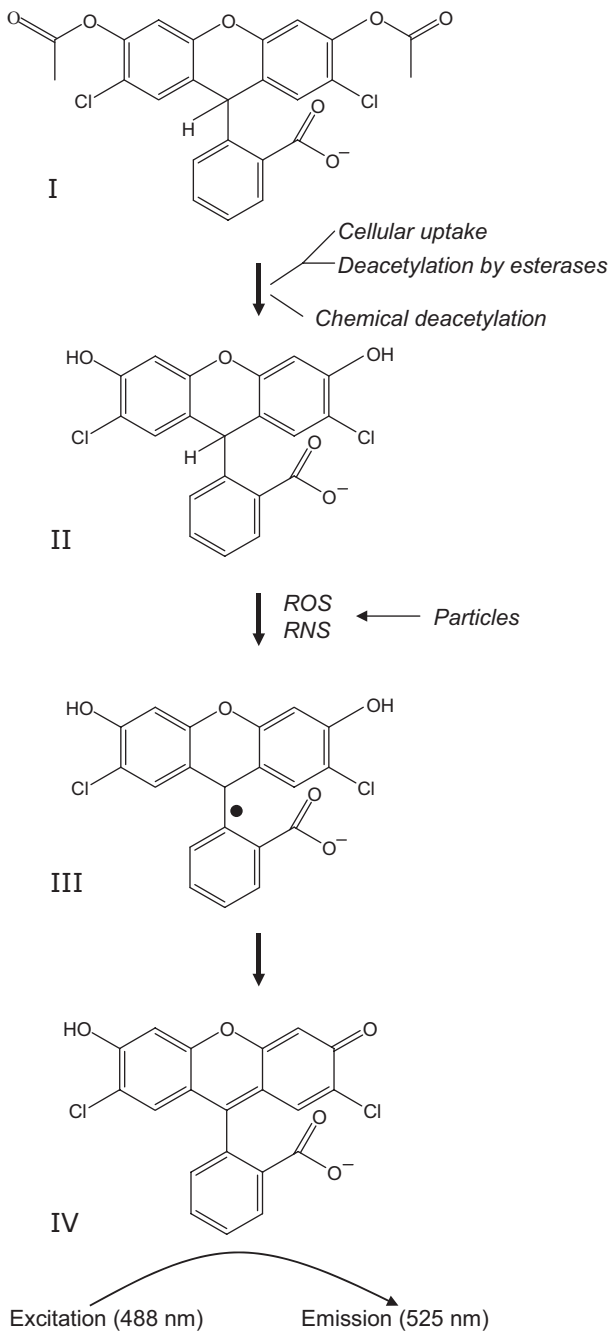

Figure **2.** Oxidation of the 2',7'-dichlorofluorescin diacetate (DCFH-DA) by particles. DCFH-DA (I) is either loaded to cells before treatment with particles or chemically deacetylated 2',7'-dichlorofluorescein (DCFH (II)) prior to acellular detection of ROS or RNS. The reaction with ROS or RNS yields the fluorescent 2',7'-dichlorofluorescein (DCF (IV)) via an intermediate radical (III).

the carbonaceous matrix. However, it should also be recognized that particulates display bell-shaped concentration–response relationships. In our hands, Printex 90 at a concentration above 100 μg/ml is associated with lower oxidation of DCFH when compared to lower concentrations [66]. Mixed results have been obtained in studies on TiO_2 showing either increased [69–71] or unaltered [56,72,73] ROS generation. Studies on silica particles have shown increased generation of ROS by DQ12 [49,50,74–76], Min-U-Sil 5 [77,78] and other types of crystalline silica and quartz [48,79,80], whereas one study found that Cap-O-Sil M-5 quartz did not generate ROS [81].

Most of the studies on authentic air pollution particles have used collected particulates as $PM_{2.5}$, coarse particles (fraction of particles between PM_{10} and $PM_{2.5}$) or TSP. It should be emphasized that these size fractions of authentic air pollution particles have both different size distributions and chemical composition. These types of particulates contain ultrafine particles, but the mass of the sample is dominated by large particles. There appears to be no relationship between the particle size of large air pollution particles and ROS production [82–85]; some studies show that coarse rather than fine particles had the highest ROS production [86,87]. However, a few studies have shown that ultrafine air pollution particles had higher DTT oxidation potential than the fine and coarse fraction of the same samples collected at the same location [60,88]. This indicates that the level of ROS production is determined by the chemical composition and large surface area of particles in the ultrafine range (less than 100 nm), whereas the chemical composition is more important than the surface area for large particles. In addition, air pollution particles collected at different locations or the same location at different times of the year have different ROS generating ability [82,83,86,87,89]. This clearly highlights the complexity of comparing the hazard of various authentic air pollution particles. The air pollution particles can generate high levels of ROS in the presence of H_2O_2 [82,85–87,89–91], but co-incubation with H_2O_2 is not required for the ROS generation by air pollution particles, as evidenced by several studies showing increased levels of ROS in aqueous solutions in the absence of H_2O_2 [60,81,83,84,92–98]. The ROS generating ability of air pollution particulates can be reduced by coincubation with deferoxamine or catalase [83,90,93], suggesting that Fenton-type chemistry is important for the acellular ROS production of air pollution particles. This is supported by observations that iron is released from urban air PM_{10} samples [99]. Leakage of transition metals is probably also a major variable explaining the ROS generating ability of DEP. It has been shown that DEP preparations generate ROS in the presence [73,85,98,100] and absence of H_2O_2 [68,73,83,97,101,102]. The generation of ROS by DEP does not appear to be mediated by carbon-centred radicals or single electrons moving freely within the carbonaceous matrix of the particulates [52]. However, wood smoke samples show signs of carbon-centred radicals and semiquinones as well as H_2O_2-dependent oxidation reactions suggesting Fenton-type of free radical oxidation reactions [85,98,103,104].

C_{60} fullerenes seem to provide a special case in studies assessing the ROS generating ability of particulates. C_{60} fullerenes are highly insoluble in aqueous solution and require vigorous mixing for an

extended period before suspension of small particles is obtained. An alternative procedure is dissolution of C_{60} fullerenes in organic solvent with subsequent mixing in aqueous solution and evaporation of the organic solvent. Tetrahydrofuran has been used as an organic solvent in several studies, but there is evidence that it is toxic to cells because of generation of reactive tetrahydrofuran-derived peroxides [105]. In addition, it has been shown that C_{60} fullerenes, initially suspended in tetrahydrofuran and then diluted in aqueous solution, generated higher levels of ROS as compared to C_{60} fullerenes suspended directly in aqueous solution [106]. It has been hypothesized that water molecules might quench C_{60} fullerenes generated singlet oxygen when the particles were directly dispersed in aqueous solution, whereas tetrahydrofuran intercalates in the lattice structure of C_{60} fullerenes during the initial solubilization, which thus mitigates the quenching by water molecules [106]. Studies of C_{60} fullerenes in aqueous solution indicate a small ability to generate ROS [66,68,107,108]. However, it has also been shown that C_{60} fullerenes can oxidize the DCFH probe [109]. This implies that the detection of ROS might be regarded as a methodological artifact rather than C_{60} fullerenes mediated generation of ROS. In addition, C_{60} fullerenes generate singlet oxygen by photochemical reactions in organic solvents, but similar reactions have not been found in aqueous solution [110].

Studies on CNT have provided mixed results; it was shown that only samples of SWCNT with high content of iron gave rise to ESR signals [111]. Studies using the DCFH oxidation assay have shown concentration-dependent ROS generation by SWCNT with low content of iron [66,68]. MWCNT in aqueous suspension did not generate ROS or carbon-centred free radicals in the presence of H_2O_2; on the contrary MWCNT exhibited radical scavenging capacity toward hydroxyl radicals and superoxide anion radicals [78].

ROS can also be detected indirectly in acellular assays by the consumption of antioxidants, for instance by suspension of particles in synthetic lung lining fluid. Thus, depletion of ascorbic acid and glutathione was differently affected by different preparations of carbon black, silicon dioxide and silica [112].

The generation of ROS is inevitably linked to increased risk of oxidative damage to biomolecules such as lipids and DNA. The lipid peroxidation products can be measured by a number of different assays such as thiobarbituric reactive substances (TBARS) and isoprostanes, whereas oxidized DNA base lesions include 8-oxo-7,8-dihydroguanine (8-oxoGua), 8-oxodG or lesions detected as formamidopyrimidine DNA glycosylase (FPG) or endonuclease III (ENDOIII) by e.g. the comet assay [63]. There are considerably fewer reports on the ability of particulates to oxidize DNA and lipids as compared to the studies on the ROS production ability. These studies appear only to encompass studies of air pollution particles, DEP and C_{60} fullerenes (Table III). Air pollution particles possess the ability to oxidize DNA in acellular conditions [84–87,90,113–115]. It has been reported that A-DEP and DEP collected from a light-duty engine generated 8-oxodG [116,117] and that diesel soot oxidized *α*-linolenic acid [118]. However, SRM1650 and SRM2975 did not generate 8-oxodG in calf thymus DNA in the presence or absence of H_2O_2 [113]. Mixing C_{60} fullerenes with liver microsomes was associated with increased levels of TBARS [119]. In another study it was shown that C_{60} fullerenes in the presence of visible light generated 8-oxodG from dG [120].

Oxidation potential of particulates in cultured cells

The ROS generating ability of particulates in cultured cells have been reported in numerous publications (Table IV). The primary assays for these types of studies are oxidation of DCFH, DTT consumption, deoxyribose assay and lucigenin chemiluminescence (superoxide production). Overall there is consistent data supporting intracellular ROS production by various particulates. All studies on C_{60} fullerenes [66,107,121,122] have reported increased intracellular ROS generation, although it should be emphasized that the intracellular ROS generation by C_{60} fullerenes is small. The majority of the studies on carbon black [58,65–67,123–131], air pollution particles [95,123,127,131–140], DEP [101,102,127,129–133,141–145] and CNT [59,66,111,124–126,142,143,146–150] have shown positive associations between exposure and intracellular ROS generation, although a few studies have not shown increased intracellular ROS generation [123,129,143,150]. The studies on silica [51,77,80,124,125,136,151–155], TiO_2 [56,58,71,122,138,142,143,149,156–160] and wood smoke particles [104,133,142] have yielded mixed results or no association between exposure and intracellular ROS production. Unfortunately, it is not possible to compare the ROS production by the particles on surface area basis because only a small fraction of the studies have reported the dose in this unit, whereas a number of studies have used the mass as metric for the dose. Still, direct comparison between studies is also difficult on mass basis because the exposures are reported in different units, including the mass of particulates per volume of dispersing solution (μg/ml), dish area (μg/cm^2) or number of exposed cells (μg/10^6 cells). The dish area can be used as a proxy-measure of the cell number because most studies on adherent cell lines use cell density that is near confluence. Figure 3 depicts an analysis of the potency of the particulates to generate ROS in terms of DCFH oxidation. We have calculated the increase in ROS production by 10 μg particles per cell area (cm^2) or number of cells (10^6 cells); these units are equivalent because they

Table III. *In vitro* generation of oxidized DNA and lipid oxidation products.

Particulate	Substrate	Co-oxidant	Concentration	Method	Effect	Reference
Air pollution particles						
SRM1649, Urban air dust Düsseldorf, Germany	Calf thymus DNA	No	1 mg/ml	8-oxodG (HPLC-ECD)	Increased production of 8-oxodG by SRM1649 (2.1-fold) and urban air dust (2.4-fold)	[114]
Duisburg, Germany	Calf thymus DNA	H_2O_2	160 μg/ml	8-oxodG (dot-blot)	Only increased in the presence of H_2O_2	[90]
Düsseldorf, Germany	Calf thymus DNA	H_2O_2	≤ 200 μg/ml	8-oxodG (dot-blot)	Coarse PM generated more 8-oxodG than fine PM when compared at equal mass	[86]
Ambient particles, Germany	Calf thymus DNA	H_2O_2	280–320 μg/ml	8-oxodG (dot-blot)	Higher generation of 8-oxodG by PM from Duisburg than rural location	[87]
Ambient particles Maastrcht, The Netherlands	Salmon testis DNA	No	Equivalent to 50 m^3 of sampled air	8-oxodG (HPLC-ECD)	Similar generation of 8-oxodG by $PM_{2.5}$, PM_{10} and TSP samples	[84]
Urban street (PM_{10}), Stockholm, Sweden	dG	H_2O_2	400 μg/ml	8-oxodG (HPLC-ECD)	Only increased in the presence of H_2O_2	[115]
TSP, PM_{10}, $PM_{2.5}$, DEP (Athens, Greece)	dG	H_2O_2	Not reported	8-oxodG (HPLC-ECD)	Particle preparations generated 8-oxodG in descending order as follows: DEP, $PM_{2.5}$, PM_{10}, TSP (statistics not reported and the level of 8-oxodG is reported in the unusual unit of μg lesions per 10^6 dG)	[85]
Urban street (TSP) Copenhagen, Denmark	Calf thymus DNA	H_2O_2	≤ 50 μg/ml	8-oxodG (HPLC-ECD)	Concentration-dependent increase	[113]
Wood smoke particles						
Wood smoke soot	dG	H_2O_2	Not reported	8-oxodG (HPLC-ECD)	Increased generation of 8-oxodG (statistics not reported and the level of 8-oxodG is reported in the unusual unit of μg lesions per 10^6 dG)	
Diesel exhaust particles						
DEP from a light-duty engine	Calf thymus DNA	H_2O_2	10 mg/ml	8-oxodG (HPLC-ECD)	Only increased 8-oxodG in the presence of H_2O_2	[116]
A-DEP	Calf thymus DNA	No	≤ 20 mg DEP/ mg DNA	8-oxodG (HPLC-ECD)	Concentration-dependent increase (max:9.5-fold)	[117]
SRM1650 and SRM2975	Calf thymus DNA	H_2O_2	≤ 200 μg/ml	8-oxodG (HPLC-ECD)	Unaltered 8-oxodG with or without presence of H_2O_2	[113]
Diesel soot	α-linolenic acid	No	100 μg/ml	TBARS (spectrophotometric assay)	Increased lipid peroxidation (7-fold)	[118]
Engineered nanomaterials						
C_{60} fullerenes	dG	Visible light	0.02–20 mg/mg dG	8-oxodG (HPLC-ECD)	Concentration-dependent increase in 8-oxodG (max: 12-fold). Highest level of 8-oxodG observed after 24 h exposure	[120]
C_{60} fullerenes	Liver microsomes	No	25–100 μg/mg protein	TBARS, conjugated dienes and lipid hydroperoxides	Concentration-dependent increase (max: 2.6-fold)	[119]

Table IV. *In vitro* short-term cellular exposure to particulates effects on ROS production.

Particulate	Cell	Duration	Concentration	Method	Effect	Reference
Silica						
SiO_2 (20.2 nm)	Primary mouse embryo fibroblasts	24 h	≤ 100 μg/ml	DCFH	Concentration-dependent increased ROS production (max: 2.2-fold)	[125]
SiO_2 (12 nm)	RAW264.7	24 h	5–40 ppm	DCFH	Concentration-dependent increase (max: 1.4-fold)	[154]
Crystalline silica (0.2–0.5 mm)	Alveolar macrophages	< 96 h	1 mg/ml	NBT	Increased ROS production	[80]
Silica particles (130 nm)	Mouse macrophages and human leukocytes (and cell lines)	5 min–72 h	≤ 32 μg/ml	DCFH	Increased ROS production	[155]
DQ12	Human bronchial cells	15 min	50 μg/ml	DCFH	Increased ROS production (1.4-fold)	[151]
DQ12	N8383 alveolar macrophages	1 h	3.1–62.5 μg/cm^2	DCFH	Unaltered ROS production	[124]
DQ12	Human neutrophils	40 min	0.05 and 0.25 mg/ml	Chemiluminescence (lucigenin)	Concentration-dependent increase (max: 1.7-fold)	[51]
Min-U-Sil 5	Human aortic endothelial cells	18–48 h	1 and 400 cm^2	DCFH and deoxyribose assay	High conc. (400 cm^2) resulted in ROS production, whereas low conc. (1 cm^2) did not. ROS generation inhibited by deferoxamine. Time-dependent generation of ROS in the DCFH assay	[77]
Min-U-Sil 5	Rat alveolar macrophages	20 h	20 μg/cm^2	DCFH	Unaltered ROS production (results not shown)	[136]
Min-U-Sil 5	MH-S macrophages	6 h	50 μg/cm^2	DCFH	Unaltered ROS production (1-fold)	[152]
Min-U-Sil 5	RAW264.7	1 h	15–100 μg/ml	DCFH	Increased ROS production (max: 1.5-fold)	[153]
Titanium dioxide						
Fine (40–300 nm) and ultrafine (20–80 nm)	A549	2 or 4 h	400 μg/cm^2	ESR with DMPO or TEMPOL	Increased ROS production, but similar production by fine and ultrafine TiO_2	[56]
Fine (1 μm) and ultrafine (21 nm)	RAW264.7	4 or 24 h	0.5–100 μg/ml	DCFH	Increased ROS production for the ultrafine (max: 2.3-fold) and fine (max:1.4-fold) particles	[156]
Anatase or rutile	Primary dermal fibroblasts	48 h	400 μg/ml	Amplex red	Increased ROS production by the rutile (1.24-fold) and anatase (1.7-fold) form of particles	[160]
Anatase (300 nm)	RAW 264.7	4 h	62.5 μg/cm^2	DCFH	Unaltered ROS production	[138]
Anatase (32 nm)	Human skin fibroblasts	Not reported	0.05 mg/ml	DCFH	Unaltered ROS production in absence of UV-A irradiation	[158]
Anatase (5 nm and 40 nm)	Mouse primary embryo fibroblasts	Not reported	0.1–30 μg/ml	Dihydrorhodamine 123	Concentration-dependent increase, whereas the induction was similar between the 5 nm (1.9-fold) and 40 nm (2.5-fold) particles	[122]
Anatase (15 nm) and anatase/rutile (50 nm)	Glomerular mesengial cell line (IP15) and proximal epithelial tubular cell line (LLC-PK_1)	6 h	5 μg/cm^2	DCFH	Unaltered ROS production by both type of particulates	[58]

Anatase (90%) and rutile (10%) p articles (45 m^2/g)	U937 monocytes	12 h	≤ 5 μg/ml	DCFH	Unaltered ROS production (1-fold)	[157]
Ultrafine (20–30 nm)	Neonatal rat ventricular cardiomyocytes	24 h	≤ 2.5 μg/ml	DCFH	Concentration-dependent increased ROS production	[143]
Ultrafine (63 nm)	A549	4 h	20 and 40 μg/cm^2	DCFH	Statistically non-significant ROS production (2-fold)	[149]
Anatase	A549	48 h	5 μg/ml	DCFH	Increased ROS production (5-fold; statistics not reported)	[142]
Anatase	L929 mouse macrophages	40 min	3–600 μg/ml	DCFH	Concentration-dependent ROS production (max: 2-fold)	[159]
TiO_2 (20–75 nm)	A549	4 h	30 μg/ml	DCFH	Increased ROS production (1.6-fold)	[71]
Carbon black						
Printex 90	A549 and NR8383 alveolar macrophages	1 or 24 h	3.1–62.5 μg/cm^2	DCFH	Increased ROS production in A549 cells (11.4-fold) and NR8383 alveolar macrophages (5.4-fold)	[124]
Printex 90 (14 nm)	MonoMac-6	30 min	30 μg/ml	DCFH	Increased ROS production (1.5-fold)	[67]
Printex 90 (14 nm)	THP-1 and A549	4 h	100 μg/ml	DCFH	Increased ROS production in THP-1 (13-fold) and A549 cells (11.6-fold)	[128]
Printex 90 (14 nm) and Huber 990 (260 nm)	Mono-Mac 6	24 h	15 μg/ml	DCFH	Increased and unaltered ROS production by Printex 90 (27-fold) and Huber 990 particles, respectively	[65]
Regal 250R (35 nm, 60 m^2/g)	Alveolar macrophages	2 h	0.63–20 μg/ml	DCFH	Dose-dependent increase (max 4.7-fold)	[123]
FR103 (95 nm)	Human bronchial epithelial cells (16-HBE)	4 h	10 μg/cm^2	DCFH	Unaltered ROS generation (1.07 fold)	[131]
FR103 (95 nm)	Human bronchial epithelial cells (16-HBE) and human nasal epithelial cells	4 h	10 μg/cm^2	DCFH	Unaltered ROS generation (1.1 fold)	[129]
FR103 (95 nm)	A549	1 h	10 μg/cm^2	DCFH	Unaltered ROS generation (1.1 fold)	[130]
Printex 90	FE1-MML cells	3 h	≤ 18.75 μg/ml	DCFH	Concentration-dependent increased ROS production (max: 11-fold)	[66]
Carbon black (12.3 nm)	Primary mouse embryo fibroblasts	24 h	≤ 100 μg/ml	DCFH	Concentration-dependent increased ROS production (max: 2.1-fold)	[125]
FW2 (13 nm), Printex 60 (21 nm), LB101(85 nm)	Glomerular mesengial cell line (IP15) and proximal epithelial tubular cell line (LLC-PK_1)	6 h	5 μg/cm^2	DCFH	Increased ROS production by FW2 (1.8–1.9 fold). No effect by Printex 60 and LB101	[58]
Cabot (20 nm)	Neuroblastoma cells and macrophages	24 h	25–100 μg/ml	DCFH	Increased concentration-dependently in macrophages (max: 12.3-fold), whereas the increase in neuroblastoma cells was considerably smaller	[126]

(Continued)

Table IV. (*continued*)

Particulate	Cell	Duration	Concentration	Method	Effect	Reference
Unspecified carbon black (1.8 nm)	Human mononuclear blood cells	200 min	≤ 650 μg/ml	Chemiluminescence (lucigenin) and deoxyribose assay	Unaltered chemiluminescence, but increased hydroxyl radical production (deoxyribose assay) as compared to dry-heated carbon particles	[127]
Air pollution particles						
$PM_{2.5}$ (Vitry-sur-Seine, France)	Human bronchial epithelial cells (16-HBE)	4 h	10 μg/cm^2	DCFH	Increased ROS production (2.8-fold)	[131]
$PM_{2.5}$ (Porte d'Auteuil, France)	Human nasal epithelial cells	3 h	10–80 μg/cm^2	DCFH	Increased ROS production (SRM 1650 generated more ROS at lower concentration than authentic air pollution $PM_{2.5}$ particles)	[132]
Boston, USA (CAPs)	Hamster alveolar macrophages	0.5 h	≤ 180 μg/ml	DCFH	Increased ROS production (max: 3.5-fold), but large variability of CASs collected on different days	[134]
Stockholm, Sweden (PM_{10})	A549	2 h	20 μg/cm^2	DCFH	Increased ROS production (1.2-fold)	[133]
Utah Valley dust (PM_{10}) from three different years	Alveolar macrophages	20 min or 24 h	≤ 1 mg/ml	Chemiluminescence and dihydrorhodamine 123	Increased ROS production (chemiluminescence) by samples from the year of collection. Unaltered (or decreased) ROS production by dihydrorhodamine 123 where the cells had been incubated 24 h before the probe was added to the cells	[137]
Denver, Colorado ($PM_{2.5}$)	NR8383 alveolar macrophages	2 h	20–200 pg/cell	DCFH	Increased ROS production	[139]
Southern California	Macrophages	Not reported	Not reported	DCFH	Increased ROS production	[140]
Urban air from the roof of a five-story building (Osaka, Japan)	Human mononuclear blood cells	200 min	≤ 650 μg/ml	Chemiluminescence (lucigenin) and deoxyribose assay	Lower chemiluminescence by DEP as compared to control. Increased hydroxyl radical production (deoxyribose assay) as compared to dry-heated carbon particles	[127]
Air pollution particles	Human bronchial epithelial (IB3-1 and S-9 CF) cells	1 h	25 μg/cm^2	DCFH	Increased ROS production in IB3-1 (5-fold) and S-9 CF (4.4-fold) cells	[135]
SRM1648	Alveolar type 2 cells	20 h	20 μg/cm^2	DCFH	Increased ROS production (1.4-fold)	[136]
SRM1648	Human pulmonary artery endothelial cells	5–120 min	1–100 μg/ml	Amplex red	Concentration- and time-dependent increase in the ROS (H_2O_2) production (max: 2.3-fold)	[95]
SRM1648	RAW 264.7	4 h	62.5 μg/cm^2	DCFH	Increased ROS production (max: 1.2-fold)	[138]
Wood smoke particles						
Wood smoke particles	A549	2 h	20 μg/cm^2	DCFH	Unaltered ROS production (0.83-fold)	[133]
Wood smoke soot	A549	48 h	5 μg/ml	DCFH	Slightly increased ROS production (statistics not reported)	[142]
Wood smoke particles	RAW 264.7	30 min	100 μg/ml	Bioxtech kit (H_2O_2)	Particle-size dependent increase in lipid peroxidation; coarse (4.3–24 μm; 4.0-fold), fine (0.42-2.4 μm; 5.6-fold, ultrafine (0.042–0.24 μm; 7.5-fold)	[104]

Diesel exhaust particles						
SRM1650	Human nasal epithelial cells	3 h	10–80 μg/cm^2	DCFH	Increased ROS production (SRM 1650 generated more ROS at lower concentration than authentic air pollution $PM_{2.5}$ particles)	[132]
SRM1650	Human bronchial epithelial cells (16-HBE)	4 h	10 μg/cm^2	DCFH	Increased ROS production (4.6-fold)	[141]
SRM1650a	MML FE1	3 h	1.3–11.7 μg/cm^2	DCFH	Increased (1.6–1.9-fold)	[102]
SRM1650	Human bronchial epithelial cells (16-HBE)	4 h	10 μg/cm^2	DCFH	Increased ROS production (2.9-fold)	[131]
SRM1650	Human bronchial epithelial cells (16-HBE) and primary cultures of nasal epithelial cells	4 h	10–30 μg/cm^2	DCFH	Markedly higher ROS production in 16-HBE cell cultures (3.0–7.3-fold) as compared to primary cultures of epithelial cells (2.3–3.1-fold)	[129]
SRM2975	A549	1 h	10 μg/cm^2	DCFH	Increased ROS production (1.6-fold)	[130]
A-DEP	BEAS-2B and THP-1	2 h	100 μg/ml	DCFH and DHE	Unaltered ROS production by DCF, whereas the oxidation of hydroethidine (indicator of superoxide anion radicals) was associated with increased ROS production in BEAS-2B cells (4.5-fold) and THP-1 cells (1.6-fold)	[145]
A-DEP	Murine L-929 fibrosarcoma cells	3 h	50 μg/ml	DCFH	Increased ROS production	[101]
DEP, Fiat engine	A549	2 h	20 μg/cm^2	DCFH	Statistically non-significant increased ROS production (1.3-fold)	[143]
DEP, Japanese National Institute of Environmental Studies	Human mononuclear blood cells	200 min	≤ 650 μg/ml	Chemiluminescence (lucigenin) and deoxyribose assay	Highest ROS production at the lowest doses (50 and 200 μg/ml) and unaltered at the highest dose. Increased hydroxyl radical production (deoxyribose assay) as compared to dry-heated carbon particles	[127]
DEP, heavy-duty engine	Neonatal rat ventricular cardiomyosites	24 h	≤ 25 μg/ml	DCFH	Concentration-dependent increased ROS production	[143]
DEP, Kenworth truck	Human aorta endothelial cells	1 h	≤ 50 μg/ml	NBT	Concentration-dependent ROS generation (max 13.8-fold)	[144]
Diesel soot	A549	48 h	5 μg/ml	DCFH	Increased ROS production (statistics not reported)	[142]
Engineered nanomaterials						
C_{60} fullerenes	FE1-MML	3 h	≤ 25 μg/ml	DCFH	Low level of ROS production that was not concentration-dependent (2.5-fold)	[66]
C_{60} fullerenes	Rat glioma cell line C6	3 h	1 μg/ml	Dihydrorhodamine 123 (fluorescence)	Increased ROS production (max 2.2 fold)	[121]

(Continued)

Table IV. (*continued*)

Particulate	Cell	Duration	Concentration	Method	Effect	Reference
C_{60} fullerenes	Rat glioma cell line C6	3 h	1 μg/ml	Dihydrorhodamine 123 (fluorescence)	Concentration-dependent increased ROS production	[107]
C_{60} fullerenes	Mouse primary embryo fibroblasts	Not reported	0.1–30 μg/ml	Dihydrorhodamine 123	Concentration-dependent increased ROS production (2.6-fold)	[122]
SWCNT	FE1-MML	3 h	≤ 25 μg/ml	DCFH	Bell-shaped ROS production with highest effect at 8.33 (8-fold)	[66]
SWCNT and MWCNT	A549	1 h	31.3 μg/cm^2	DCFH	Increased ROS production by SWCNT (7.8-fold) and MWCNT (4.2-fold)	[124]
SWCNT	HaCaT	12 h	0.1–10 μg/ml	DCFH	Dose-dependent increase (max: 3.9-fold)	[146]
SWCNT	Primary mouse embryo fibroblasts	24 h	≤ 100 μg/ml	DCFH	Concentration-dependent increased ROS production (max: 4.1-fold)	[125]
SWCNT (containing 0.23% iron)	RAW 264.7	6 h	100 μg/ml	DHE assay and DAF2	Unaltered generation of ROS	[150]
SWCNT (containing 30% iron)	HaCaT	15 min	240 μg/ml	ESR with DMPO as spin trap	Increased ESR signal, which was suppressed by deferoxamine	[147]
SWCNT (containing 0.23% or 26% iron)	RAW264.7 (with or without stimulation)	30 min	≤ 150 μg/ml	ESR with DMPO as spin trap, DHE, or DAF2	Only ROS production (ESR signals) in zymosan-stimulated cells. Unaltered ROS generation measured by DHE and DAF2	[111]
SWCNT and MWCNT	Neuroblastoma cells and macrophages	24 h	25–100 μg/ml	DCFH	Increased ROS at the lowest concentration of SWCNT and MWCNT in macrophages (19.5-fold), whereas the increase in neuroblastoma cells was considerably smaller.	[126]
SWCNT	Neonatal rat ventricular cardiomyosites	24 h	≤ 25μg/ml	DCFH	Unaltered ROS production	[143]
SWCNT	Mesothelioma cells	1.5 h	150 μg/ml	ESR, DHE assay and DCFH	Increased ROS production	[148]
SWCNT	Hela	1 h	Not reported	MitoSOX red	Unaltered ROS	[59]
MWCNT	A549	48 h	5 μg/ml	DCFH	Strong ROS production by Ni-catalyst grown MWCNT, whereas arc evaporation grown MWCNT was associated with less DCFH oxidation	[142]
MWCNT	A549	4 h	20 and 40 μg/cm^2	DCFH	Unaltered ROS production	[149]

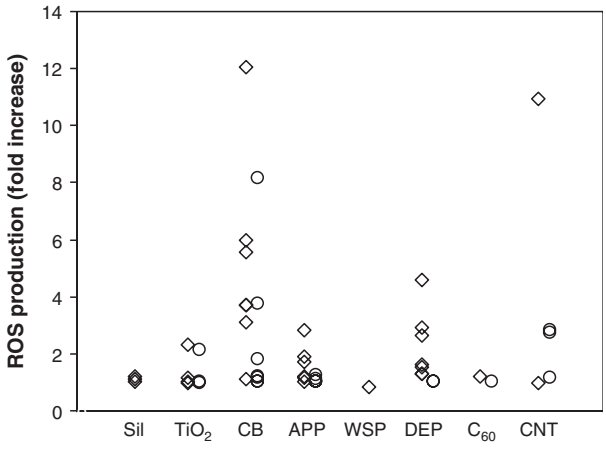

Figure 3. ROS production detected by the DCFH-DA probe in cultured cells exposed to silica (Sil), titanium dioxide (TiO_2), carbon black (CB), air pollution particles (APP), wood smoke particles (WSP), diesel exhaust particles (DEP), C60 fullerenes (C_{60}) or carbon nanotubes (CNT). The symbols indicate the ROS production per 10 $\mu g_{particles}/cm^2{}_{dish}$ (diamonds) or 10 $\mu g_{particles}/106_{cells}$ (circles) Original data have been collected from publications as follows: silica [124,136,152], TiO2 [58,138,149], carbon black [58,65–67,123,124,126,128,129,131], air pollution particles [131,133–136,138,284], wood smoke particles [133], DEP [102,129,131–133,141], C_{60} fullerenes [66] and CNT [66,126,146,149]. The ROS production per cell area or number of cells has been calculated from linear regression analysis. High concentrations of PM, which have resulted in plateau or bell-shaped concentration-response curves, have been omitted from the analysis.

relate the mass of particles to the amount of target molecules (assuming that cells have about the same volume and uptake of DCFDA). The concentration of particles in terms of mass per volume depends on the amount of liquid that the cells are exposed to; this is problematic because particles sediment during culture and the adherent cells might be exposed to higher concentration than assumed by the concentration in the fluid. As can be seen in Figure 3, expression of the ROS generating ability in terms of mass of particulates per surface area or number of cells indicates that the particulates have different potency. The particles differ considerably in potency, with carbon black being the most potent compound. The DEP preparations (SRM1650, SRM2975, A-DEP and authentic DEP preparations) and air pollution particles (SRM1648, SRM1649 and authentic air pollution particles) also generate high levels of ROS. The other particles appear to be associated with lower DCFH oxidation potential.

The intracellular ROS production may occur directly on the surface of the particles, as suggested by studies on carbon black, SWCNT and C_{60} fullerenes showing that the dynamics of ROS production in cell-free environment is similar to that observed inside cells [66]. However, constituents in the cell culture media are important, as has been shown in experiments with carbon black dispersed in different media containing either bovine serum albumin or dipalmitoyl-phosphatidylcholine (lung surfactant phospholipid) that gave different ROS production between a cell-free system and cultured cells [67]. It is possible that different dispersion agents may alter surface reactivity and particle size distribution, explaining differences in ROS production. In addition, it has been hypothesized that macrophages generate ROS primarily by activation of NADPH oxidase, as documented in studies of carbon black where inhibition of NADPH oxidase activity abolished ROS production in alveolar macrophages [123].

Depletion of endogenous antioxidants by particulates

The level of endogenous free radical scavengers and antioxidant enzymes serve to counteract the detrimental effects of ROS. Depletion of ROS scavenging compounds or reduced activity of antioxidant enzymes after acute exposure to particulates can be regarded as indices of oxidative stress. Glutathione (GSH) is oxidized to glutathione disulphide (GSSG). A reduced GSH/GSSG ratio or a reduced GSH/GSH ratio indicates a depletion of GSH. A concentration-dependent decrease of the GSH/GSSG ratio has been observed in THP-1, BEAS-2B and RAW 264.7 cells exposed to A-DEP [145,161]. Similar results have been obtained in cell cultures exposed to Printex 90 where the intracellular GSH concentration was decreased modestly in J774 murine macrophage cells [145,161] and more pronounced in A549 cells [162]. Concentration-dependent depletion of GSH and vitamin E has also been observed in cells exposed to SWCNT containing ~ 30% iron [111,147]. Studies on air pollution particles further indicate that the particle size fraction is important, since the GSH/GSSG ratio decreased in RAW 264.7 cells exposed to fine and ultrafine particles, whereas exposure to coarse particles did not alter the GSH/GSSG ratio [60]. Collectively these data indicate that particulates might generate oxidative stress by depletion of the endogenous free radical scavenging compounds in cultured cells.

Investigations of the effect of particulates on the antioxidant defense system in animals have provided more mixed results as compared to the effects observed in cultured cells. The complexity of the effect on antioxidant enzymes and endogenous antioxidants can be exemplified by studies on pulmonary exposure to combustion particles. It has been shown that pulmonary exposure to A-DEP was associated with reduced activity of glutathione peroxidase (GPx), superoxide dismutase (SOD) and glutathione reductase (GR) in mice 2 and 24 h after i.t. instillation [100]. These observations are supported by a study with a longer duration of pulmonary exposure to A-DEP by i.t. instillation (once a week for 10 weeks); the SOD activity was reduced in lung tissue of mice concomitantly with increased activity of cytochrome P-450 reductase that may over-produce superoxide

anion radicals from quinone compounds [163]. However, the GSH/GSSG ratio in lung tissue in another study of A-DEP was unaltered, even though there was increased level of lipid peroxidation products in the lung [161]. In addition, it has been shown that i.t. instillation of SRM1650 was associated with increased levels of 8-oxodG in the lung tissue of guinea pigs, although the concentration of ascorbate and the activities of GPx and SOD were unaltered [164]. Inhalation of cold wood smoke resulted in higher GPx activity (24–48 h) and lower Mn-SOD (12 h) activity in the lung of rats, whereas the GR and CuZn-SOD activities remained unaltered [165]. In another study it was shown that the GSH/GSSG ratio decreased concentration-dependently in the lung of sheep after inhalation of cold wood smoke [166]. The chemical profile of particles generated from different combustion processes may differ and the effect of such complex mixtures could be difficult to predict based alone on the type of particulates.

The results obtained from studies on nanomaterials in animal experimental models suggest the same kind of complexity as observed in studies of combustion particles. For instance, inhalation of SWCNT on 4 consecutive days did not alter the GSH level in the lung of mice, whereas there was an inflammatory response and increased lipid peroxidation in terms of malondialdehyde (MDA) content [167]. However, during the following 28 days there was accumulation of MDA, decreased level of inflammation, depletion of GSH and clear histopathological changes culminating in the development of multifocal granulomatous lesions and interstitial fibrosis [167]. The pulmonary lipid peroxidation was explained by a two-phase model where the early increase in lipid peroxidation arose from inflammation-generated oxidative stress, whereas tissue injury contributed to lipid peroxidation in the late phase. It should also be emphasized that some types of nanomaterials may act as radical scavengers *in vivo*. This has been observed in a study on intraperitoneal injection of C_{60} fullerenes that did not affect the GSH status, whereas it inhibited CCl_4-induced oxidation of GSH in the liver [168].

Collectively, the data from animal experimental models indicate that depletion of the antioxidant system is not a pre-requisite for the generation of oxidatively damaged DNA and lipids. The oxidative stress may be explained by a sequence of events such as (1) depletion of endogenous antioxidants by excessive particle-generated ROS and oxidation of biomolecules or (2) depletion of the endogenous antioxidant system and oxidation of cellular biomolecules as independent events of particle-generated ROS. However, it should also be emphasized that studies of animal experimental models usually employ relatively long exposure periods and lower doses as compared to cultured cells, which are not well-suited for the study of endogenous antioxidant depletion and decreased levels of antioxidant enzymes. Additionally, it is likely that prolonged exposure to particulates is associated with increased activity of the antioxidant defense system.

The role of the organic fraction of particulates

Particles generated by combustion processes, such as air pollution particles, wood smoke particles and DEP contain organic compounds such as quinones and PAH, including nitro-derivatives of PAH, oxygenated PAH and halogenated aromatic hydrocarbons [169,170]. These substances can be extracted in organic solvents (referred to as organic extracts of particles). The organic extracts have considerable effect, as shown by studies of dichloromethane-based organic extract of SRM1650 that generated the same level of intracellular ROS as the native particulate did [129,141]. Methanol extracts of wood smoke particles generated higher levels of FPG sites in THP-1 and A549 cells as compared to cultures exposed to native particles [171]. In RAW264.7 cells, organic extract of fine air pollution particles, which had a high content of organic compounds, was associated with a larger induction of heme oxygenase-1 than extracts of other size modes of air pollution particles [172]. RAW264.7 cell cultures exposed to extracts of A-DEP also showed evidence of ROS generation, which was inhibited by concomitant treatment with the free radical scavenger *N*-acetyl-cysteine [173]. Despite these observations, it should be noted that stimulation of inflammatory cells may alter the response to organic extracts of particulates. It has been shown that organic extract of DEP (SRM1975) generated ROS in neutrophils and macrophages, whereas the same preparation decreased the ROS production by neutrophils and macrophages that had been stimulated by treatment with phorbol-12, 13-myristate acetate [174].

The extractable organic compounds usually contain quinone substances that generate superoxide anion radicals via redox cycling processes [175]. Some types of PAH (e.g. β-naphthoflavone) have been shown to generate oxidative stress and induce antioxidant response element reporter gene activity [176]. The PAH compounds may also undergo biotransformation to quinone compounds [177]. Figure 4 depicts the transformation of benzo[*a*]pyrene to quinone species by two different mechanisms. The first pathway involves oxidation of benzo[*a*]pyrene by peroxidase activity of cytochrome P450, whereas the second reaction occurs by pathways involving aldo-keto reductase activity leading to a pro-oxidant cellular state with elevated ROS generation, GSH depletion and oxidatively generated DNA lesions [177,178]. The association between exposure to benzo[*a*]pyrene and oxidative stress is supported by studies in animal experimental models. Oral exposure of benzo[*a*]pyrene induced a complex array of genotoxic effects where a high dose increased the level of 8-oxodG in the liver [179], whereas a lower dose decreased the level of 8-oxodG in the lung and liver but increased

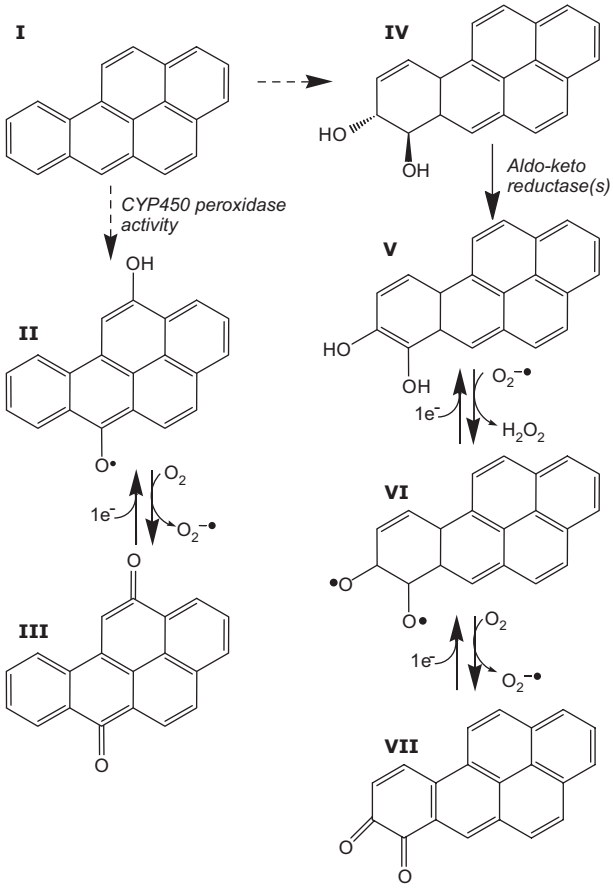

Figure 4. Conversion of benzo[*a*]pyrene (I) to quinone species via cytochrome P450 peroxidase activity benzo[a]pyrene-diones (II and III) that can generate ROS by redox-cycling. Benzo[*a*]pyrene can also be biotransformed to nenzo[*a*]pyrene-7,8-trans-dihydrodiol (IV) that can be further metabolized to catechol (V) that are capable of redox-cycling to semiquinone anion radicals (VI) and benzo[*a*]pyrene-7,8-dione (VII). The figure has been adapted from references [177,178].

the urinary excretion of 8-oxodG [177]. It is possible that these observations can be explained by different metabolic routes associated with marked difference in exposure, although it should also be noted that the high levels of 8-oxodG in control animals, suggesting spurious oxidation, might hamper the interpretation of the results. However, supporting evidence of the *in vivo* pro-oxidant effect of benzo[*a*] pyrene comes from a study showing increased levels of lipid peroxidation-induced etheno-DNA adducts in aorta tissue of dyslipidemic apoE-deficient mice receiving a single oral dose of benzo[*a*]pyrene [180].

Collectively, there is evidence that extractable organic compounds can be important contributors to ROS generation and oxidative damage in cultured cells and animal experimental models, but it must be expected that the effect depends on the cell type and bioavailability of the adhered organic compounds.

The role of mitochondrial dysfunction

Damage to mitochondria is considered to be a key event in the particle-induced cytotoxicity which may lead to generation of ROS, especially superoxide radical anions. At sufficiently high doses it is also possible that particulates elicit apoptosis. Using authentic air pollution particles it has been shown that the ultrafine fraction induced structural mitochondrial damage in RAW 264.7 and BEAS-2B cells, whereas the mitochondrial architecture remained intact by exposure to coarse particles [60]. It has also been shown that methanol-extracts of DEP promoted swelling of mitochondria in RAW264.7 cells; the quinone-enriched polar fraction rather than the PAH-enriched aromatic fraction mediated this effect by opening permeability transition pores and depolarization of the mitochondrial membrane potential [181]. Various particulates collected from ambient street air, wood burning and diesel exhaust (DE) also increases the mitochondrial depolarization in A549 cells [133,135]. The mitochondrial dysfunction might arise as a consequence of direct interference of particles with mitochondrial enzymes or it might be caused by cytosolic ROS generation. Support of the latter hypothesis comes from a study in A549 cells exposed to air pollution particles; the mitochondrial dysfunction could be attenuated by addition of free radical scavenger (sodium benzoate) or the iron chelator deferoxamine [182]. In this regard it should be emphasized that the mitochondrial dysfunction, especially a hampered function of the electron transport chain, may be associated with increased generation of ROS. This may provoke the onset of a vicious circle activating pro-inflammatory cascades. Another pathway leading to mitochondrial dysfunction has been suggested by results from a mouse alveolar macrophage cell line that had increased lysosomal permeability, unaltered intracellular ROS generation and mitochondrial depolarization after exposure to quartz [152]. Studies on TiO_2 particles have shown unaltered mitochondrial membrane potential in A549 cells, but it should be emphasized that the size of TiO_2 particles was not reported and it might have been pigment grade preparations rather than nanosized particles [183,184]. In addition, C_{60} fullerenes did not alter the mitochondrial activity in HepG2 cells, whereas there was evidence of lipid peroxidation (TBA RS) that could be prevented by concomitant exposure to ascorbic acid [185].

Oxidative damage to biomolecules by exposure to particulates in cell culture systems

Table V summarizes studies that have investigated the ability of particulates to oxidatively damage lipids and DNA in cultured cells. There is similar distribution between statistically significant results and null effects between publications on oxidized DNA and lipids (the positive and negative results were 18/6 and 18/2 for the effects of oxidized DNA and lipid products, respectively, $\chi^2 = 1.65$, $p = 0.20$). We can therefore consider these endpoints as equivalent for the purpose of overall analysis, although it should be emphasized that the simple TBARS assay is not an optimal

Table V. *In vitro* cellular exposure and oxidatively damaged DNA and lipids.

Particulate	Cell	Duration	Concentration	Endpoint	Effect	Reference
Silica						
SiO_2 (12.3 nm)	Primary mouse embryo fibroblasts	24 h	5–100 μg/ml	MDA (kit)	Concentration-dependent increased lipid peroxidation (max:1.9-fold)	[125]
DQ12	Rat lung epithelial type II cells (RLE)	4 h	100 μg/cm^2	8-oxodG (immunoassay)	Increased immunostaining in DQ12 exposed cells	[188]
DQ12	Rat lung epthelial type II cells (RLE)	4 h	80 μg/cm^2	8-oxodG (immunoassay)	Increased immunostaining in DQ12 exposed cells (2.1-fold)	[50]
DQ12	A549	4 h	80 μg/cm^2	8-oxodG (immunoassay)	Increased immunostaining in DQ12 exposed cells (3.5-fold)	[49]
Silica nanoparticles	A549	72 h	≤ 50 μg/cm^2	8-oxodG (antibody-based western blot)	Unaltered 8-oxodG	[57]
SRM1878a	FE1 MML	3 h	15 μg/cm^2	FPG sites (comet assay)	Statistically non-significant increase (1.86-fold)	[189]
SRM1878a	A549	2–4 h	25, 50, 100 μg/ml	FPG sites (comet assay)	Increased level of FPG sites	[187]
Min-U-Sil 5	RAW 246.7	24 h	15–120 μg/ml	8-isoprostanes (immunoassay)	Concentration-dependent increase (10–33-fold)	[186]
Min-U-Sil 5	RAW 246.7	1 h	100 μg/ml	BODIPY 581/591	Increased level of lipid peroxidation (18-fold)	[153]
Titanium dioxide						
Anatase and rutile	BEAS-2B	1 h	10 μg/ml	FPG sites (comet assay) and TBARS (spectrophotometric assay)	Increased FPG sites and lipid peroxidation products	[193]
Anatase (25%) and rutile (75%) with 24.4 nm (mean)	RTG-2	24 h	5 and 50 μg/ml	FPG sites (comet assay)	Unaltered FPG sites by 5 μg/ml (1.13-fold) and 50 μg/ml (0.93-fold)	[192]
Ultrafine (63 nm)	A549	4 h	20 and 40 μg/cm^2	FPG sites (comet assay)	Statistically non-significantly unaltered FPG sites at 20 μg/cm^2 (1.3-fold) and 40 μg/cm^2 (2.0-fold)	[149]
Anatase (450 nm)	Human skin fibroblasts	18 h	10 μg/cm^2	8-oxodG (HPLC-ECD)	Unaltered 8-oxodG (high baseline level of DNA damage and detection limit of 9.5 lesions/10^6 dG	[72]
Anatase (30-50 nm; 20-120 m^2/g)	Chinese hamster ovary V79	24–72 h	1–10 μg/cm^2	TBARS (spectrophotometric assay)	Lipid peroxidation reported to be increased although the data presented do not support the conclusion	[69]
Carbon black						
Printex 90	A549	3 h	11.3 μg/cm^2	FPG sites (comet assay)	Increased level of FPG sites (2.2-fold)	[189]
Printex 90 (300 m^2/g), Printex G (30 m^2/g)	Alveolar macrophages	1 h	3.2–100 μg/10^6 cells/ml	8-isoprostanes	Unaltered level of lipid peroxidation	[52]
Carbon black (12.3 nm)	Primary mouse embryo fibroblasts	24 h	5–100 μg/ml	MDA (kit)	Concentration-dependent increased lipid peroxidation (max:2.3-fold)	[125]
Air pollution particles						
Urban street (TSP), Copenhagen, Denmark	A549	24 h	2.5–100 μg/ml	FPG sites (comet assay)	Concentration-dependent increase (max: 2.3-fold)	[113]
Coarse and fine, Düsseldorf, Germany	A549	2 h	50 μg/ml	8-oxodG (antibody-based detection)	Coarse and fine PM generate similar extent of 8-oxodG	[86]
Urban street (PM_{10}), Stockholm, Sweden	A549	4 h	10 μg/cm^2	8-oxodG (HPLC-ECD)	Unaltered (8-oxodG increased by PM collected from subway)	[115]

Urban street (PM_{10}), Stockholm, Sweden)	RAW 264.7	18 h	100 μg/ml	TBARS	Increased level of lipid peoxidation products (5.7-fold)	[93]
Dunkerque, France	Human lung embryo tissue cells (L132)	24, 48, 72 h	19 and 75 μg/ml	MDA (HPLC) and 8-oxodG (antibody-based)	Concentration- and time-dependent increase of 8-oxodG (max: 28-fold). Only increased MDA at the highest concentration after 72 h (12-fold), which was associated with significant toxicity	[190]
Tunnel street, Oslo, Norway	A549 and THP-1	3 h	2.5–200 μg/ml	FPG sites (comet assay)	Increased FPG sites in A549 and THP-1 cells	[171]
Ambient particles (Taiwan)	BEAS-2B	8 h	100 μg/ml	Lipid peroxidation products (kit)	$PM_{1.0}$ significantly increased (2.3-fold), whereas larger particles generated less lipid peroxidation products	[191]
Urban air dust, Dussendorf, Germany and SRM1649	BEAS-2B	2 h	400 mg/ml	8-oxodG (HPLC-ECD)	Increased 8-oxodG by urban dust (2.4-fold) and SRM1649 (2.7-fold)	[114]
Wood smoke particles						
Wood smoke particles	RAW 264.7	1 h	Not reported	TBARS (spectrophotometric assay)	Increased lipid peroxidation (max: 2.9-fold)	[103]
Wood smoke particles	RAW 264.7	1 h	100 μg/ml	Lipid peroxidation (kit)	Particle-size dependent increase in lipid peroxidation; coarse (4.3–24 μm; 1.2-fold), fine (0.42–2.4 μm; 1.4-fold, ultrafine (0.042–0.24 μm; 1.6-fold)	[104]
Wood smoke particles	A549 and THP-1	3 h	2.5–200 μg/ml	FPG sites (comet assay)	Increased FPG sites in A549 and THP-1 cells	[171]
Diesel exhaust particles						
SRM1650, SRM2975	A549	3, 24 and 48 h	2.5–250 μg/ml	FPG sites (comet assay)	Concentration-dependent increase by SRM1650 (max: 4-fold) and SRM2975 (max: 3-fold)	[113]
SRM1650a	Alveolar macrophages	1 h	3.2–32 μg/10^6 cells/ml	8-isoprostanes	Unaltered level of lipid peroxidation	[52]
SRM2975	A549 or THP-1	3 h	2.5–200 μg/ml	FPG sites (comet assay)	Concentration-dependent increase in A549 cells (max 17-fold), whereas the level of FPG sites was increased at the two lowest concentrations in THP-1 cells (1.8-fold)	[171]
A-DEP	RAW 264.7	5 h	50 μg/ml	Lipid hydroperoxides (spectrophotometry)	Increased lipid peroxidation (1.8-fold)	[161]
Engineered nanomaterials						
C_{60} fullerenes	FE1-MML cells	3 h	100 μg/ml	FPG sites (comet assay)	Increased DNA damage (1.2-fold)	[66]
C_{60} fullerenes	Rat glioma cell line C6	3 h	1 μg/ml	TBARS (colorimetric assay)	Increased lipid peroxides (2.9-fold)	[121]
C_{60} fullerenes	Rat glioma cell line C6	3 h	1 μg/ml	TBARS (colorimetric assay)	Increased lipid peroxides (2.9-fold)	[107]
C_{60} fullerenes (in THF)	HepG2, neuronal human astrocytes and human dermal fibroblasts	48 h	0.24–2400 ppb	TBARS	Increased in HepG2 (max: 3.1-fold), neuronal human astrocytes (max: 4.8-fold), human dermal fibroblasts (max: 5.4-fold)	[185]

(Continued)

Table V. (*continued*)

Particulate	Cell	Duration	Concentration	Endpoint	Effect	Reference
SWCNT	FE1-MML cells	3 h	100 μg/ml	FPG sites (comet assay)	Increased DNA damage (1.6-fold)	[66]
SWCNT (30% iron)	HaCaT cells	18 h	≤ 240 μg/ml	TBARS (spectrophotometry)	Concentration-dependent increase (max: 1.48-fold)	[147]
SWCNT (26% or 0.23% iron)	RAW264.7 (stimulated)	30–120 min	125 μg/ml	Lipid hydroperoxides	Higher level of lipid peroxidation in the iron-rich SWCNT (3.5-fold) than the purified SWCNT (2.0-fold)	[111]
SWCNT	Primary mouse embryo fibroblasts	24 h	5–100 μg/ml	MDA	Concentration-dependent increased lipid peroxidation (max: 1.9-fold)	[125]
MWCNT	A549	4 h	20 and 40 μg/cm^2	FPG sites (comet assay)	Unaltered after both 20 μg/cm^2 (0.98-fold) and 40 μg/cm^2 (0.94-fold)	[149]

assay of lipid oxidation damage in biological samples because it detects other compounds than lipid peroxidation products too. In this regard improved methods using a high performance liquid chromatography (HPLC) purification step are more reliable [63].

The majority of studies on generation of lipid peroxidation products and oxidized DNA lesions in cell cultures have shown increased generation of oxidized biomolecules by exposure to silica [49,50,57,125,153, 186–189], air pollution particles [86,93,113–115, 171,190,191], wood smoke particles [103,104,171], DEP [52,113,161,171], C_{60} fullerenes [66,107, 121, 185] and SWCNT [66,111,125,147,149]. However, it has also been shown that C_{60} fullerenes directly oxidize thiobarbituric acid, indicating that increased TBARS in cell cultures may be a methodological artifact that is not indicative of lipid peroxidation [109]. Studies on carbon black have provided mixed results, with studies showing an unaltered level of 8-isoprostanes [52], whereas other studies reported an increased level of MDA detected with a commercial kit and oxidatively damaged DNA lesions [125,189]. Exposure to TiO_2 in cell cultures has yielded mainly null effect [69,72,149,192] and only one positive effect in terms of increased TBARS detected with the unreliable spectrophotometric assay [193].

The cell culture studies reported in Table V provide important qualitative information about the ability of particulates to generate oxidized lipids and DNA in cultured cells, but the differences in assays and reported unit of concentration precludes an assessment of the quantitative differences of particulates across publications. However, such an analysis can be made by use of the simple form of the alkaline comet assay that detects strand breaks and alkaline labile lesions. Nowadays, the comet assay is among the most popular tests for DNA damage in genetic toxicology, research on particle genotoxicity and it has been validated in biomonitoring studies [194]. The production of ROS is associated with generation of strand breaks that can be measured by the simple version of the comet assay, but this version of the comet assay can also detect DNA damage originating from PAH-rich coal tar and compounds that damage DNA by non-oxidative reactions such as heterocyclic aromatic amines and coal tar [195,196]. Figure 5 indicates that there is considerable difference in the genotoxic potency between particulates assessed by the comet assay. Collectively, the studies on strand breaks indicate that carbon black, DEP and air pollution particles consistently have the highest DNA damaging potency, whereas C_{60} fullerenes have the lowest potency. Between these extremes are TiO_2, wood smoke particles, silica and CNT that have modest genotoxic potential. In addition, it is interesting to note that the genotoxic potency of the particles (Figure 5) is similar to the potency of DCFH oxidation potential (Figure 3). This implies that the presence of intracellular ROS and oxidative insults to biomolecules are part of the

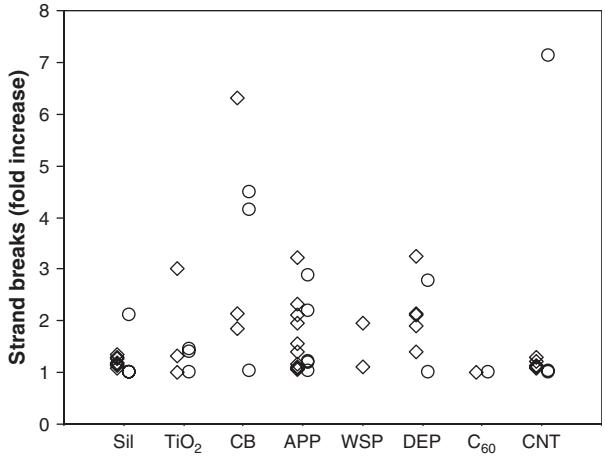

Figure 5. Generation of strand breaks detected by the comet assay in cultured cells exposed to silica (Sil), titanium dioxide (TiO_2), carbon black (CB), air pollution particles (APP), wood smoke particles (WSP), diesel exhaust particles (DEP), C60 fullerenes (C60) or carbon nanotubes (CNT). The symbols indicate the generation of strand breaks per 10 mgparticles/cm^{2}dish (diamonds) or 10 mgparticles/10^{6}cells (circles). Original data have been collected from publications as follows: silica [49,50,74,124,125,187–189,240,241], TiO2 [149,193,280,285, 286], carbon black [125, 189,287,288], air pollution particles [87,90,113,115,171, 182,287–291], wood smoke particles [171,290], diesel exhaust particles [113,171,213,288], C60 fullerenes [66] and CNT [66,125,148,149, 292,293]. One study on the genotoxic effect of C60 fullerenes has not been included in the graph because this study reported a very high level of strand breaks (95-fold increase per 10 μgparticles/10^{6}cells [294]. The generation of strand breaks per cell area or number of cells has been calculated from linear regression analysis. High concentrations of PM, which have resulted in plateau or bell-shaped concentration-response curves, have been omitted from the analysis.

same phenomenon of particle exposure, but it is obviously premature to regard one or the other assay as a redundant endpoint.

Association between particulates and oxidative damage in experimental animal models

Investigations of the association between exposure to particulates and oxidatively damaged biomolecules in experimental animal models have mainly focused on the respiratory system by inhalation or i.t. instillation (Table VI), whereas the effect elicited by alternative exposure routes have been investigated in fewer studies (Table VII). For the pulmonary route of exposure, it has been hypothesized that the mechanism of action acts through two thresholds: (1) A dosimetric threshold. That is the dose at which lung clearance mechanisms cannot remove particles at sufficient rate and accumulation of particulates occurs. (2) A mechanistic threshold where the level of the antioxidant defenses is overwhelmed by production of ROS [45]. Both mechanisms can include contribution from inflammation to ROS formation targeting non-inflammatory cells. It is rather difficult to measure ROS in animal experimental models, whereas it is feasible to measure the levels of oxidized biomolecules such as lipid peroxidation products and oxidized DNA lesions.

The number of studies on particle-induced oxidatively damaged DNA or lipids indicate clearly that the majority of studies have reported positive effects of silica (seven studies: [197–203]) and DEP (18 studies [116,117,161,164,204–217], whereas only two [108, 218] and three [219–221] studies have reported null effect of exposure to silica and DEP, respectively. The studies on air pollution particles [222–225], wood smoke particles [165,166] and C_{60} fullerenes [68,108] have reported increased levels of lipid and DNA oxidation products, but it should be emphasized that the number of studies are low. The studies on TiO_2 [201,210,226,227], carbon black [40,228,229] and CNT [68,167,230,231] have shown mixed results.

It should be acknowledged that some of the methods for the detection of lipid peroxidation products have been criticized for being unsuitable for the detection of damage to lipids because they are unspecific [63]. In addition, the antibody-based detection of 8-oxodG generates values that are higher than those obtained by HPLC with electrochemical detection (ECD), indicating that the antibodies are unspecific [232,233]. Still, immunohistochemistry (IHC) for the detection of 8-oxoGua has the unique ability of localization of the lesion histologically to a specific type of cells. The studies using IHC for the detection of 8-oxoGua after exposure to DQ12 quartz have shown increased levels of DNA damage in the lung of rats, including alveolar epithelial cells [198–201]. The induction of 8-oxoGua by pulmonary exposure to quartz was less pronounced in Chinese hamsters compared to rats [202]. However, the immunostaining of 8-oxoGua in unexposed hamsters was ~ 4-fold stronger than in rats, which could be explained by limited specificity of the antibody in that species. As such, it is interesting that the detection of 8-oxodG by HPLC-ECD did not indicate any increase in the level of oxidatively damaged DNA in rats exposed to DQ12 quartz [218]. Pulmonary exposure to Printex 90 and DE have also been associated with an increased level of 8-oxoGua measured by IHC [216,228]. The level of 8-oxodG in plasma was marginally increased in the plasma of rats exposed to nano-sized carbon black [229]. The association between effect of pulmonary exposure to TiO_2 and oxidized lipids and DNA lesions remains unclear because the studies are difficult to interpret. The level of 8-oxoGua in the lung tissue was unaltered in one study using IHC [199], whereas another study reported an unrealistically high level of 8-oxodG (40 lesions/10^6 dG) in unexposed animals [210]. Measurement of TBARS by the spectrophotometric assay in brain tissue indicated that intranasal exposure to TiO_2 was associated with an increased level of lipid peroxidation at day 30 after exposure, whereas the level of TBARS was unaltered at days 2, 10 and 20 after exposure [226,227].

Table VI. Studies on pulmonary exposure to particulates and association with levels of oxidized DNA and lipids in animal experimental models.

Exposure	Size	Biomarker	Effect	References
Silica				
DQ12 (0.3, 1.5 or 7.5 mg/rat) by i.t. instillation in female Wistar rats	3.2 m^2/g[a]	8-oxodG (IHC)	Detection of 8-oxoGua at the highest dose (7.5 mg/rat) 3 days after instillation. Increased 8-oxodG at the two highest doses at days 21 and 90 after instillation	[199]
DQ12 (2.5 mg/rat) by i.t. instillation in Wistar rats	900 nm (3.2 m^2/g)	8-oxoGua (IHC)	Increased 8-oxoGua staining in the lung at days 7 (3-fold), 21 (2.2-fold) and 90 (3.6-fold) after instillation	[200]
DQ12 (0.6 mg/rat) by i.t. instillation in female Wistar rat	900 nm	8-oxoGua (IHC)	Increased 8-oxoGua in the lung 90 days after instillation, which also displayed signs of pulmonary inflammation	[201]
DQ12 (0.15, 0.30, 0.60, 1.2, or 2.4 mg/rat) by i.t. instillation and killed 21 or 90 days after exposure	900 nm	8-oxoGua (IHC)	Increased 8-oxoGua in the lung of rats exposed to 1.2 (1.5-fold) and 2.4 mg (1.8-fold) 90 days after instillation. No effect 21 days after exposure	[198]
DQ12 (3 or 12 mg/kg) by i.t. instillation in female Wistar rats or Chinese hamsters and killed 90 days after the instillation	900 nm (3.2 m^2/g)[a]	8-oxoGua (IHC)	Increased 8-oxoGua in the lung of rats (1.8-fold; 12 mg/kg bodyweight), whereas the level of DNA damage was not statistically significant in the hamsters (1.4-fold)	[202]
DQ12 (2 mg/rat) exposed by i.t instillation in female Wistar rats	3.2 m^2/g[a]	8-oxodG (HPLC-ECD)	Unaltered 8-oxodG in the lung 7 days after instillation	[218]
Min-U-Sil 5 (10 mg/kg) i.t. instillation in male Wistar rats	5 μm	8-oxodG (HPLC-ECD)	Increased 8-oxodG in the lung at days 1 (2.2-fold), 3 (2.6-fold) and 5 (2.9-fold) after instillation, whereas there were unaltered levels of 8-oxodG at weeks 1, 4, 24 and 32 after the exposure. High baseline level of 8-oxodG (13 lesions/10^6 dG)	[203]
Min-U-Sil 5 (15 mg/m^3), 6 h/day for 20, 40 or 60 days male Fisher 344 rats	1.78 μm	Lipid peroxidation (colorimetric assay)	Increased lipid peroxidation in the lung (1.2–1.9-fold)	[197]
Min-U-Sil 5 (0.2–3 mg/rat) by i.t. instillation	Not reported	TBARS (spectrophotometry)	Unaltered levels of lipid peroxidation products in bronchoalveolar lavage fluid	[108]
Titanium dioxide				
TiO_2 (0.15, 0.3, 0.6 mg/rat) by i.t. instillation in female Wistar rats	20 nm	8-oxoGua (IHC)	Unaltered levels of 8-oxoGua in the lung 90 days after instillation of P25 (untreated, hydrophilic surface) and T805 (silanized, hydrophobic surface) types of TiO_2. No signs of pulmonary inflammation.	[201]
TiO_2 (amorphous) by i.t. instillation once weekly for 10 weeks in ICR mice (0.1 mg/mouse)	Not reported	8-oxodG (HPLC-ECD)	Unaltered 8-oxodG in the lung (1.1-fold). High baseline level of 8-oxodG (40 lesions/10^6 dG)	[210]
TiO_2 (rutile or anatase) by intranasal instillation in female CD-1 (ICR) mice	80 nm (22.7 m^2/g) and 155 nm (10.5 m^2/g)	TBARS (spectrophotometry)	Increased levels of TBARS in brain homogenate 30 days after exposure, which was higher in the mice exposed to anatase (1.4-fold) as compared to rutile TiO_2 (1.1-fold). Unaltered levels of lipid peroxidation products in the brain at days 2, 10 and 20 after exposure	[226,227]
Carbon black				
Printex 90 (1, 7, 50 mg/m^3) or Sterling V for 13 weeks (6 h/day and 5 days/week). Female Fisher 344 rats	16 nm (300 m^2/g; Printex 90) and 70 nm (37 m^2/g, Sterling V)	8-oxodG (HPLC-ECD)	Elevated 8-oxodG in the lung of rats that inhaled 50 mg/$m^3$of Printex 90 (1.21-fold), whereas there was no effect of Sterling V. High baseline level of 8-oxodG (24 lesions/10^6 dG)	[40]
Printex 90 or Printex 25 once weekly for 6 weeks by i.t. instillation in male ICR mice	14 nm (300 m^2/g; Printex 90) and 56 nm (45 m^2/g; Printex 25)	8-oxodG (IHC)	Increased 8-oxodG in the lung by Printex 90 (2.5-fold increased staining score), whereas Printex 25 was not statistically significant (1.9-fold)	[228]
Carbon black (15.6 mg/m^3, 6 h/day, 5 d/week) for 4 weeks in rats	120 nm	8-oxodG (antibody-based ELISA)	Statistically non-significant increased level of 8-oxodG in the plasma of carbon black exposed rats (1.5-fold)	[229]

Air pollution particles				
CAPs breathing for 5 h (1.06 mg/m^3) in male Sprague Dawley rats	0.1–2.5 μm	TBARS (spectrofluorometry)	Increased levels in the lung (2-fold)	[224]
CAPs breathing for 75 h (5 h/d and 3 d/week) in *ApoE*$^{-/-}$ mice. Exposures included CAPs ($PM_{2.5}$) and filtered air representing exposure to ultrafine particles	$PM_{2.5}$ and ultrafine particles	MDA (colorimetric assay)	Increased MDA in the liver in groups of mice exposed to CAPs (1.2-fold) and filtered CAPs air with ultrafine particles (1.2-fold)	[225]
$PM_{2.5}$ particulates (Taiyuan, China) by i.t. instillation (1.5, 7.5, 37.5 mg/kg) male Wistar rats	Not reported	TBARS (fluorometric method)	Increased levels in the heart, liver, lung (1.4–1.7-fold; 7.5 mg/kg) and testicles (1.6-fold; 37.5 mg/kg) 24 h after instillation. Unaltered levels in the spleen, kidney and brain	[223]
Authentic air pollution particles (6 h, 20 h, or 5 h/d for consecutive days)	Not reported	TBARS (spectrofluorometry)	Increased lung lipid peroxidation after 20 h of exposure, whereas 6 h of exposure and intermittent short-term (6 h) did not increase the level of TBARS in the lung	[222]
Wood smoke particles				
Cold wood smoke (from fir and pine) inhalation fro 16.25 min in Sprague Dawley rats	Not reported	TBARS	Bell-shaped time curves with peak at 24 h in the lung (4-fold). Increased TBARS in the liver 48 h after exposure (1.6-fold)	[165]
Cold wood smoke (western pine bark) in male adult sheep	Not reported	TBARS	Concentration-dependent increase in TBARS in the lung (max: 4-fold) 48 h after inhalation Elevated carboxyhaemoglobin concentration in the blood	[166]
Diesel exhaust particles				
SRM1650 by i.t. instillation (0.7 or 2.1 mg/guinea pig) and killed 5 days later in male and female Ssc:AL guinea pigs	18–30 nm (108 m^2/g)	8-oxodG (HPLC-ECD)	8-oxodG increased in the lung of both sexes at 2.1 mg/guinea pig. Urinary excretion of 8-oxodG (per 24 h) was unaltered in the last 24 h of the exposure period	[164]
A-DEP by i.t instillation (2 mg/rat or 4 mg/rat) in female Fischer 344 rats	0.3–3 μm	8-oxodG (HPLC-ECD)	8-oxodG increased in the lung in a dose-dependent manner 2 h and 8 h after instillation. No statistical significance at 1, 2, 5 and 7 days after instillation. Markedly induction of OGG1 mRNA in the lung at days 5 and 7 after instillation. Decreased 8-oxodG repair activity at days 1 and 2 after instillation	[208]
A-DEP by i.t. instillation (0.1–0.6 mg/mouse) in male ICR mice sacrificed 12 h later. Time-effects examined after i.t. instillation with 0.3 mg/mouse. Sacrificed after 3, 6, 12 h; 1, 2, 3, 5 and 7 days after exposure[b]	400 nm[c]	8-oxodG (HPLC-ECD)	Bell-shaped induction of 8-oxodG in the lung of mice killed 12 h after administration, with maximal effect observed in mice exposed to 0.3 mg (3.3-fold). In mice exposed to 0.3 mg, there was a gradual increase of 8-oxodG during the first 2 days and it then declined in the following time points. High baseline level of 8-oxodG (48 lesions/10^6 dG)	[117]
A-DEP by i.t. instillation once a week for 10 week (0.05, 0.1 and 0.2 mg/mouse) in male ICR mice and killed 24 h after the last instillation	400 nm[c]	8-oxodG (HPLC-ECD)	Dose-dependent increase in pulmonary 8-oxodG (statistically significant in mice i.t. administrated with 0.1 and 0.2 mg/mouse). High baseline level of 8-oxodG (30 lesions/10^6 dG)	[207]
A-DEP by i.t. instillation once a week for 10 weeks (0.1 mg/mouse) in ICR mice	400 nm[c]	8-oxodG (HPLC-ECD)	Increased 8-oxodG in the lung of mice (1.79-fold), whereas mice exposed to washed A-DEP had lower level of 8-oxodG generation in the lung (1.42-fold). High baseline level of 8-oxodG (40 lesions/10^6 dG)	[210]

(Continued)

Table VI. (*continued*)

Exposure	Size	Biomarker	Effect	References
A-DEP (500 μg/mouse) by i.t. instillation in male ICR mice and killed 24 h later	400 nm[c]	8-oxodG (IHC)	Increased staining in the lung of DEP-exposed mice and less staining in lung tissue of mice pre-treated with rosmarinic acid	[209]
A-DEP (1, 2.5 or 5 mg/mouse) by i.t instillation in male DDY mice and killed 24 h later	400 nm[c]	8-oxodG (HPLC-ECD)	Highest level of pulmonary 8-oxodG following 2.5 (3.15-fold) and 5 (2.56-fold) mg/mouse of DEP and probably no effect at 1 mg/mouse (1.23-fold).	[211]
A-DEP (2 mg/m^3) for 1 h/day on 10 days in female BALB/c mice sensitized with OVA	400 nm[c]	Lipid hydroperoxides (spectrophotometry)	Increased lipid peroxidation (2.9-fold) in DEP-exposed mice	[161]
Inhalation of SRM1650 as a single bout (1.5 h of 20 or 80 mg/m^3) or four bouts of 1.5 h of 5 or 20 mg/m^3 on 4 consecutive days in female Balb/CJ (DNA damage) and Muta^{TM}mice (mutation frequency)	18–30 nm (108 m^2/g)	8-oxodG (HPLC-ECD)	Elevated 8-oxodG in the lung at 80 mg/m^3 at 1 and 22 h after a single inhalation (20 mg/m^3 was not associated increased level of 8-oxodG). Unaltered levels of 8-oxodG in mice exposed to 4 × 1.5 h exposure to 5 and 20 mg/m^3	[212] [213]
SRM2975 (1.5-h inhalation exposure to 20 mg/m^3 on 4 consecutive days in C57BL/6 and *Ogg1*$^{-/-}$ mice	215 nm (91 m^2/g)[d]	8-oxodG (HPLC-ECD) and FPG sites (comet assay)	Increased 8-oxodG in the lung of *Ogg1*$^{-/-}$ mice; unaltered levels of FPG sites and 8-oxodG in the wild-type mice. Unaltered levels of 8-oxodG and FPG sites in the liver of DEP exposed mice. Unaltered OGG1 mRNA expression in the wild-type mice (OGG1 mRNA was not detectable in *Ogg1*$^{-/-}$ mice)	[214]
DE exposure (1 or 6 mg/m^3) for 4 weeks (12 h/day and 7 days/week) generated from a light-duty diesel engine in male BigBlue rats	Not reported	8-oxodG (HPLC-ECD)	Increased pulmonary 8-oxodG after exposure to 1 mg/m^3 (1.7-fold) and 6 mg/m^3 (2.2-fold). High baseline level of 8-oxodG (35 lesions/10^6 dG)	[215]
Diesel exhaust exposure (3.5 mg/m^3, 17 h/day, 3 days/week) for 1, 3, 6, 9 or 12 months generated by a light-duty diesel engine in female Fisher 344 rats	1.4–8.4 μm (peak: 2.2–2.8 μm)	8-oxodG (HPLC-ECD)	Elevated after 1 month (2.29-fold) and approximately the same after 3–12 months of exposure (3-fold). High baseline level of 8-oxodG (13 lesions/10^6 dG)	[116]
DE exposure (3 mg/m^3) for 4 weeks (12 h/day and 7 days/week) from a light-duty diesel engine in male *nrf2*$^{+-}$ and *nrf2*$^{-/-}$ mice	Not reported	8-oxodG (IHC)	Detection of 8-oxodG in *nrf2*$^{-/-}$ mice exposed to DE, whereas heterozygote mice had similar adduct level as non-exposed	[216]
Engineered nanomaterials				
C_{60} fullerenes by i.t. instillation (0.2–3 mg/rat)	160 nm	TBARS (spectrophotemetry)	Increased levels of lipid peroxidation products in bronchoalveolar fluid	[108]
MWCNT administered by pharyngeal aspiration (20 μg/mouse) with or without ozone exposure in female C57BL mice	20–30 nm (diameter) and up to 50 μm in length	8-isoprostanes and TBARS	Unaltered levels of 8-isoprostanes (serum) and TBARS (lung) at 17 and 36 h	[231]
SWCNT (99.7% elemental carbon) administered by pharyngeal aspiration (40 μg/mouse) in female C57BL mice	1–4 nm (diameter), 100–1000 nm (length) and 1040 m^2/g	MDA (with HPLC pre-purification)	Increased MDA in lung tissue 28 days after pharyngeal aspiration in mice on basal (1.9-fold) and vitamin E deficient (3.3-fold) diet	[230]
SWCNT (17.7% iron) inhalation exposure (5 mg/m^3) for 4 days (5 h/day) in female C57BL mice	0.8–1.2 nm (diameter) and 508 m^2/g	MDA (with HPLC pre-purification)	Increased MDA at day 1 after the last exposure (1.2-fold), which increased further on day 7 (1.3-fold) and day 28 (1.4-fold) after the exposure	[167]

[a] Obtained from Cakmak et al. [74].
[b] The investigation included parallel groups given normal diet, high-fat diet (16% corn-oil) and β-carotene containing diet (0.02 w/w). Only data from the normal diet are reported. The results from the high-fat diet suggest single-factor effects of DEP and fat, whereas mice fed concomitantly with β-carotene had lower induction of 8-oxodG.
[c] Obtained from Sagai et al. [100].
[d] Obtained from Saber et al. [279].

Table VII. Studies on non-pulmonary exposure to particulates in animal experimental models.

Exposure	Size	Biomarker	Effect	References
Diesel exhaust particles				
Single dose of SRM2975 (0.064 and 0.64 mg/kg bodyweight) and sacrificed 6 or 24 h later. Male Fischer 344 rats	215 nm (91 m^2/g)[a]	8-oxodG (HPLC-ECD)	Elevated levels of 8-oxodG in colon mucosa tissue, liver and lung at 0.64 mg/kg bodyweight at 6 and 24 h after administration. Increased *OGG1* mRNA levels in the lung 24 h after the administration	[217]
I.p. injection of SRM2975 (50, 500 or 5000 μg/kg). Sacrificed 6 or 24 h later. Female C57 or *ApoE*$^{-/-}$ mice	215 nm (91 m^2/g)[a]	FPG sites (comet assay)	Increased level of FPG sites in the liver 24 h after administration. No effect after 6 h. FPG sites in the aorta and lung tissue were unaltered after both time points	[204]
A-DEP administrated by oral gavage on five consecutive days at doses of 31.25, 62.5, 125 or 500 mg/kg/day in C57BL/6Jp^{un}/p^{un}	400 nm[b]	8-oxodG (HPLC-ECD)	No increase in 8-oxodG in embryos at 4 h (only 500 mg/kg bodyweight/day) or 2 days after exposure (31.25, 62.5, 125 or 500 mg/kg bodyweight/day). Baseline levels of 8-oxodG were ~ 15 lesions/10^6 dG	[219]
Dietary administration of SRM1650 (0.8 and 8 mg/kg) for 21 days. Male *Ogg1*$^{-/-}$ and wt mice	18–30 nm (108 m^2/g)	8-oxodG (HPLC-ECD) and ENDOIII and FPG sites (comet assay)	Unaltered levels of oxidatively damaged DNA in colon, liver and lung of both *Ogg1*$^{-/-}$ and wild type mice. Unaltered expression level of *Ogg1* in the colon and lung (the liver was not analysed)	[220]
Dietary administration of SRM1650 (0.2, 0.8, 2, 8, 20, 80 ppm) for 21 days in Male Big Blue Fischer rats	18–30 nm (108 m^2/g)	8-oxodG (HPLC-ECD, MDA (HPLC-ECD) and ENDOIII and FPG sites (comet assay)[b]	Unaltered 8-oxodG in the colon mucosa, liver and urine. Bell-shaped concentration-response curves for ENDOIII and FPG sites in the lung (statistically significant at 8 ppm). Unaltered plasma concentration in plasma	205–206
Two-way factorial study of dietary administration of SRM2975 in the feed (0.08 ppm) with low or high sucrose content (3.45% vs 6.85% w/w sucrose) for 21 days in male Big Blue Fischer rats.	215 nm (91 m^2/g)[a]	8-oxodG (HPLC-ECD), ENDOIII and FPG sites (comet assay)	Unaltered 8-oxodG, ENDOIII and FPG sites in the colon mucosa and liver tissue	[221]
Engineered nanomaterials				
Single dose of C_{60} fullerenes (0.064, 0.64 mg/kg) suspended in corn oil or saline. Sacrifice 6 or 24 h after. Male Big Blue Fischer rats	< 20 m^2/g	8-oxodG (HPLC-ECD)	Increased 8-oxodG in the liver (max: 1.25-fold) and lung (max: 1.20-fold), whereas the level of 8-oxodG was unaltered in the colon mucosa tissue	[68]
Single dose of SWCNT (0.064, 0.64 mg/kg) suspended in corn oil or saline. Sacrifice 6 or 24 h after in Male Big Blue Fischer rats	731 m^2/g	8-oxodG (HPLC-ECD)	Increased 8-oxodG in the liver (max: 1.25-fold) and lung (max: 1.23-fold), whereas the level of 8-oxodG was unaltered in the colon mucosa tissue	[68]

[a]Obtained from Saber et al. [279].
[b]Obtained from Sagai et al. [100].

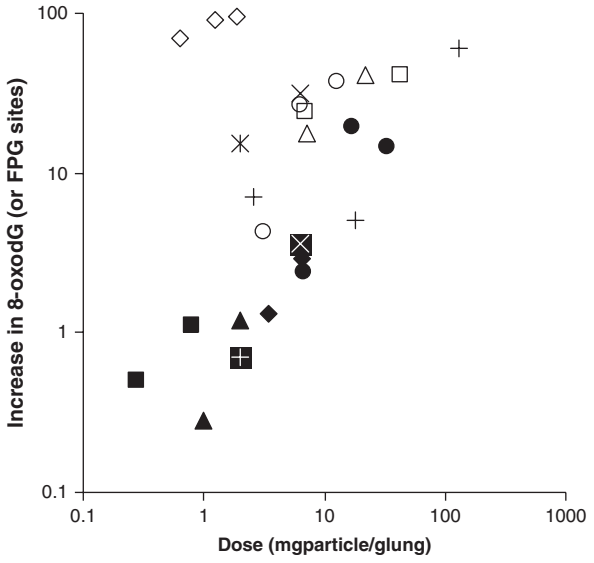

Figure 6. Generation of 8-oxodG or FPG sites in lung tissue of animals by pulmonary exposure. Solid and open symbols indicate studies that have reported levels of 8-oxodG in control groups that were below and above 10 lesions/106 dG, respectively. The doses of particles are reported as mg/g lung weight, based on calculations and assumption reported earlier [236]. The level of FPG sites have been calculated from the primary comet assay endpoint and assuming that 1% DNA in the tail corresponds to 111 lesions per diploid cells that contains 6 3 109 basepairs and 22% of the bases are guanines as reported previously [295]. The symbols refer to studies as follows: solid triangle [212], solid square [164], solid diamond [208], solid circle [211], open circle [207], open triangle [116], open diamond [117], cross [210], solid square with plus [218], solid square with cross [210], plus [40] and askers [203]. There is a linear relationship between the dose and generation of 8-oxodG (r 5 0.78, p , 0.001 linear regression analysis) after excluding one study showing very high baseline level of 8-oxodG in unexposed animals (48 lesions/106 dG [117]).

Figure 6 provides an analysis of the potency of different particulates to generate 8-oxodG in lung tissue by pulmonary exposure. An overall comparison of the studies for the purpose of comparing the potency of different particulates is hampered because of problems in the methodology of some of the endpoints. Results from the European Standards Committee on Oxidative Damage to DNA (ESCODD) suggested that publications reporting levels of 8-oxoGua in DNA, which exceeded 5 lesions/10^6 dG in baseline samples should be interpreted with caution [234]. We have previously used 10 lesions/10^6 dG as a cut-off value in assessment of the associations between the level of DNA damage and exposure to air pollution or dietary intake of antioxidants [235,236]. The cut-off was chosen because the ESCODD threshold was established on data of lymphocytes from young healthy humans and analysis of pig liver samples by ESCODD partner laboratories indicated a median of about 10 lesions/10^6 dG [234,237,238]. The investigations included in Figure 6 have been stratified into publications reporting levels of 8-oxodG that were lower or higher than the threshold of 10 lesions/10^6 dG. As can be seen, there appears to be a linear relationship, suggesting that the different types of particulates generate a similar level of 8-oxodG on mass basis, although it is also clear that those studies with high baseline levels of 8-oxodG have reported the largest generation of 8-oxodG as an effect of exposure.

The relationship between the duration and dose of exposure has been investigated in a few studies. It was shown that a single inhalation exposure of a large concentration of SRM1650 was associated with increased 8-oxodG, whereas the same dose administered as four low-concentration inhalation exposures on 4 consecutive days was associated with increased expression of 8-oxo-guanine DNA glycosylase 1 (OGG1) and unaltered 8-oxodG in lung tissue [212]. In *Ogg1*$^{-/-}$ mice, this exposure was associated with increased 8-oxodG, indicating a strong effect modification of OGG1-mediated DNA repair [214]. Among the oxidatively generated DNA base lesions, 8-oxoGua has been of special interest because it is abundant in the genome of mammalian cells and it is pro-mutagenic [239]. However, despite increased generation of 8-oxodG by SRM1650, inhalation exposures associated with elevated levels of 8-oxodG have not been associated with elevated mutant frequency in the Muta-Mouse model (Table VIII), which may be due to the insufficient follow-up period or importance of the gaseous phase [213]. It should be noted that exposure to DE was associated with increased 8-oxodG, elevated mutant frequency and altered mutation spectrum in mice [215]. These differences in the mutagenicity are intriguing because both exposures gave rise to 8-oxodG and PAH-related bulky DNA adducts, suggesting that the differences cannot be explained by a different content of PAH compounds, although there were most likely different concentrations of other organic compounds and exhaust gasses were part of the exposure only in the study on DE [215]. Studies on the pulmonary exposure to quartz also suggest that the relationship between DNA damage and mutations is not straight forward. Cell culture studies have shown both increased mutagenicity by quartz [240,241] and unaltered effect on mutant frequency even after long periods of exposure [189,242]. On the other hand, pulmonary exposure to quartz was associated with increased mutant frequency in type II alveolar cells [242] and increased expression of mutated p53 protein in lung cells [199]. However, studies on pulmonary exposure of quartz suggest that the most consistent increase in 8-oxodG levels appears months after the exposure and might be ascribed to persistent inflammation or tissue injury [198–202,218]. The studies on carbon black suggest that the particle size is an important determinant of the genotoxicity; Printex 90, which has a primary particle size of 14 nm, generated 8-oxodG, whereas Printex 25 (56 nm) and Sterling V (70 nm), with larger sizes, did not [40,228]. In this respect, it is

Table VIII. Association between exposure to particulates and mutant frequency in animal models and cultured mammalian cells.[a]

Particulate	Cultured cells	Animals
Silica	• Unaltered in rat lung epithelial RLE-6TN cells exposed to quartz [242] • Unaltered in mouse FE1-MML cells exposed to SRM1878a quartz [189] • Concentration-dependent increase in WIL2-NS human B-cell lymphoblastoid cells exposed to ultrafine silicon dioxide [240] • Concentration-dependent increase in HPRT mutants WIS-NS human B-cell lymphoblastoid cells exposed to Min-U-Sil 5 quartz [241]	• Increased HPRT mutations in alveolar type II cells after i.t. instillation of α-quartz [242] • Increased expression of mutated p53 protein in lung cells detected by whole lung immunostaining after exposure to DQ12 [199]
TiO_2	• Unaltered in rat lung epithelial RLE-6TN cells [242] • Concentration-dependent increase in WIL2-NS human B-cell lymphoblastoid cells ultrafine TiO_2 [280] • Increased kilo-base pair deletion mutations [122]	• Increased HPRT mutations in alveolar type II cells after i.t. instillation to analtase TiO_2 [242]
Carbon black	• Unaltered in rat lung epithelial RLE-6TN cells [242] • Increased in mouse FE1-MML cells exposed to Printex 90 [189] • Unaltered in the L5178Y mouse lymphoma assay when cells were exposed to N-339 carbon black [243]	• Increased HPRT mutations in alveolar type II cells after i.t. instillation to ultrafine Monarch 900 [242]
Diesel exhaust (particles)	• Unaltered 6-thioguanine-resistant gene mutation in V79 cells exposed to particulates collected from a diesel engine [281] • Increased in mouse FE1-MML cells exposed to SRM1650a [102] • increased in a human-hamster hybrid cell line exposed to SRM2975 [282]	• Concentration-dependent increased mutant frequency (and mutation spectrum) in *lacI* of BigBlue rat lung tissue after inhalation [215] • Unaltered mutant frequency in *cII* of lung tissue of BigBlue rats ingesting SRM1650 for 21 days [206] • Unaltered mutant frequency in *cII* of BigBlue rats in colon mucosa cells and liver after ingestion of SRM1650 for 21 days [221] • Decreased *cII* mutant frequency in lung tissue of MutaMouse after a single inhalation exposure of SRM1650 (20 mg/m^3) whereas a higher concentration (80 mg/m^3) and repeated exposures did not alter the mutant frequency [213]
C_{60} fullerenes	• Unaltered in mouse FE1-MML cells [66] • Increased kilo-base pair deletion mutations [122]	• Not reported
Carbon nanotubes	• Unaltered in mouse FE1-MML cells exposed to SWCNT [66] • Increased APRT mutant frequency in mouse embryonic stem cells [283]	• Increased K-ras mutations in lung tissue inhalation and pharyngeal aspiration of SWCNT [167]

[a] Wood smoke particles are not included in the table because there are no studies on the mutagenicity in mammalian cells.

interesting that cell culture experiments have shown increased levels of ROS production, FPG sites and mutant frequency after exposure to Printex 90 [189]. Carbon black with larger primary particle size did not increase the mutagenicity in cultured cells [242,243], although increased mutagenicity was observed in type II alveolar cells of rats exposed to ultrafine carbon black by i.t. instillation [242].

Exposure to PM by inhalation is mainly considered to be a pulmonary problem, but it should be kept in mind that deposition of particulates gives rise to gastrointestinal exposure because most particles are removed from the surface of the epithelium by the mucociliary escalator and swallowed [18,244]. Therefore the gastrointestinal exposure route is highly relevant for a range of inhalable particles, but also for engineered nanomaterials which are added to dietary products directly or used in composite wrapping materials. Table VII outlines the studies on the effect of extra-pulmonary exposure to particulates. It has been shown that gastrointestinal exposure to SRM2975, C_{60} fullerenes and SWCNT were associated with elevated levels of 8-oxodG in the lung and liver, whereas only SRM2975 generated elevated levels of 8-oxodG in colon mucosa cells [68,217]. Another study showed an increased level of FPG sites in the liver following intra-peritoneal injection of SRM2975 in dyslipidemic *ApoE*$^{-/-}$ mice, whereas there was no effect in the aorta and lung tissue, which could be due to the route of exposure [204]. In another study, the level of 8-oxodG was unaltered in embryos at 4 h or 2 days post-exposure after the mothers had been exposed to DEP by oral gavage [219]. Studies of longer exposure periods have incorporated the particulates in the feed. The effect of oral SRM1650 exposure was investigated in a study of male BigBlue rats. Particulates were administered in the diet for 21 days and increased levels of FPG sites were observed in lung [206], whereas the regulation of *Ogg1* was unaltered. There were unaltered levels of 8-oxodG and increased strand breaks and *Ogg1* mRNA expression in the liver and colon mucosa tissue, as well as unaltered urinary excretion of 8-oxodG and plasma concentration of MDA [205]. Interestingly, the DEP exposure did not result in induction of mutations in either liver, lung or colon mucosa cells (Table VIII) [205,206]. A subsequent study with the same design but a different type of DEP (SRM2975) showed that the plasma concentration of MDA was unaltered, 8-oxodG and FPG sites were unaltered in the colon mucosa and liver, whereas the expression level of *Ogg1* was increased in the liver, but not in the colon, and the mutation frequency was not increased [221]. These data suggest an association between increased OGG1 repair activity and unaltered levels of oxidative damage to DNA, but it should be emphasized that a study in *Ogg1*$^{-/-}$ mice, exposed to SRM1650 through the diet for 21 days, did not show accumulation of 8-oxodG, ENDOIII or FPG sites in the colon, liver and lung tissue [220]. This might be due to differences in species; mice might be less susceptible than rats to oxidative effects of particulates when exposed via the diet. Collectively, the data from the investigations of non-pulmonary exposure support the findings from the studies of inhalation exposure to particles, showing that short-term exposure is associated with increased levels of oxidized DNA lesions and lipid peroxidation products, whereas prolonged exposure periods could be associated with increased activity of the DNA repair system.

Association between exposure to particulates and oxidatively damaged biomolecules in human biomonitoring studies

Investigations of the effect of particulates in humans encompass biomarker-based biomonitoring studies and epidemiological studies on hard endpoints such as cardiovascular diseases and cancer in subjects exposed in occupational settings and urban air. These types of studies serve as excellent platforms investigating the association between exposure to particulates, oxidative stress and hard endpoints, although they do not provide firm conclusions regarding the association between biomarkers of oxidized DNA and lipids and disease endpoints. In fact, there is lack of information about the predictive value of most biomarkers of oxidative stress, which can only be firmly assessed in prospective studies [194,232,245]. Urinary excretion of 8-oxodG and the concentration of TBARS in plasma are among the few biomarkers that have been studied in prospective cohort studies; they have predictive value in regards to development of lung cancer and cardiovascular diseases, respectively [246–249].

The biological effect of particulates is difficult to measure in target tissue of humans because of ethical reasons and most of the research is therefore carried out on surrogate tissue cells such as blood cells (e.g. leukocytes, mononuclear blood cells or lymphocytes) or urine. Table IX outlines a number of studies that have assessed the exposure of air pollution particles in terms of oxidative damage to DNA in blood cells or urine; there is to the best of our knowledge no published biomonitoring studies on nanoparticle exposure containing data on oxidatively damaged DNA and lipids. In keeping with the general consideration about methodological problems of biomarkers of oxidatively damaged DNA, it should be recognized that some of these studies have problems with high levels of 8-oxodG, suggesting spurious oxidation of the samples [250,251]. In addition, the design of the biomonitoring studies is crucial for the interpretation of the results; especially the effect of confounding variables is important. It should be emphasized that some studies have shown that the comet assay detects DNA damage that

Table IX. Studies on exposure to particulates in humans.

Subjects	Exposure assessment	Effects	References
Air pollution particles			
98 police men and 105 controls (e.g. office clerks). Prague, Czech Republic and Kosice, Slovak Republic	Concentration of polycyclic aromatic hydrocarbons in personal $PM_{2.5}$ samples	Higher 8-oxodG level in lymphocytes of policemen in Kosice compared to controls, whereas no effect in policemen from Prague. Levels of 8-oxodG were very high (i.e. 53.6 lesions/10^6 nucleotides, corresponding to 244 lesion/10^6 dG)	[255]
41 non-smoking men (36 ± 5 yr)	Urban air pollution in Cotonou and a rural village (Republic of Benin)	Higher level of oxidized DNA in taxi drivers (20.5 8-oxodG/10^6 dG) compared to controls in a rural village (11.1 8-oxodG/10^6 dG)	[251]
135 non-smoking men (34 ± 10 yr)	Population in Benin, incl. inhabitants in a rural village (6961 particles/cm^3), and three groups living in Cotonou, incl. suburban (19980 particles/cm^3), and dense traffic (> 200 000 particles/cm^3)[a]	Gradient in FPG sites in mononuclear blood cells as follows: 0.11 FPG sites/10^6 bp (rural), 0.19 FPG sites/10^6 bp (people living in the suburb), 0.21 FPG sites/10^6 bp (people living near roads with heavy traffic) and 0.27 FPG sites/10^6 bp (taxi-motodrivers)	[256]
50 students (20–33 yr) living in the centre of Copenhagen	Personal $PM_{2.5}$ exposure and stationary monitoring station concentrations of PM	Correlation between personal exposure to $PM_{2.5}$ and 8-oxodG content in lymphocytes and MDA in plasma (only women), whereas there were no correlations between $PM_{2.5}$ mass concentration and FPG sites in lymphocytes or 24-h urinary excretion of 8-oxodG. No correlation between biomarkers and stationary (urban background) measurements of $PM_{2.5}$	[266,273]
15 non-smokers (25 ± 3 yr)	Bicycling in Copenhagen (32 400 particles/cm^3) or indoor (13 400 particles/cm^3)[a]	Increased level of FPG sites after cycling in the traffic (0.08 FPG sites/10^6 bp) compared to cycling in the laboratory (0.02 FPG sites/10^6 bp)	[274]
29 non-smokers (20–40 yr)	Normal air (6169–15 362 particles/cm^3) or filtered air (91–542 particles/cm^3)[b]	Filtered air was associated with lower levels of FPG sites in mononuclear blood cells (0.38 FPG sites/10^6 bp) compared to normal air (0.53 FPG sites/10^6 bp)	[275]
57 non-smokers (45 ± 8 yr)	Urban air pollution exposure among bus drivers in the city centre or rural/suburban area at the day of work and a day off	Bus drivers in the city centre had higher level of urinary 8-oxodG excretion as compared to bus drivers from the rural/suburban area, whereas clear differences between urinary excretions a working days and a day off was not observed. Unaltered MDA in plasma between bus drivers in the city centre and rural/suburban area	[261,268]
Cross-sectional study of 47 female highway toll station workers (26 ± 6 yr) and 27 controls (27 ± 5 yr) consisting of females training to become toll station workers	Exposure assessed as average exposure to vehicles/h and urinary 1-hydroxypyreneglucuronide excretion	Highway toll workers had higher spot urinary 8-oxodG excretion (antibody-based detection) at the end of the workday than the controls	[250]
50 male non-smoking bus drivers and controls	Stationary sampling of $PM_{2.5}$ and PM_{10} at two locations in Prague with heavy and light traffic	Higher urinary excretion of 8-oxodG (antibody-based detection) and 15-F_{2t}- isoprostanes among bus drivers compared to controls	[259,262, 265]
95 male taxi drivers and 75 controls (community subjects) in Taipei city, Taiwan	Urinary 1-hydroxypyrene excretion	Higher spot morning urinary excretion of 8-oxodG (antibody-based) among taxi drivers compared to controls and a positive correlation between 1-hydroxypyrene and 8-oxodG	[260]
City policemen from different districts of Prague, Czech Republic	$PM_{2.5}$ (stationary monitoring stations)	Higher levels of FPG and ENDOIII sites in lymphocytes from exposed policemen	[258]
Panel study of 107 children (9.5 ± 2.1 yr) with asthma, Mexico City	$PM_{2.5}$, O_3 and NO_2 (stationary monitoring stations)	Positive association between ambient $PM_{2.5}$ levels and concentration of MDA in exhaled breath	[270]
25 subjects with diabetes mellitus (28–63 yr)	Personal PM_{10} samplers	Positive association between personal PM_{10} levels and the concentration of TBARS in plasma	[267]
Children (6–11 yr) living in areas of low (Prachatice) and high (Teplice) exposure (Czech republic) (n = 894)	Stationary monitoring station concentrations of $PM_{2.5}$ and PM_{10}	Positive association between air pollution exposure and urinary excretion of 8-oxodG (antibody-based detection) in Teplice, whereas there the same association was statistically non-significant in children from Prachatice	[269]

(Continued)

Table IX. (*continued*)

Subjects	Exposure assessment	Effects	References
Male subjects with stable coronary heart disease and controls	Two hours exposure to CAPs or filtered air	Increased 8-isoprostane concentration in exhaled breath by CAPs exposure	[272]
Children (n = 75, 9–13 yr) living in an rural and urban area of Thailand	Benzene	Increased level of 8-oxodG in leukocytes and urine (HPLC-ECD)	[257]
Subjects in a rural and urban area of Mexico	PM_{10} and ozone (stationary monitoring station)	Increased level of plasma TBARS in subjects living in Mexico City	[264]
Subjects living in areas of high (Los Angeles) and low (San Francisco Bay Area) pollution, USA	PM_{10}, ozone, NO_2 (stationary monitoring stations)	Increased plasma 8-isoPGF in subjects living in the most polluted area	[263]
Wood smoke particles			
28 women exposed to residential biomass smoke and 15 reference subjects (31–63 yr)	None	Increased serum concentration of TBARS (spectrophotometric assay) in woman exposed to biomass smoke as compared to reference subjects (3.2 vs 1.5 nmol/ml, respectively)	[276]
13 subjects exposed to wood smoke (20–56 yr) for 4 h	$PM_{2.5}$ and ultrafine particles	Increased urinary excretion of 8-iso-PGFα (2.3-fold) and MDA levels in exhaled breath	[271,277]

[a] The number concentration (particles/cm^3) is measured with a condensation particle counter (TSI 3007) that detects particles in the 10–100 nm range.
[b] The number concentration (particles/cm^3) is measured with a custom built differential-mobility particle sizer apparatus that detects particles in the 6–700 nm range.

displays seasonal variation [252–254]. Problems with the experimental design and/or confounding can result from attempts of providing gradients in the exposure levels. Studies that are designed to detect differences between a group of exposed subjects relative to a reference group or temporal (seasonal) differences in exposure and oxidative stress have shown increased level of oxidatively damaged DNA in leukocytes [251,255–258], urinary excretion of 8-oxodG [257,259–262] and plasma lipid peroxidation products [263–267], although one study showed no effect of MDA in plasma of bus drivers working in the city centre as compared to drivers working in the rural/suburban areas [268]. A very large study on urinary excretion of 8-oxodG from children in the Czech Republic showed only a positive association in samples collected from children in the most polluted area, whereas there was a difference in 8-oxodG excretion between this location and children living in the less polluted area [269]. In a different design there was an increased urinary excretion in post-shift spot urine samples of female highway toll workers compared to a reference group consisting of females training to become toll station workers [250]. Some studies have also shown associations between exposure to PM and lipid peroxidation products in exhaled breath [270–272].

The exposure characterization in biomonotoring studies encompass data obtained from stationary monitor stations and personal monitors, including concentration of PAH or mass concentration of particles (e.g. the $PM_{2.5}$ fraction) as markers of air pollution or biomarkers of air pollution components such as PAH metabolites. Sampling of personal exposure data obviously requires a more demanding experimental set-up because it is important to follow the subjects over time and the sampled air pollution constituents should be representative of the emission. Using this approach of personal exposure characterization, it has been shown that students living in the central area of Copenhagen had a positive correlation between personal exposure to $PM_{2.5}$ (mass concentration) and the level of 8-oxodG in lymphocytes, whereas the exposure did not correlate with the level of FPG sites in lymphocytes or urinary excretion of 8-oxodG [273]. Later studies with focus on controlled exposure to ultrafine traffic-generated air pollution particles showed that healthy humans bicycling for ~ 90 min in the laboratory or in the most traffic-intense streets of Copenhagen had the highest levels of FPG sites in mononuclear blood cells after the bicycling in the traffic as compared to the laboratory [274]. In a subsequent experiment, air from a traffic-intense street in Copenhagen was sucked into a chamber with or without filtering the particulate fraction; it was shown that reducing the exposure to ultrafine particles by filtering the air was associated with lower levels of FPG sites in mononuclear blood cells [275]. Interestingly, similar experiments with exposure to wood smoke, containing very high mass concentration of particles, indicated increased levels of lipid peroxidation products in serum and urine [276,277], whereas no clear association was observed with respect to oxidatively damaged DNA in mononuclear blood cells, which could be due to low statistical power [278].

Concluding remarks

Various types of particulates are able to both generate ROS (Table II) and oxidize lipids and DNA (Table III) in an acellular environment. These data suggest that particles have a direct oxidizing ability that most likely arises from both surface-mediated reactions (e.g. quartz) and leakage of transition metals and redox-active quinone substances (e.g. air pollution particles). There is also compelling evidence from studies in cultured cells that particles generate ROS (Table IV and Figure 3) and oxidize biomolecules such as lipids and DNA (Table V and Figure 4). Carbon black, air pollution particles and DEP generates higher level of ROS and strand breaks in cultures cells on the same mass basis as compared to silica, TiO_2 and CNT, whereas exposure to wood smoke particles and C_{60} fullerenes is associated with the lowest level of ROS generation and strand breaks. In keeping with the importance of the surface area, it would have been interesting to rank the particles according to this metric. One of the major caveats in regard to the DNA damaging ability is the numerous reports that particles seem not to be present in the nuclei of the cells. This could imply that particles do not need to be present at the site of injury and that the effect is mediated by leached substances or stable ROS generated at the surface of particles. In addition, cellular exposure to some type of particulates inflicts upon normal mitochondrial function, which may lead to excess generation of ROS by the electron transport chain. In intact organisms, ROS production from inflammation induced by particulates can also contribute. The data from animal experimental models are too few to determine whether some type of particles are more potent in generating oxidative damage to DNA. However, the data outlined in Figure 4 indicate a relationship between the mass of particles and net increase in oxidative damage in lung tissue, although the particles have different primary particle size.

Figure 7 outlines an overall analysis where we have assessed whether particles produce the same effect in experimental systems detecting different aspects of oxidative stress. The figure encompasses oxidizing ability in acellular conditions (Tables II and III), intracellular ROS generation (Table IV), oxidatively damaged DNA and lipids in cultured cells (Table V) and oxidatively damaged DNA and lipids in animal experiments (Tables VI and VII). The results were regarded as either showing positive or null effect; the type of particles

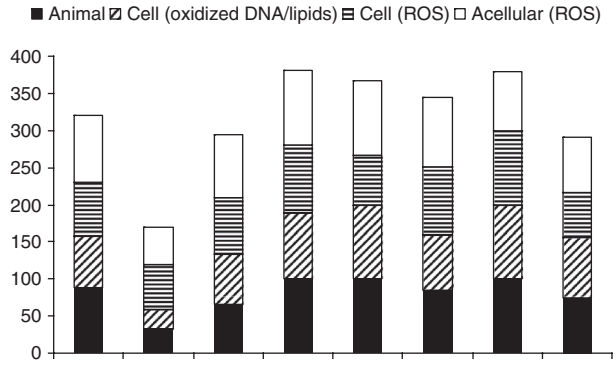

Figure 7. Associations between exposure to silica (Sil), titanium dioxide (TiO2), carbon black (CB), air pollution particles (APP), wood smoke particles (WSP), diesel exhaust particles (DEP), C60 fullerenes (C60) or carbon nanotubes (CNT) particles and oxidative damage in acellular conditions, cells and animal tissues. The columns represent the number of studies having shown increased level of oxidative damage in acellular conditions (cf. Tables II and III), intracellular ROS (cf. Table IV), intracellular oxidized biomarkers (cf. Table V) and animal experimental models (cf. Tables VII and VIII). The studies have been classified as showing positive effect or null effect. Acellular studies showing positive effect: silica [48–50,74,76–80], TiO_2 [69,70], carbon black [41,65–68], air pollution particles [60,81–94,96–98,113–115,140], wood smoke particles [85,98,103,104], DEP [68,73,83,85,97,98,100,102,113,116–118], C60 fullerenes [66,68,106–109,119,120], CNT [66,68,111]. Acellular studies showing null effect: silica [81], TiO_2 [56,72,73] carbon black [52], DEP [52], C60 fullerenes [105,110], CNT [78]. Studies on intracellular ROS showing positive effect: silica [51,77,80,125,151,153–155], TiO_2 [56,71, 122,142,143,156,159,160], carbon black [58,65–67,123–128], air pollution particles [95,127,131,132,134–140], wood smoke particles [104,142], DEP [101,102,127,129–132,141–145], C60 fullerenes [66,107,121,122], CNT [66,124–126,142,146–148]. Studies on intracellular ROS showing null effect: silica [124,136,152], TiO_2 [58,138,149,157,158], carbon black [129–131], air pollution particles [133], wood smoke particles [133], DEP [133], CNT [59,111,143,149,150]. Studies on intracellular oxidized biomolecules showing positive effect: silica [50,125,153,186–188], TiO_2 [193], carbon black [125,189], air pollution particles [86,93,113–115,171,190,191], wood smoke particles [103,104,171], diesel exhaust particles [113,161,171], C60 fullerenes [66,107,121,185], CNT [66,111,125,147]. Studies on intracellular oxidized biomolecules showing null effect: silica [57,189], TiO_2 [72,149,192], carbon black [52], DEP [52], CNT [149]. Animal experimental models showing positive effect: silica [197–203], TiO_2 [226], carbon black [40,228], air pollution particles [204,206,217,225], DEP [116,117,161,164,207–213,215,216], wood smoke particle [165,166], C_{60} fullerenes [68,108], CNT [68, 167,230]. Animal experimental models showing null effect: silica [108,218], TiO_2 [201,210], carbon black [229], air pollution particles [219–221], CNT [231]. The statistical analysis showed that the occurrence of effect, test system and particle type is mutually dependent ($\chi^2 = 81.3$; $\chi^2_{0.01,\,52} = 78.6$). The post-hoc breakdown analysis showed that the occurrence of test system depends on type of particle and effect ($\chi^2 = 54.2$; $\chi^2_{0.05,\,45} = 61.7$) and the effect depends on the test system and type of particle ($\chi^2 = 40.8$; $\chi^2_{0.05,\,31} = 45.0$), whereas the type of particle that have been investigated does not depend on the type of detection system and effect (c2 = 75.3; $\chi^2_{0.01,\,49} = 74.9$).

were stratified into silica, TiO_2, carbon black, air pollution particles, wood smoke particles, DEP, C_{60} fullerenes and CNT (the details of the statistical design, results and interpretation are described in the legend text of Figure 7). Overall, the analysis shows mutual dependency of the reported effect, test system that has been used and the types of particles that have been tested. The analysis has two important implications: (1) the effect, which has been reported, depends on both the types of particles being tested and the type of test system; and (2) the detection system that has been used depends on the types of particles that have been tested and the effect. As for the first conclusion, it implies some types of particles (especially TiO_2) are more likely to show null effect than other types of particles (air pollution particles, wood smoke particles, DEP and C_{60} fullerenes). The second implication indicates a propensity of researchers to study effects on some types of particles with detection systems that provide some type of result. This is clearly visualized by the high number of studies on air pollution particles and DEP that have reported increased ROS generation and oxidized biomolecules in acellular conditions and cultured cells. Furthermore, the reasonable concurrence of results from all four levels of experimental complexity support the use of simple acellular and cellular assays for ROS production as an early screening of potential hazards related to oxidative damage to DNA from particulates. Moreover, the concurrence could also suggest that direct ROS production may be more important for this endpoint than indirect ROS production from for instance inflammation.

The studies of oxidative stress effects in humans are less abundant than the studies on acellular and cellular model systems as well as animal experimental models. Still, the data from combustion particles indicate that environmental exposure to particulates is associated with increased biomarker levels of oxidative damage in leukocytes, plasma and urine. This is interesting considering that animals and humans are evolutionarily adapted to deal with particulates in epithelium with large surface area, designed for transmembrane passage of molecules, such as the lung epithelium and gastrointestinal tract. The defense barriers that protect against biological pathogens seem to play a pivotal role in the removal of particulates. However, intense exposures may overwhelm the defense systems, especially in vulnerable subjects such as the elderly and patients with respiratory and cardiovascular diseases. Based on the analogy shown in Figure 7, it must be expected that humans exposed to engineered nanomaterials could have higher levels of oxidatively damaged DNA and lipids.

Acknowledgements

The authors are supported by grants from the Danish Research Councils.

***Declaration of interest*:** The authors report no conflict of interest. The authors alone are responsible for the content and writing of the paper.

References

[1] Castranova V, Vallyathan V. Silicosis and coal workers' pneumoconiosis. Environ Health Perspect 2000;108(Suppl 4):675–684.

[2] Nemery B, Hoet PH, Nemmar A. The Meuse Valley fog of 1930: an air pollution disaster. Lancet 2001;357:704–708.

[3] Bell ML, Davis DL, Fletcher T. A retrospective assessment of mortality from the London smog episode of 1952: the role of influenza and pollution. Environ Health Perspect 2004;112:6–8.

[4] Brunekreef B, Holgate ST. Air pollution and health. Lancet 2002;360:1233–1242.

[5] Mauderly JL, Snipes MB, Barr EB, Belinsky SA, Bond JA, Brooks AL, Chang I-Y, Cheng YS, Gillett NA, Griffith WC, Henderson RF, Mitchell CE, Nikula KJ, Thomassen DG. Pulmonary toxicity of inhaled diesel exhaust and carbon black in chronically exposed rats - Part I: neoplastic and nonneoplastic lung lesions. HEI Res Report 1994;68:1–75.

[6] Heinrich U, Fuhst R, Rittinghausen S, Creutzenberg O, Bellmann B, Koch W, Levsen K. Chronic inhalation exposure of Wistar rats and two different strains of mice to diesel engine exhaust, carbon black, and titanium dioxide. Inhal Toxicol 1995;7:533–556.

[7] Nikula KJ, Snipes MB, Barr EB, Griffith WC, Henderson RF, Mauderly JL. Comparative pulmonary toxicities and carcinogenicities of chronically inhaled diesel exhaust and carbon black in F344 rats. Fundam Appl Toxicol 1995;25:80–94.

[8] Baan RA. Carcinogenic hazards from inhaled carbon black, titanium dioxide, and talc not containing asbestos or asbestiform fibers: recent evaluations by an IARC Monographs Working Group. Inhal Toxicol 2007;19(Suppl 1):213–228.

[9] Takagi A, Hirose A, Nishimura T, Fukumori N, Ogata A, Ohashi N, Kitajima S, Kanno J. Induction of mesothelioma in p53+/– mouse by intraperitoneal application of multi-wall carbon nanotube. J Toxicol Sci 2008;33:105–116.

[10] Poland CA, Duffin R, Kinloch I, Maynard A, Wallace WAH, Seaton A, Stone V, Brown S, MacNee W, Donaldson K. Carbon nanotubes introduced into the abdominal cavity of mice show asbestos-like pathogenicity in a pilot study. Nature Nanotechnol 2008;3:423–428.

[11] Vesterdal LK, Folkmann JK, Jacobsen NR, Sheykhzade M, Wallin H, Loft S, Møller P. Modest vasomotor dysfunction induced by low doses of C_{60} fullerenes in apolipoprotein E knockout mice with different degree of atherosclerosis. Part Fibre Toxicol 2009;6:5.

[12] Li Z, Hulderman T, Salmen R, Chapman R, Leonard SS, Young SH, Shvedova A, Luster MI, Simeonova PP. Cardiovascular effects of pulmonary exposure to single-wall carbon nanotubes. Environ Health Perspect 2007;115:377–382.

[13] Nel A, Xia T, Madler L, Li N. Toxic potential of materials at the nanolevel. Science 2006;311:622–627.

[14] Ayres JG, Borm P, Cassee FR, Castranova V, Donaldson K, Ghio A, Harrison RM, Hider R, Kelly F, Kooter IM, Marano F, Maynard RL, Mudway I, Nel A, Sioutas C, Smith S, Baeza-Squiban A, Cho A, Duggan S, Froines J. Evaluating the toxicity of airborne particulate matter and nanoparticles by measuring oxidative stress potential - a workshop report and consensus statement. Inhal Toxicol 2008;20:75–99.

[15] Donaldson K, Stone, V, Clouter A, Renwick L MacNee W. Ultrafine particles. Occup Environ Med 2001;58:211–216.

[16] Shimada A, Kawamura N, Okajima M, Kaewamatawong T, Inoue H, Morita T. Translocation pathway of the intratracheneally instilled ultrafine particles from the lung into the blood circulation in the mouse. Toxicol Pathol 2006;34:949–957.

[17] Mühlfeld C, Geiser M, Kapp N, Gehr P, Rothen-Rutishauser B. Re-evaluation of pulmonary titanium dioxide nanoparticle distribution using the 'reactive deposition inden': evidence for clearance through microvasculature. Part Fibre Toxicol 2007;4:7.

[18] Oberdörster G, Sharp Z, Atudorei V, Elder A, Gelein R, Lunts A, Kreyling W, Cox C. Extrapulmonary translocation of ultrafine carbon particles following whole-body inhalation exposure of rats. J Toxicol Environ Health A 2002;65:1531–1543.

[19] Carr KE, Hazzard RA, Reid S, Hodges GM. The effect of size on uptake of orally administered latex microparticles in the small intestine and transport to mesenteric lymph nodes. Pharm Res 1996;13:1205–1209.

[20] Kreyling WG, Semmler M, Erbe F, Mayer P, Takenaka S, Schulz H, Oberdörster G, Ziesenis A. Translocation of ultrafine insoluble iridium particles from lung epithelium to extrapulmonary organs is size dependent but very low. J Toxicol Environ Health A 2002;65:1513–1530.

[21] Smyth SH, Feldhaus S, Schumacher U, Carr KE. Uptake of inert microparticles in normal and immune deficient mice. Int J Pharm 2008;346:109–118.

[22] Lwin S, Isoshima Y, Ueno H, Ishiguro N. Uptake and transport if foreign particles in Peyer's patches of both distal and ileum and jejunum of calves. Cell Tissue Res 2009;337:125–135.

[23] Mills NL, Amin N, Robinson SD, Anand A, Davies J, Patel D, de la Fuente JM, Cassee FR, Boon NA, MacNee W, Millar AM, Donaldson K, Newby DE. Do inhaled carbon nanoparticles translocate directly into the circulation in humans? Am J Respir Crit Care Med 2006;173:426–431.

[24] Wiebert P, Sanchez-Crespo A, Falk R, Philipson K, Lundin A, Larsson S, Moller W, Kreyling WG, Svartengren M. No significant translocation of inhaled 35-nm carbon particles to the circulation in humans. Inhal Toxicol 2006;18:741–747.

[25] Moller W, Felten K, Sommerer K, Scheuch G, Meyer G, Meyer P, Haussinger K, Kreyling WG. Deposition, retention, and translocation of ultrafine particles from the central airways and lung periphery. Am J Respir Crit Care Med 2008;177:426–432.

[26] Kreyling WG, Semmler-Behnke M, Seitz J, Scymczak W, Wenk A, Mayer P, Takenaka S, Oberdörster G. Size dependence of the translocation of inhaled iridium and carbon nanoparticle aggregates from the lung of rats to the blood and secondary organs. Inhal Toxicol 2009;21:55–60.

[27] Semmler-Behnke M, Kreyling WG, Lipka J, Fertsch S, Wenk S, Takenaka S, Schmid G, Brandau W. Biodistribution of 1.4- and 18-nm gold particles in rats. Small 2008;4:2108–2111.

[28] Mossmann BT, Borm PJ, Castranova V, Costa DL, Donaldson K, Kleeberger SR. Mechanisms of action of inhaled fibers, particles and nanoparticles in lung and cardiovascular diseases. Part Fibre Toxcol 2007;4:4.

[29] Li N, Xia T, Nel AE. The role of oxidative stress in ambient particulate matter-induced lung diseases and its implications in the toxicity of engineered nanoparticles. Free Radic Biol Med 2008;44:1689–1699.

[30] US Environmental Protection Agency. Role of particle agglomeration in nanoparticle toxicity (EPA grant Number: R832528). Available online at: http://cfpub.epa.gov/ncer_abstracts/index.cfm/fuseaction/display.abstractDetail/abstract/7814, accessed 24 August 2009.

[31] DeMarini DM, Brooks LR, Warren SH, Kobayashi T, Gilmour MI, Singh P. Bioassay-directed fractionation and salmonella mutagenicity of automobile and forklift diesel exhaust particles. Environ Health Perspect 2004;112:814–819.

[32] Singh P, DeMarini DM, Dick CA, Tabor DG, Ryan JV, Linak WP, Kobayashi T, Gilmour MI. Sample characterization of automobile and forklift diesel exhaust particles and

comparative pulmonary toxicity in mice. Environ Health Perspect 2004;112:820–825.
[33] Oberdörster G, Oberörster E, Oberdörster J. Nanotoxicology: an emerging discipline evolving from studies of ultrafine particles. Environ Health Perspect 2005;113:823–839.
[34] Donaldson K, Stone V, Clouter A, Renwick L, MacNee W. Ultrafine particles. Occup Environ Med 2001;58:211–216.
[35] Maynard AD, Aitken RJ. Assessing exposure to airborne nanomaterials: current abilities and future requirements. Nanotoxicology 2007;1:26–41.
[36] Knaapen AM, Borm PJ, Albrecht C, Schins RP. Inhaled particles and lung cancer. Part A: mechanisms. Int J Cancer 2004;109:799–809.
[37] Renwick LC, Brown D, Clouter A, Donaldson K. Increased inflammation and altered macrophage chemotactic responses caused by two ultrafine particle types. Occup Environ Med 2004;61:442–447.
[38] Duffin R, Tran L, Brown D, Stone V, Donaldson K. Proinflammogenic effects of low-toxicity and metal nanoparticles *in vivo* and *in vitro*: highlighting the role of particle surface area and surface reactivity. Inhal Toxicol 2007;19: 849–856.
[39] Monteiller C, Tran L, MacNee W, Faux S, Jones A, Miller B, Donaldson K. The pro-inflammatory effects of low-toxicity low-solubility particles, nanoparticles and fine particles, on epithelial cells *in vitro*: the role of surface area. Occup Environ Med 2007;64:609–615.
[40] Gallagher J, Sams II R, Inmon J, Gelein R, Elder A, Oberdörster G, Prahalad AK. Formation of 8-oxo-7,8-dihydro-2'-deoxyguanosine in rat lung DNA following subchronic inhalation of carbon black. Toxicol Appl Pharmacol 2003;190:224–231.
[41] Koike E, Kobayashi T. Chemical and biological oxidative effects of carbon black nanoparticles. Chemosphere 2006;65:946–951.
[42] Grassian VH, O'shaughnessy PT, Mcakova-Dodd A, Pettibone JM, Thorne PS. Inhalation exposure study of titanium dioxide nanoparticles with a primary particle size of 2 to 5 nm. Environ Health Perspect 2007;115:397–402.
[43] Warheit DB, Webb TR, Colvin VL, Reed KL, Sayes CM. Pulmonary bioassay studies with nanoscale and fine-quartz particles in rats: toxicity is not dependent upon particle size but on surface characteristics. Toxicol Sci 2007;95:270–280.
[44] Warheit DB, Webb TR, Reed KL, Frerichs S, Sayes CM. Pulmonary toxicity study in rats with three forms of ultrafine-TiO_2 particles: differential responses related to surface properties. Toxicology 2007;230:90–104.
[45] Oberdörster G. Toxicokinetics and effects of fibrous and nonfibrous particles. Inhal Toxicol 2002;14:29–56.
[46] Borm PJ, Schins RP, Albrecht C. Inhaled particles and lung cancer, part B: paradigms and risk assessment. Int J Cancer 2004;110:3–14.
[47] Fubini B, Hubbard A. Reactive oxygen species (ROS) and reactive nitrogen species (RNS) generation by silica in inflammation and fibrosis. Free Radic Biol Med 2003;34: 1507–1516.
[48] Fenoglio I, Fonsato S, Fubini B. Reaction of cysteine and glutathione (GSH) at the freshly fractured quartz surface: a possible role in silica-related diseases? Free Radic Biol Med 2003;35:752–762.
[49] Schins RP, Knaapen AM, Cakmak GD, Shi T, Weishaupt C, Borm PJ. Oxidant-induced DNA damage by quartz in alveolar epithelial cells. Mutat Res 2002;517:77–86.
[50] Schins RP, Duffin R, Hohr D, Knaapen AM, Shi T, Weishaupt C, Stone V, Donaldson K, Borm PJ. Surface modification of quartz inhibits toxicity, particle uptake, and oxidative DNA damage in human lung epithelial cells. Chem Res Toxicol 2002;15:1166–1173.
[51] Knaapen AM, Albrecht C, Becker A, Hohr D, Winzer A, Haenen GR, Borm PJ, Schins RP. DNA damage in lung epithelial cells isolated from rats exposed to quartz: role of surface reactivity and neutrophilic inflammation. Carcinogenesis 2002;23:1111–1120.
[52] Beck-Speier I, Dayal N, Karg E, Maier KL, Schumann G, Schulz H, Semmler M, Takenaka S, Stettmaier K, Bors W, Ghio A, Samet JM, Heyder J. Oxidative stress and lipid mediators induced in alveolar macrophages by ultrafine particles. Free Radic Biol Med 2005;38:1080–1092.
[53] Unfried K, Albrecht C, Klotz L, von Mikecz A, Grether-Beck S, Schins RPF. Cellular responses to nanoparticles:Target struntures and mechanisms. Nanotoxicology 2007;1:52–71.
[54] Conner SD, Schmid SL. Regulated portals of entry into the cell. Nature 2003;422:37–44.
[55] Stearns RC, Paulauskis JD, Godleski JJ. Endocytosis of ultrafine particles by A549 cells. Am J Respir Cell Mol Biol 2001;24:108–115.
[56] Singh S, Shi T, Duffin R, Albrecht C, van BD, Hohr D, Fubini B, Martra G, Fenoglio I, Borm PJ, Schins RP. Endocytosis, oxidative stress and IL-8 expression in human lung epithelial cells upon treatment with fine and ultrafine TiO_2: role of the specific surface area and of surface methylation of the particles. Toxicol Appl Pharmacol 2007;222: 141–151.
[57] Jin Y, Kannan S, Wu M, Zhao JX. Toxicity of luminescent silica nanoparticles to living cells. Chem Res Toxicol 2007;20:1126–1133.
[58] Lazou B, Jorly J, On D, Sellier E, Moisan F, Fleury-Feith J, Cambar J, Brochard P, Ohayon C. *In vitro* effects of nanoparticles on renal cells. Part Fibre Toxicol 2008;5:22.
[59] Yehia HN, Draper RK, Mikoryak C, Walker EK, Bajaj P, Musselman IH, Daigrepont MC, Dieckmann GR, Pantano P. Single-walled carbon nanotube interactions with HeLa cells. J Nanobiotechnol 2007;5:8.
[60] Li N, Sioutas C, Cho A, Schmitz D, Misra C, Sempf J, Wang M, Oberley T, Froines J, Nel A. Ultrafine particulate pollutants induce oxidative stress and mitochondrial damage. Environ Health Perspect 2003;111:455–460.
[61] Terry LJ, Shows EB, Wente SR. Crossing the nuclear envelope: hierarchical regulation of nucleocytoplasmic transport. Science 2007;318:1412–1416.
[62] Geiser M, Rothen-Rutishauser B, Kapp N, Schurch S, Kreyling W, Schulz H, Semmler M, Im H, V, Heyder J, Gehr P. Ultrafine particles cross cellular membranes by nonphagocytic mechanisms in lungs and in cultured cells. Environ Health Perspect 2005;113:1555–1560.
[63] Halliwell B, Whiteman M. Measuring reactive species and oxidative damage *in vivo* and in cell culture: how should you do it and what do the results mean? Br J Pharmacol 2004;142:231–255.
[64] Wardman P. Fluorescent and luminescent probes for measurement of oxidative and nitrosative species in cells and tissues: progress, pitfalls, and prospects. Free Radic Biol Med 2007;43:995–1022.
[65] Wilson MR, Lightbody JH, Donaldson K, Sales J, Stone V. Interactions between ultrafine particles and transition metals *in vivo* and *in vitro*. Toxicol Appl Pharmacol 2002;184: 172–179.
[66] Jacobsen NR, Pojana G, White P, Møller P, Cohn CA, Korsholm KS, Vogel U, Marcomini A, Loft S, Wallin H. Genotoxicity, cytotoxicity and reactive oxygen species induced by single-walled carbon nanotubes and C_{60} fullerenes in the FE1-Muta^{TM}Mouse lung epithelial cells. Environ Mol Mutagen 2008;49:476–487.
[67] Foucaud L, Wilson MR, Brown DM, Stone V. Measurement of reactive species production by nanoparticles prepared in biologically relevant media. Toxicol Lett 2007;174:1–9.
[68] Folkmann JK, Risom L, Jacobsen NR, Wallin H, Loft S, Møller P. Oxidatively damaged DNA in rats exposed by oral

gavage to C_{60} fullerenes and single-walled carbon nanotubes. Environ Health Perspect 2009;117:703–708.

[69] Bhattacharya K, Cramer H, Albrecht C, Schins R, Rahman Q, Zimmermann U, Dopp E. Vanadium pentoxide-coated ultrafine titanium dioxide particles induce cellular damage and micronucleus formation in V79 cells. J Toxicol Environ Health A 2008;71:976–980.

[70] Elder A, Yang H, Gwiazda R, Teng X, Thurston S, He H, Oberdörster G. Testing nanomaterials of unknown toxicity: an example based on platinum nanoparticles of different shapes. Adv Matter 2007;19:3124–3129.

[71] Limbach LK, Wick P, Manser P, Grass RN, Bruinink A, Stark WJ. Exposure of engineered nanoparticles to human lung epithelial cells: influence of chemical composition and catalytic activity on oxidative stress. Environ Sci Technol 2007;41: 4158–4163.

[72] Wamer WG, Yin JJ, Wei RR. Oxidative damage to nucleic acids photosensitized by titanium dioxide. Free Radic Biol Med 1997;23:851–858.

[73] Park S, Nam H, Chung N, Park JD, Lim Y. The role of iron in reactive oxygen species generation from diesel exhaust particles. Toxicol In Vitro 2006;20:851–857.

[74] Cakmak GD, Schins RP, Shi T, Fenoglio I, Fubini B, Borm PJ. *In vitro* genotoxicity assessment of commercial quartz flours in comparison to standard DQ12 quartz. Int J Hyg Environ Health 2004;207:105–113.

[75] Geh S, Shi T, Shokouhi B, Schins RP, Armbruster L, Rettenmeier AW, Dopp E. Genotoxic potential of respirable bentonite particles with different quartz contents and chemical modifications in human lung fibroblasts. Inhal Toxicol 2006;18:405–412.

[76] Duffin R, Gilmour PS, Schins RP, Clouter A, Guy K, Brown DM, MacNee W, Borm PJ, Donaldson K, Stone V. Aluminium lactate treatment of DQ12 quartz inhibits its ability to cause inflammation, chemokine expression, and nuclear factor-kappaB activation. Toxicol Appl Pharmacol 2001;176: 10–17.

[77] Santarelli L, Recchioni R, Moroni F, Marcheselli F, Governa M. Crystalline silica induces apoptosis in human endothelial cells *in vitro*. Cell Biol Toxicol 2004;20:97–108.

[78] Fenoglio I, Tomatis M, Lison D, Muller J, Fonseca A, Nagy JB, Fubini B. Reactivity of carbon nanotubes: free radical generation or scavenging activity? Free Radic Biol Med 2006; 40:1227–1233.

[79] Øvrevik J, Hetland RB, Schins RP, Myran T, Schwarze PE. Iron release and ROS generation from mineral particles are not related to cytokine release or apoptosis in exposed A549 cells. Toxicol Lett 2006;165:31–38.

[80] Vallyathan V, Shi XL, Dalal NS, Irr W, Castranova V. Generation of free radicals from freshly fractured silica dust. Potential role in acute silica-induced lung injury. Am Rev Respir Dis 1988;138:1213–1219.

[81] Dellinger B, Pryor WA, Cueto R, Squadrito GL, Hegde V, Deutsch WA. Role of free radicals in the toxicity of airborne fine particulate matter. Chem Res Toxicol 2001;14: 1371–1377.

[82] Schins RP, Lightbody JH, Borm PJ, Shi T, Donaldson K, Stone V. Inflammatory effects of coarse and fine particulate matter in relation to chemical and biological constituents. Toxicol Appl Prmacol 2004;195:1–11.

[83] Briede JJ, de Kok TM, Hogervorst JG, Moonen EJ, Op Den Camp CL, Kleinjanst JC. Development and application of an electron spin resonance spectrometry method for the determination of oxygen free radical formation by particulate matter. Environ Sci echnol 2005;39: 8420–8426.

[84] de Kok TM, Hogervorst JG, Briede JJ, van Herwijnen MH, Maas LM, Moonen EJ, Driece HA, Kleinjans JC. Genotoxicity and physicochemical characteristics of traffic-related ambient particulate matter. Environ Mol Mutagen 2005;46:71–80.

[85] Valavanidis A, Vlahoyianni T, Fiotakis K. Comparative study of the formation of oxidative damage marker 8-hydroxy-2'-deoxyguanosine (8-OHdG) adduct from the nucleoside 2'-deoxyguanosine by transition metals and suspensions of particulate matter in relation to metal content and redox reactivity. Free Radic Res 2005;39:1071–1081.

[86] Shi T, Knaapen AM, Begerow J, Birmili W, Borm PJ, Schins RP. Temporal variation of hydroxyl radical generation and 8-hydroxy-2'-deoxyguanosine formation by coarse and fine particulate matter. Occup Environ Med 2003;60:315–321.

[87] Shi T, Duffin R, Borm PJ, Li H, Weishaupt C, Schins RP. Hydroxyl-radical-dependent DNA damage by ambient particulate matter from contrasting sampling locations. Environ Res 2006;101:18–24.

[88] Cho AK, Sioutas C, Miguel AH, Kumagai Y, Schmitz DA, Singh M, Eiguren-Fernandez A, Froines JR. Redox activity of airborne particulate matter at different sites in the Los Angeles Basin. Environ Res 2005;99:40–47.

[89] Kunzli N, Mudway IS, Gotschi T, Shi T, Kelly FJ, Cook S, Burney P, Forsberg B, Gauderman JW, Hazenkamp ME, Heinrich J, Jarvis D, Norback D, Payo-Losa F, Poli A, Sunyer J, Borm PJ. Comparison of oxidative properties, light absorbance, total and elemental mass concentration of ambient PM 2.5 collected at 20 European sites. Environ Health Perspect 2006;114:684–690.

[90] Knaapen AM, Shi T, Borm PJA, Schins RPF. Soluble metals as well as the insoluble particle fraction are involved in cellular DNA damage induced by particulate matter. Mol Cell Biochem 2002;234–235:317–326.

[91] Ghio AJ, Stonehuerner J, Dailey LA, Carter JD. Metals associated with both the water-soluble and insoluble fractions of an ambient air pollution particle catalyze an oxidative stress. Inhal Toxicol 1999;11:37–49.

[92] de Kok TM, Hogervorst JG, Kleinjans JC, Briede JJ. Radicals in the church. Eur Respir J 2004;24:1069–1070.

[93] Lindbom J, Gustafsson M, Blomqvist G, Dahl A, Gudmundsson A, Swietlicki E, Ljungman AG. Wear particles generated from studded tires and pavement induces inflammatory reactions in mouse macrophage cells. Chem Res Toxicol 2007;20: 937–946.

[94] Hogervorst JG, de Kok TM, Briede JJ, Wesseling G, Kleinjans JC, van Schayck CP. Relationship between radical generation by urban ambient particulate matter and pulmonary function of school children. J Toxicol Environ Health A 2006;69: 245–262.

[95] Li Z, Hyseni X, Carter JD, Soukup JM, Dailey LA, Huang YC. Pollutant particles enhanced H_2O_2 production from NAD(P)H oxidase and mitochondria in human pulmonary artery endothelial cells. Am J Physiol Cell Physiol 2006;291: C357–C365.

[96] Donaldson K, Brown DM, Mitchell C, Dineva M, Beswick PH, Gilmour P, MacNee W. Free radical activity of PM10: iron-mediated generation of hydroxyl radicals. Environ Health Perspect 1997;105(Suppl 5):1285–1289.

[97] Ball JC, Straccia AM, Young WC, Aust AE. The formation of reactive oxygen species catalyzed by neutral, aqueous extracts of NIST ambient particulate matter and diesel engine particles. J Air Waste Manag Assoc 2000;50:1897–1903.

[98] Valavanidis A, Fiotakis K, Bakeas E, Vlahogianni T. Electron paramagnetic resonance study of the generation of reactive oxygen species catalysed by transition metals and quinoid redox cycling by inhalable ambient particulate matter. Redox Rep 2005;10:37–51.

[99] Gilmour PS, Brown DM, Lindsay TG, Beswick PH, MacNee W, Donaldson K. Adverse health effects of PM10 particles: involvement of iron in generation of hydroxyl radical. Occup Environ Med 1996;53:817–822.

[100] Sagai M, Saito H, Ichinose T, Kodama M, Mori Y. Biological effects of diesel exhaust particles. I. *In vitro* production of superoxide and *in vivo* toxicity in mouse. Free Radic Biol Med 1993;14:37–47.

[101] Kaimul AM, Nakamura H, Tanito M, Yamada K, Utsumi H, Yodoi J. Thioredoxin-1 suppresses lung injury and apoptosis induced by diesel exhaust particles (DEP) by scavenging reactive oxygen species and by inhibiting DEP-induced downregulation of Akt. Free Radic Biol Med 2005;39: 1549–1559.

[102] Jacobsen NR, Moller P, Cohn CA, Loft S, Vogel U, Wallin H. Diesel exhaust particles are mutagenic in FE1-Muta-Mouse lung epithelial cells. Mutat Res 2008;641:54–57.

[103] Leonard SS, Wang S, Shi X, Jordan BS, Castranova V, Dubick MA. Wood smoke particles generate free radicals and cause lipid peroxidation, DNA damage, NFkappaB activation and TNF-alpha release in macrophages. Toxicology 2000;150:147–157.

[104] Leonard SS, Castranova V, Chen BT, Schwegler-Berry D, Hoover M, Piacitelli C, Gaughan DM. Particle size-dependent radical generation from wildland fire smoke. Toxicology 2007;236:103–113.

[105] Zhang B, Cho M, Fortner JD, Lee J, Huang CH, Hughes JB, Kim JH. Delineating oxidative processes of aqueous C_{60} preparations: role of THF peroxide. Environ Sci Technol 2009;43:108–113.

[106] Markovic Z, Todorovic-Markovic B, Kleut D, Nikolic N, Vranjes-Djuric S, Misirkic M, Vucicevic L, Janjetovic K, Isakovic A, Harhaji L, Babic-Stojic B, Dramicanin M, Trajkovic V. The mechanism of cell-damaging reactive oxygen generation by colloidal fullerenes. Biomaterials 2007; 28:5437–5448.

[107] Harhaji L, Isakovic A, Raicevic N, Markovic Z, Todorovic-Markovic B, Nikolic N, Vranjes-Djuric S, Markovic I, Trajkovic V. Multiple mechanisms underlying the anticancer action of nanocrystalline fullerene. Eur J Pharmacol 2007;568:89–98.

[108] Sayes CM, Marchione AA, Reed KL, Warheit DB. Comparative pulmonary toxicity assessments of C60 water suspensions in rats: few differences in fullerene toxicity *in vivo* in contrast to *in vitro* profiles. Nano Lett 2007;7: 2399–2406.

[109] Lyon DY, Brunet L, Hinkal GW, Wiesner MR, Alvarez PJ. Antibacterial activity of fullerene water suspensions (nC_{60}) is not due to ROS-mediated damage. Nano Lett 2008;8:1539–1543.

[110] Lee J, Fortner JD, Hughes JB, Kim JH. Photochemical production of reactive oxygen species by C_{60} in the aqueous phase during UV irradiation. Environ Sci Technol 2007;41:2529–2535.

[111] Kagan VE, Tyurina YY, Tyurin VA, Konduru NV, Potapovich AI, Osipov AN, Kisin ER, Schwegler-Berry D, Mercer R, Castranova V, Shvedova AA. Direct and indirect effects of single walled carbon nanotubes on RAW 264.7 macrophages: role of iron. Toxicol Lett 2006;165:88–100.

[112] Zielinski H, Mudway IS, Berube KA, Murphy S, Richards R, Kelly FJ. Modeling the interactions of particulates with epithelial lining fluid antioxidants. Am J Physiol 1999;277:L719–L726.

[113] Danielsen PH, Loft S, Møller P. DNA damage and cytotoxicity in type II lung epithelial (A549) cell cultures after exposure to diesel exhaust and urban street particles. Part Fibre Toxicol 2008;5:6.

[114] Prahalad AK, Inmon J, Dailey LA, Madden MC, Ghio AJ, Gallagher JE. Air pollution particles mediated oxidative DNA base damage in a cell free system and in human airway epithelial cells in relation to particulate metal content and bioreactivity. Chem Res Toxicol 2001;14:879–887.

[115] Karlsson HL, Nilsson L, Moller L. Subway particles are more genotoxic than street particles and induce oxidative stress in cultured human lung cells. Chem Res Toxicol 2005;18:19–23.

[116] Iwai K, Adachi S, Takahashi M, Möller L, Udagawa T, Mizuno S, Sugawara I. Early oxidative DNA damages and late development of lung cancer in diesel exhaust-exposed rats. Environ Res 2000;84:255–264.

[117] Nagashima M, Kasai H, Yokota J, Nagamachi Y, Ichinose T, Sagai M. Formation of an oxidative DNA damage, 8-hydroxydeoxyguanosine, in mouse lung DNA after intratracheal instillation of diesel exhaust particles and effects of high dietary fat and beta-carotene on this process. Carcinogenesis 1995;16:1441–1445.

[118] Vogl G, Elstner EF. Diesel soot particles catalyze the production of oxy-radicals. Toxicol Lett 1989;47:17–23.

[119] Kamat JP, Devasagayam TP, Priyadarsini KI, Mohan H. Reactive oxygen species mediated membrane damage induced by fullerene derivatives and its possible biological implications. Toxicology 2000;155:55–61.

[120] Sera N, Tokiwa H, Miyata N. Mutagenicity of the fullerene C60-generated singlet oxygen dependent formation of lipid peroxides. Carcinogenesis 1996;17:2163–2169.

[121] Isakovic A, Markovic Z, Todorovic-Markovic B, Nikolic N, Vranjes-Djuric S, Mirkovic M, Dramicanin M, Harhaji L, Raicevic N, Nikolic Z, Trajkovic V. Distinct cytotoxic mechanisms of pristine versus hydroxylated fullerene. Toxicol Sci 2006;91:173–183.

[122] Xu A, Chai Y, Hei TK. Genotoxic responses to titanium dioxide nanoparticles and fullerene in gpt delta transgenic MEF cells. Part Fibre Toxicol 2009;6:3.

[123] Aam BB, Fonnum F. Carbon black particles increase reactive oxygen species formation in rat alveolar macrophages *in vitro*. Arch Toxicol 2007;81:441–446.

[124] Pulskamp K, Diabate S, Krug HF. Carbon nanotubes show no sign of acute toxicity but induce intracellular reactive oxygen species in dependence on contaminants. Toxicol Lett 2007;168:58–74.

[125] Yang H, Liu C, Yang D, Zhang H, Xi Z. Comparative study of cytotoxicity, oxidative stress and genotoxicity induced by four typical nanomaterials: the role of particle size, shape and composition. J Appl Toxicol 2008;29:69–78.

[126] Schrand AM, Dai L, Schlager JJ, Hussain SM, Osawa E. Differential biocompatibility of carbon nanotubes and nanodiamonds. Diamond Relat Mater 2007;16: 2118–2123.

[127] Ohyama M, Otake T, Adachi S, Kobayashi T, Morinaga K. A comparison of the production of reactive oxygen species by suspended particulate matter and diesel exhaust particles with macrophages. Inhal Toxicol 2007;19(Suppl 1):157–160.

[128] Chang CC, Chiu HF, Wu YS, Li YC, Tsai ML, Shen CK, Yang CY. The induction of vascular endothelial growth factor by ultrafine carbon black contributes to the increase of alveolar-capillary permeability. Environ Health Perspect 2005;113:454–460.

[129] Baulig A, Garlatti M, Bonvallot V, Marchand A, Barouki R, Marano F, Baeza-Squiban A. Involvement of reactive oxygen species in the metabolic pathways triggered by diesel exhaust particles in human airway epithelial cells. Am J Physiol Lung Cell Mol.Physiol 2003;285: L671–L679.

[130] Amara N, Bachoual R, Desmard M, Golda S, Guichard C, Lanone S, Aubier M, Ogier-Denis E, Boczkowski J. Diesel exhaust particles induce matrix metalloprotease-1 in human lung epithelial cells via a NADP(H) oxidase/NOX4 redox-dependent mechanism. Am J Physiol Lung Cell Mol.Physiol 2007;293:L170–L181.

[131] Baulig A, Sourdeval M, Meyer M, Marano F, Baeza-Squiban A. Biological effects of atmospheric particles on human bronchial epithelial cells. Comparison with diesel exhaust particles. Toxicol In Vitro 2003;17:567–573.

[132] Auger F, Gendron MC, Chamot C, Marano F, Dazy AC. Responses of well-differentiated nasal epithelial cells exposed to particles: role of the epithelium in airway inflammation. Toxicol Appl Pharmacol 2006;215:285–294.

[133] Karlsson HL, Holgersson A, Moller L. Mechanisms related to the genotoxicity of particles in the subway and from other sources. Chem Res Toxicol 2008;21:726–731.

[134] Goldsmith CA, Imrich A, Danaee H, Ning YY, Kobzik L. Analysis of air pollution particulate-mediated oxidant stress in alveolar macrophages. J Toxicol Environ Health A 1998;54:529–545.

[135] Kamdar O, Le W, Zhang J, Ghio AJ, Rosen GD, Upadhyay D. Air pollution induces enhanced mitochondrial oxidative stress in cystic fibrosis airway epithelium. FEBS Lett 2008;582:3601–3606.

[136] Becher R, Bucht A, Ovrevik J, Hongslo JK, Dahlman HJ, Samuelsen JT, Schwarze PE. Involvement of NADPH oxidase and iNOS in rodent pulmonary cytokine responses to urban air and mineral particles. Inhal Toxicol 2007;19: 645–655.

[137] Soukup JM, Ghio AJ, Becker S. Soluble components of Utah Valley particulate pollution alter alveolar macrophage function *in vivo* and *in vitro*. Inhal Toxicol 2000;12:401–414.

[138] Schneider JC, Card GL, Pfau JC, Holian A. Air pollution particulate SRM 1648 causes oxidative stress in RAW 264.7 macrophages leading to production of prostaglandin E2, a potential Th2 mediator. Inhal Toxicol 2005;17:871–877.

[139] Zhang Y, Schauer JJ, Shafer MM, Hannigan MP, Dutton SJ. Source apportionment of *in vitro* reactive oxygen species bioassay activity from atmospheric particulate matter. Environ Sci Technol 2008;42:7502–7509.

[140] Verma V, Polidori A, Schauer JJ, Shafer MM, Cassee FR, Sioutas C. Physicochemical and toxicological profiles of particulate matter in Los Angeles during the October 2007 southern California wildfires. Environ Sci Technol 2009;43:954–960.

[141] Bonvallot V, Baeza-Squiban A, Baulig A, Brulant S, Boland S, Muzeau F, Barouki R, Marano F. Organic compounds from diesel exhaust particles elicit a proinflammatory response in human airway epithelial cells and induce cytochrome p450 1A1 expression. Am J Respir Cell Mol Biol 2001;25:515–521.

[142] Garza KM, Soto KF, Murr LE. Cytotoxicity and reactive oxygen species generation from aggregated carbon and carbonaceous nanoparticulate materials. Int J Nanomed 2008; 3:83–94.

[143] Helfenstein M, Miragoli M, Rohr S, Muller L, Wick P, Mohr M, Gehr P, Rothen-Rutishauser B. Effects of combustion-derived ultrafine particles and manufactured nanoparticles on heart cells *in vitro*. Toxicology 2008;253:70–78.

[144] Li R, Ning Z, Cui J, Khalsa B, Ai L, Takabe W, Beebe T, Majumdar R, Sioutas C, Hsiai T. Ultrafine particles from diesel engines induce vascular oxidative stress via JNK activation. Free Radic Biol Med 2009;46:775–782.

[145] Li N, Wang M, Oberley TD, Sempf JM, Nel AE. Comparison of the pro-oxidative and proinflammatory effects of organic diesel exhaust particle chemicals in bronchial epithelial cells and macrophages. J Immunol 2002;169:4531–4541.

[146] Manna SK, Sarkar S, Barr J, Wise K, Barrera EV, Jejelowo O, Rice-Ficht AC, Ramesh GT. Single-walled carbon nanotube induces oxidative stress and activates nuclear transcription factor-kappaB in human keratinocytes. Nano Lett 2005;5:1676–1684.

[147] Shvedova AA, Castranova V, Kisin ER, Schwegler-Berry D, Murray AR, Gandelsman VZ, Maynard A, Baron P. Exposure to carbon nanotube material: assessment of nanotube cytotoxicity using human keratinocyte cells. J Toxicol Environ Health A 2003;66:1909–1926.

[148] Pacurari M, Yin XJ, Zhao J, Ding M, Leonard SS, Schwegler-Berry D, Ducatman BS, Sbarra D, Hoover MD, Castranova V, Vallyathan V. Raw single-wall carbon nanotubes induce oxidative stress and activate MAPKs, AP-1, NF-kappaB, and Akt in normal and malignant human mesothelial cells. Environ Health Perspect 2008;116:1211–1217.

[149] Karlsson HL, Cronholm P, Gustafsson J, Moller L. Copper oxide nanoparticles are highly toxic: a comparison between metal oxide nanoparticles and carbon nanotubes. Chem Res Toxicol 2008;21:1726–1732.

[150] Shvedova AA, Kisin ER, Mercer R, Murray AR, Johnson VJ, Potapovich AI, Tyurina YY, Gorelik O, Arepalli S, Schwegler-Berry D, Hubbs AF, Antonini J, Evans DE, Ku BK, Ramsey D, Maynard A, Kagan VE, Castranova V, Baron P. Unusual inflammatory and fibrogenic pulmonary responses to single-walled carbon nanotubes in mice. Am J Physiol Lung Cell Mol Physiol 2005;289:L698–L708.

[151] Deshpande A, Narayanan PK, Lehnert BE. Silica-induced generation of extracellular factor(s) increases reactive oxygen species in human bronchial epithelial cells. Toxicol Sci 2002;67:275–283.

[152] Thibodeau MS, Giardina C, Knecht DA, Helble J, Hubbard AK. Silica-induced apoptosis in mouse alveolar macrophages is initiated by lysosomal enzyme activity. Toxicol Sci 2004;80:34–48.

[153] Scarfi S, Magnone M, Ferraris C, Pozzolini M, Benvenuto F, Benatti U, Giovine M. Ascorbic acid pre-treated quartz stimulates TNF-alpha release in RAW 264.7 murine macrophages through ROS production and membrane lipid peroxidation. Respir Res 2009;10:25.

[154] Park EJ, Park K. Oxidative stress and pro-inflammatory responses induced by silica nanoparticles *in vivo* and *in vitro*. Toxicol Lett 2009;184:18–25.

[155] Diaz B, Sanchez-Espinel C, Arruebo M, Faro J, de ME, Magadan S, Yague C, Fernandez-Pacheco R, Ibarra MR, Santamaria J, Gonzalez-Fernandez A. Assessing methods for blood cell cytotoxic responses to inorganic nanoparticles and nanoparticle aggregates. Small 2008;4:2025–2034.

[156] Kang JL, Moon C, Lee HS, Lee HW, Park EM, Kim HS, Castranova V. Comparison of the biological activity between ultrafine and fine titanium dioxide particles in RAW 264.7 cells associated with oxidative stress. J Toxicol Environ Health A 2008;71:478–485.

[157] Wan R, Mo Y, Zhang X, Chien S, Tollerud DJ, Zhang Q. Matrix metalloproteinase-2 and -9 are induced differently by metal nanoparticles in human monocytes: the role of oxidative stress and protein tyrosine kinase activation. Toxicol Appl Pharmacol 2008;233:276–285.

[158] Shen B, Scaiano JC, English AM. Zeolite encapsulation decreases TiO_2-photosensitized ROS generation in cultured human skin fibroblasts. Photochem Photobiol 2006;82:5–12.

[159] Jin CY, Zhu BS, Wang XF, Lu QH. Cytotoxicity of titanium dioxide nanoparticles in mouse fibroblast cells. Chem Res Toxicol 2008;21:1871–1877.

[160] Pan Z, Lee W, Slutsky L, Clark RA, Pernodet N, Rafailovich MH. Adverse effects of titanium dioxide nanoparticles on human dermal fibroblasts and how to protect cells. Small 2009;5:511–520.

[161] Whitekus MJ, Li N, Zhang M, Wang M, Horwitz MA, Nelson SK, Horwitz LD, Brechun N, az-Sanchez D, Nel AE. Thiol antioxidants inhibit the adjuvant effects of aerosolized diesel exhaust particles in a murine model for ovalbumin sensitization. J Immunol 2002;168:2560–2567.

[162] Stone V, Shaw J, Brown DM, MacNee W, Faux SP, Donaldson K. The role of oxidative stress in the prolonged inhibitory effect of ultrafine carbon black on epithelial cell function. Toxicol in Vitro 1998;12:649–659.

[163] Lim HB, Ichinose T, Miyabara Y, Takano H, Kumagai Y, Shimojyo N, Devalia JL, Sagai M. Involvement of superoxide and nitric oxide on airway inflammation and hyperresponsiveness induced by diesel exhaust particles in mice. Free Radic Biol Med 1998;25:635–644.

[164] Møller P, Daneshvar B, Loft S, Wallin H, Poulsen HE, Autrup H, Ravn-Haren G, Dragsted LO. Oxidative DNA damage in vitamin C supplemented guinea pigs after intratracheal instillation of diesel exhaust particles. Toxicol Appl Pharmacol 2003;189:39–44.

[165] Dubick MA, Carden SC, Jordan BS, Langlinais PC, Mozingo DW. Indices of antioxidant status in rats subjected to wood smoke inhalation and/or thermal injury. Toxicology 2002;176:145–157.

[166] Park MS, Cancio LC, Jordan BS, Brinkley WW, Rivera VR, Dubick MA. Assessment of oxidative stress in lungs from sheep after inhalation of wood smoke. Toxicology 2004;195:97–112.

[167] Shvedova AA, Kisin E, Murray AR, Johnson VJ, Gorelik O, Arepalli S, Hubbs AF, Mercer RR, Keohavong P, Sussman N, Jin J, Yin J, Stone S, Chen BT, Deye G, Maynard A, Castranova V, Baron PA, Kagan VE. Inhalation vs. aspiration of single-walled carbon nanotubes in C57BL/6 mice: inflammation, fibrosis, oxidative stress, and mutagenesis. Am J Physiol Lung Cell Mol Physiol 2008;295:L552–L565.

[168] Gharbi N, Pressac M, Hadchouel M, Szwarc H, Wilson SR, Moussa F. [60]fullerene is a powerful antioxidant *in vivo* with no acute or subacute toxicity. Nano Lett 2005;5: 2578–2585.

[169] Sørensen M, Autrup H, Møller P, Hertel O, Jensen SS, Vinzents P, Knudsen LE, Loft S. Linking exposure to environmental pollutants with biological effects. Mutat Res 2003; 544:255–271.

[170] Risom L, Møller P, Loft S. Oxidative stress-induced DNA damage by particulate air pollution. Mutat Res 2005;592: 119–137.

[171] Danielsen PH, Loft S, Kocbach A, Schwarze PE, Møller P. Oxidative damage to DNA and repair induced by Norwegian wood smoke particles in human A549 and THP-1 cell lines. Mutat Res 2009;674:116–122.

[172] Li N, Kim S, Wang M, Froines J, Sioutas C, Nel A. Use of a stratified oxidative stress model to study the biological effects of ambient concentrated and diesel exhaust particulate matter. Inhal Toxicol 2002;14:459–486.

[173] Hiura TS, Kaszubowski MP, Li N, Nel AE. Chemicals in diesel exhaust particles generate reactive oxygen radicals and induce apoptosis in macrophages. J Immunol 1999;163: 5582–5591.

[174] Aam BB, Fonnum F. ROS scavenging effects of organic extract of diesel exhaust particles on human neutrophil granulocytes and rat alveolar macrophages. Toxicology 2007;230:207–218.

[175] Squadrito GL, Cueto R, Dellinger B, Pryor WA. Quinoid redox cycling as a mechanism for sustained free radical generation by inhaled airborne particulate matter. Free Radic Biol Med 2001;31:1132–1138.

[176] Ng D, Kokot N, Hiura T, Faris M, Saxon A, Nel A. Macrophage activation by polycyclic aromatic hydrocarbons: evidence for the involvement of stress-activated protein kinases, activator protein-1, and antioxidant response elements. J Immunol 1998;161:942–951.

[177] Briede JJ, Godschalk RW, Emans MT, de Kok TM, Van AE, Van MJ, van Schooten FJ, Kleinjans JC. *In vitro* and *in vivo* studies on oxygen free radical and DNA adduct formation in rat lung and liver during benzo[a]pyrene metabolism. Free Radic Res 2004;38:995–1002.

[178] Park JH, Mangal D, Tacka KA, Quinn AM, Harvey RG, Blair IA, Penning TM. Evidence for the aldo-keto reductase pathway of polycyclic aromatic trans-dihydrodiol activation in human lung A549 cells. Proc Natl Acad Sci USA 2008;105:6846–6851.

[179] Kim KB, Lee BM. Oxidative stress to DNA, protein, and antioxidant enzymes (superoxide dismutase and catalase) in rats treated with benzo(*a*)pyrene. Cancer Lett 1997;113:205–212.

[180] Godschalk R, Curfs D, Bartsch H, van Schooten FJ, Nair J. Benzo[a]pyrene enhances lipid peroxidation induced DNA damage in aorta of apolipoprotein E knockout mice. Free Radic Res 2003;37:1299–1305.

[181] Xia T, Korge P, Weiss JN, Li N, Venkatesen MI, Sioutas C, Nel A. Quinones and aromatic chemical compounds in particulate matter induce mitochondrial dysfunction: implications for ultrafine particle toxicity. Environ Health Perspect 2004;112:1347–1358.

[182] Upadhyay D, Panduri V, Ghio A, Kamp DW. Particulate matter induces alveolar epithelial cell DNA damage and apoptosis: role of free radicals and the mitochondria. Am J Respir Cell Mol.Biol 2003;29:180–187.

[183] Kamp DW, Panduri V, Weitzman SA, Chandel N. Asbestos-induced alveolar epithelial cell apoptosis: role of mitochondrial dysfunction caused by iron-derived free radicals. Mol Cell Biochem 2002;234–235:153–160.

[184] Panduri V, Weitzman SA, Chandel N, Kamp DW. The mitochondria-regulated death pathway mediates asbestos-induced alveolar epithelial cell apoptosis. Am J Respir Cell Mol Biol 2003;28:241–248.

[185] Sayes CM, Gobin AM, Ausman KD, Mendez J, West JL, Colvin VL. Nano-C60 cytotoxicity is due to lipid peroxidation. Biomaterials 2005;26:7587–7595.

[186] Balduzzi M, Diociaiuti M, De BB, Paradisi S, Paoletti L. *In vitro* effects on macrophages induced by noncytotoxic doses of silica particles possibly relevant to ambient exposure. Environ Res 2004;96:62–71.

[187] Fanizza C, Ursini CL, Paba E, Ciervo A, Di FA, Maiello R, De SP, Cavallo D. Cytotoxicity and DNA-damage in human lung epithelial cells exposed to respirable *α*-quartz. Toxicol In Vitro 2007;21:586–594.

[188] Li H, Haberzettl P, Albrecht C, Hohr D, Knaapen AM, Borm PJ, Schins RP. Inhibition of the mitochondrial respiratory chain function abrogates quartz induced DNA damage in lung epithelial cells. Mutat Res 2007;617:46–57.

[189] Jacobsen NR, Saber AT, White P, Moller P, Pojana G, Vogel U, Loft S, Gingerich J, Soper L, Douglas GR, Wallin H. Increased mutant frequency by carbon black, but not quartz, in the lacZ and cII transgenes of muta mouse lung epithelial cells. Environ Mol Mutagen 2007; 48:451–461.

[190] Garcon G, Dagher Z, Zerimech F, Ledoux F, Courcot D, Aboukais A, Puskaric E, Shirali P. Dunkerque City air pollution particulate matter-induced cytotoxicity, oxidative stress and inflammation in human epithelial lung cells (L132) in culture. Toxicol In Vitro 2006;20:519–528.

[191] Huang SL, Hsu MK, Chan CC. Effects of submicrometer particle compositions on cytokine production and lipid peroxidation of human bronchial epithelial cells. Environ Health Perspect 2003;111:478–482.

[192] Vevers WF, and Jha AN. Genotoxic and cytotoxic potential of titanium dioxide (TiO_2) nanoparticles on fish cells *in vitro*. Ecotoxicology 2008;17:410–420.

[193] Gurr JR, Wang AS, Chen CH, Jan KY. Ultrafine titanium dioxide particles in the absence of photoactivation can induce oxidative damage to human bronchial epithelial cells. Toxicology 2005;213:66–73.

[194] Møller P. The alkaline comet assay: towards validation in biomonitoring of DNA damaging exposures. Basic Clin Pharmacol Toxicol 2006;98:336–345.

[195] Thein N, Møller P, Amtoft H, Vogel U, Korsholm B, Autrup H, Wallin H. A strong genotoxic effect in mouse skin of a single painting of coal tar in hairless mice and in Muta™ Mouse. Mutat Res 2000;468:117–124.

[196] Møller P, Wallin H, Vogel U, Autrup H, Risom L, Hald MT, Daneshvar B, Dragsted LO, Poulsen HE, Loft S. Mutagenecity of 2-amino-3-methylimidazo[4,5-*f*]quinoline in colon and liver of Big Blue rats: role of DNA adducts, strand breaks and oxidative stress. Carcinogenesis 2002;23: 1379–1385.

[197] Porter DW, Millecchia LL, Willard P, Robinson VA, Ramsey D, McLaurin J, Khan A, Brumbaugh K, Beighley CM, Teass A, Castranova V. Nitric oxide and reactive oxygen species production causes progressive damage in rats after cessation of silica inhalation. Toxicol Sci 2006;90:188–197.

[198] Seiler F, Rehn B, Rehn S, Bruch J. Evidence of a no-effect level in silica-induced rat lung mutagenicity but not in fibrogenicity. Arch Toxicol 2001;74:716–719.

[199] Seiler F, Rehn B, Rehn S, Hermann M, Bruch J. Quartz exposure of the rat lung leads to a linear dose response in inflammation but not in oxidative DNA damage and mutagenicity. Am J Respir Cell Mol Biol 2001;24:492–498.

[200] Nehls P, Seiler F, Rehn B, Greferath R, Bruch J. Formation and persistence of 8-oxoguanine in rat lung cells as an important determinant for tumor formation following particle exposure. Environ Health Perspect 1997;105(Suppl 5):1291–1296.

[201] Rehn B, Seiler F, Rehn S, Bruch J, Maier M. Investigation on the inflammatory and genotoxic lung effects of two types of titanium dioxide: untreated and surface treated. Toxicol Appl Pharmacol 2003;189:84–95.

[202] Seiler F, Rehn B, Rehn S, Bruchs J. Significant differences in the cellular and molecular reactions of rat and hamster lung after quartz exposure. Toxicol Lett 2001;119:11–19.

[203] Yamano Y, Kagawa J, Hanaoka T, Takahashi T, Kasai H, Tsugane S, Watanabe S. Oxidative DNA damage induced by silica *in vivo*. Environ Res 1995;69:102–107.

[204] Folkmann JK, Risom L, Hansen CS, Loft S, Møller P. Oxidatively damaged DNA and inflammation in the liver of dyslipidemic ApoE$^{-/-}$ mice exposed to diesel exhaust particles. Toxicology 2007;237:134–144.

[205] Dybdahl M, Risom L, Møller P, Autrup H, Wallin H, Vogel U, Bornholdt J, Daneshvar B, Dragsted LO, Weimann A, Poulsen HE, Loft S. DNA adduct formation and oxidative stress in colon and liver of Big Blue rats after dietary exposure to diesel particles. Carcinogenesis 2003;24: 1759–1766.

[206] Muller AK, Farombi EO, Møller P, Autrup HN, Vogel U, Wallin H, Dragsted LO, Loft S, Binderup ML. DNA damage in lung after oral exposure to diesel exhaust particles in Big Blue((R)) rats. Mutat Res 2004;550:123–132.

[207] Ichinose T, Yajima Y, Nagashima M, Takeshita S, Nagamachi Y, Sagai M. Lung carcinogenesis and formation of 8-hydroxy-deoxyguanosine in mice by diesel exhaust particles. Carcinogenesis 1997;18:185–192.

[208] Tsurudome Y, Hirano T, Yamato H, Tanaka I, Sagai M, Hirano H, Nagata N, Itoh H, Kasai H. Changes in levels of 8-hydroxyguanine in DNA, its repair and *OGG1* mRNA in rat lungs after intratracheal administration of diesel exhaust particles. Carcinogenesis 1999;20:1573–1576.

[209] Sanbongi C, Takano H, Osakabe N, Sasa N, Natsume M, Yanagisawa R, Inoue K, Kato Y, Osawa T, Yoshikawa T. Rosmarinic acid inhibits lung injury induced by diesel exhaust particles. Free Radic Biol Med 2003;34:1060–1069.

[210] Ichinose T, Yamanushi T, Seto H, Sagai M. Oxygen radicals in lung carcinogenesis accompanying phagocytosis of diesel exhaust particles. Int J Oncol 1997;11:571–575.

[211] Tokiwa H, Sera N, Nakanishi Y, Sagai M. 8-Hydroxyguanosine formed in human lung tissue and the association with diesel exhaust particles. Free Radic Biol Med 1999;27: 1251–1258.

[212] Risom L, Dybdahl M, Bornholdt J, Vogel U, Wallin H, Møller P, Loft S. Oxidative DNA damage and defence gene expression in the mouse lung after short-term exposure to diesel exhaust particles by inhalation. Carcinogenesis 2003;24:1847–1852.

[213] Dybdahl M, Risom L, Bornholdt J, Autrup H, Loft S, Wallin H. Inflammatory and genotoxic effects of diesel particles *in vitro* and *in vivo*. Mutat Res 2004;562:119–131.

[214] Risom L, Dybdahl M, Møller P, Wallin H, Haun T, Vogel U, Klungland A, Loft S. Repeated inhalations of diesel exhaust particles and oxidatively damaged DNA in young oxoguanine DNA glycosylase (OGG1) deficient mice. Free Radic Res 2007;41:172–181.

[215] Sato H, Sone H, Sagai M, Suzuki KT, Aoki Y. Increase in mutation frequency in lung of Big Blue rat by exposure to diesel exhaust. Carcinogenesis 2000;21:653–661.

[216] Aoki Y, Sato H, Nishimura N, Takahashi S, Itoh K, Yamamoto M. Accelerated DNA adduct formation in the lung of the Nrf2 knockout mouse exposed to diesel exhaust. Toxicol Appl Pharmacol 2001;173:154–160.

[217] Danielsen PH, Risom L, Wallin H, Autrup H, Vogel U, Loft S, Møller P. DNA damage in rats after a single oral exposure to diesel exhaust particles. Mutat Res 2008;637:49–55.

[218] Albrecht C, Knaapen AM, Becker A, Hohr D, Haberzettl P, van Schooten FJ, Borm PJ, Schins RP. The crucial role of particle surface reactivity in respirable quartz-induced reactive oxygen/nitrogen species formation and APE/Ref-1 induction in rat lung. Respir Res 2005;6:129.

[219] Reliene R, Hlavacova A, Mahadevan B, Baird WM, Schiestl RH. Diesel exhaust particles cause increased levels of DNA deletions after transplacental exposure in mice. Mutat Res 2005;570:245–252.

[220] Risom L, Moller P, Dybdahl M, Vogel U, Wallin H, Loft S. Dietary exposure to diesel exhaust particles and oxidatively damaged DNA in young oxoguanine DNA glycosylase 1 deficient mice. Toxicol Lett 2007;175:16–23.

[221] Risom L, Møller P, Hansen M, Autrup H, Bornholdt J, Vogel U, Wallin H, Poulsen HE, Dragsted LO, Loft S. Dietary elevated sucrose modulation of diesel-induced genotoxicity in the colon and liver of Big Blue rats. Arch Toxicol 2003;77:651–656.

[222] Pereira CE, Heck TG, Saldiva PH, Rhoden CR. Ambient particulate air pollution from vehicles promotes lipid peroxidation and inflammatory responses in rat lung. Braz J Med Biol Res 2007;40:1353–1359.

[223] Liu X, Meng Z. Effects of airborne fine particulate matter on antioxidant capacity and lipid peroxidation in multiple organs of rats. Inhal Toxicol 2005;17:467–473.

[224] Rhoden CR, Lawrence J, Godleski JJ, Gonzalez-Flecha B. N-acetylcysteine prevents lung inflammation after short-term inhalation exposure to concentrated ambient particles. Toxicol Sci 2004;79:296–303.

[225] Araujo JA, Barajas B, Kleinman M, Wang X, Bennett BJ, Gong KW, Navab M, Harkema J, Sioutas C, Lusis AJ, Nel AE. Ambient particulate pollutants in the ultrafine range promote early atherosclerosis and systemic oxidative stress. Circ Res 2008;102:589–596.

[226] Wang J, Chen C, Liu Y, Jiao F, Li W, Lao F, Li Y, Li B, Ge C, Zhou G, Gao Y, Zhao Y, Chai Z. Potential neurological lesion after nasal instillation of TiO_2 nanoparticles in the anatase and rutile crystal phases. Toxicol Lett 2008; 183: 72–80.

[227] Wang J, Liu Y, Jiao F, Lao F, Li W, Gu Y, Li Y, Ge C, Zhou G, Li B, Zhao Y, Chai Z, Chen C. Time-dependent translocation and potential impairment on central nervous system by intranasally instilled TiO(2) nanoparticles. Toxicology 2008;254:82–90.

[228] Inoue K, Takano H, Yanagisawa R, Sakurai M, Ichinose T, Sadakane K, Yoshikawa T. Effects of nano particles on antigen-related airway inflammation in mice. Respir Res 2005;6:106.

[229] Niwa Y, Hiura Y, Sawamura H, Iwai N. Inhalation exposure to carbon black induces inflammatory response in rats. Circ J 2008;72:144–149.
[230] Shvedova AA, Kisin ER, Murray AR, Gorelik O, Arepalli S, Castranova V, Young SH, Gao F, Tyurina YY, Oury TD, Kagan VE. Vitamin E deficiency enhances pulmonary inflammatory response and oxidative stress induced by single-walled carbon nanotubes in C57BL/6 mice. Toxicol Appl Pharmacol 2007;221:339–348.
[231] Han SG, Andrews R, Gairola CG, Bhalla DK. Acute pulmonary effects of combined exposure to carbon nanotubes and ozone in mice. Inhal Toxicol 2008;20:391–398.
[232] Loft S, Møller P. Oxidative DNA damage and human cancer: need for cohort studies. Antioxid Redox Signal 2006;8:1021–1031.
[233] Cooke MS, Olinski R, Loft S. Measurement and meaning of oxidatively modified DNA lesions in urine. Cancer Epidemiol Biomarkers Prev 2008;17:3–14.
[234] ESCODD (European Standards Committee on Oxidative DNA Damage). Comparative analysis of baseline 8-oxo-7, 8-dihydroguanine in mammalian cell DNA, by different methods in different laboratories: an approach to consensus. Carcinogenesis 2003;23:2129–2133.
[235] Møller P, Loft S. Dietary antioxidants and beneficial effect on oxidatively damaged DNA. Free Radic Biol Med 2006;41:388–415.
[236] Møller P, Folkmann JK, Forchhammer L, Bräuner EV, Danielsen PH, Risom L, Loft S. Air pollution, oxidative damage to DNA, and carcinogenesis. Cancer Lett 2008;266: 84–97.
[237] ESCODD (European Standards Committee on Oxidative DNA Damage). Measurement of DNA oxidation in human cells by chromatographic and enzymic methods. Free Radic Biol Med 2003;34:1089–1099.
[238] ESCODD (European Standards Committee on Oxidative DNA Damage), Gedik CM, Collins A. Establishing the background level of base oxidation in human lymphocyte DNA: results of an inter-laboratory validation study. FASEB J 2005;19:82–84.
[239] Kasai H. Analysis of a form of oxidative DNA damage, 8-hydroxy-2'-deoxyguanosine, as a marker of cellular oxidative stress during carcinogenesis. Mutat Res 1997;387:147–163.
[240] Wang JJ, Sanderson BJ, Wang H. Cytotoxicity and genotoxicity of ultrafine crystalline SiO_2 particulate in cultured human lymphoblastoid cells. Environ Mol Mutagen 2007;48:151–157.
[241] Wang JJ, Wang H, Sanderson BJ. Ultrafine quartz-induced damage in human lymphoblastoid cells in vitro using three genetic damage end-points. Toxicol Mech Methods 2007;17:223–232.
[242] Driscoll KE, Deyo LC, Carter JM, Howard BW, Hassenbein DG, Bertram TA. Effects of particle exposure and particle-elicited inflammatory cells on mutation in rat alveolar epithelial cells. Carcinogenesis 1997;18:423–430.
[243] Kirwin CJ, LeBlanc JV, Thomas WC, Haworth SR, Kirby PE, Thilagar A, Bowman JT, Brusick DJ. Evaluation of the genetic activity of industrially produced carbon black. J Toxicol Environ Health 1981;7:973–989.
[244] Semmler M, Seitz J, Erbe F, Mayer P, Heyder J, Oberdörster G, Kreyling WG. Long-term clearance kinetics of inhaled ultrafine insoluble iridium particles from the rat lung, including transient translocation into secondary organs. Inhal Toxicol 2004;16:453–459.
[245] Møller P, Risom L, Lundby C, Mikkelsen L, Loft S. Hypoxia and oxidation levels of DNA and lipids in humans and animal experimental models. IUBMB Life 2008;60: 707–723.
[246] Loft S, Svoboda P, Kasai H, Tjonneland A, Vogel U, Møller P, Overvad K, Raaschou-Nielsen O. Prospective study of 8-oxo-7,8-dihydro-2'-deoxyguanosine excretion and the risk of lung cancer. Carcinogenesis 2006;27: 1245–1250.
[247] Boaz M, Matas Z, Biro A, Katzir Z, Green M, Fainaru M, Smetana S. Comparison of hemostatic factors and serum malondialdehyde as predictive factors for cardiovascular disease in hemodialysis patients. Am J Kidney Dis 1999; 34:438–444.
[248] Walter MF, Jacob RF, Jeffers B, Ghadanfar MM, Preston GM, Buch J, Mason RP. Serum levels of thiobarbituric acid reactive substances predict cardiovascular events in patients with stable coronary artery disease: a longitudinal analysis of the PREVENT study. J Am Coll Cardiol 2004;44: 1996–2002.
[249] Huerta JM, Gonzalez S, Fernandez S, Patterson AM, Lasheras C. Lipid peroxidation, antioxidant status and survival in institutionalised elderly: a five-year longitudinal study. Free Radic Res 2006;40:571–578.
[250] Lai CH, Liou SH, Lin HC, Shih TS, Tsai PJ, Chen JS, Yang T, Jaakkola JJ, Strickland PT. Exposure to traffic exhausts and oxidative DNA damage. Occup Environ Med 2005;62: 216–222.
[251] Ayi FL, Mobio TA, Creppy EE, Fayomi B, Fustoni S, Møller P, Kyrtopoulos S, Georgiades P, Loft S, Sanni A, Skov H, Ovrebo S, Autrup H. Survey of air pollution in Cotonou, Benin—air monitoring and biomarkers. Sci Total Environ 2006;358:85–96.
[252] Møller P, Knudsen LE, Frentz G, Dybdahl M, Wallin H, Nexø BA. Seasonal variation of DNA damage and repair in patients with non-melanoma skin cancer and referents with and without psoriasis. Mutat Res 1998;407:25–34.
[253] Møller P, Knudsen LE, Loft S, Wallin H. The comet assay as a rapid test in biomonitoring occupational exposure to DNA-damaging agents and effect of confounding factors. Cancer Epidemiol Biomarkers Prev 2000;9:1005–1015.
[254] Møller P, Wallin H, Holst E, Knudsen LE. Sunlight induced DNA damage in human mononuclear cells. FASEB J 2002;16:45–53.
[255] Singh R, Kaur B, Kalina I, Popov TA, Georgieva T, Garte S, Binkova B, Sram RJ, Taioli E, Farmer PB. Effects of environmental air pollution on endogenous oxidative DNA damage in humans. Mutat Res 2007;620:71–82.
[256] Avogbe PH, Ayi-Fanou L, Autrup H, Loft S, Fayomi B, Sanni A, Vinzents P, Møller P. Ultrafine particulate matter and high-level benzene urban air pollution in relation to oxidative DNA damage. Carcinogenesis 2005;26:613–620.
[257] Buthbumrung N, Mahidol C, Navasumrit P, Promvijit J, Hunsonti P, Autrup H, Ruchirawat M. Oxidative DNA damage and influence of genetic polymorphisms among urban and rural schoolchildren exposed to benzene. Chem Biol Interact 2008;172:185–194.
[258] Novotna B, Topinka J, Solansky I, Chvatalova I, Lnenickova Z, Sram RJ. Impact of air pollution and genotype variability on DNA damage in Prague policemen. Toxicol Lett 2007; 172:37–47.
[259] Rossner P Jr, Svecova V, Milcova A, Lnenickova Z, Solansky I, Santella RM, Sram RJ. Oxidative and nitrosative stress markers in bus drivers. Mutat Res 2007;617:23–32.
[260] Chuang CY, Lee CC, Chang YK, Sung FC. Oxidative DNA damage estimated by urinary 8-hydroxydeoxyguanosine: influence of taxi driving, smoking and areca chewing. Chemosphere 2003;52:1163–1171.
[261] Loft S, Poulsen HE, Vistisen K, Knudsen LE. Increased urinary excretion of 8-oxo-2'-deoxyguanosine, a biomarker of oxidative DNA damage, in urban bus drivers. Mutat Res 1999;441:11–19.

[262] Rossner P Jr, Svecova V, Milcova A, Lnenickova Z, Solansky I, Sram RJ. Seasonal variability of oxidative stress markers in city bus drivers. Part I. Oxidative damage to DNA. Mutat Res 2008;642:14–20.

[263] Chen C, Arjomandi M, Balmes J, Tager I, Holland N. Effects of chronic and acute ozone exposure on lipid peroxidation and antioxidant capacity in healthy young adults. Environ Health Perspect 2007;115:1732–1737.

[264] Sanchez-Rodriguez MA, Retana-Ugalde R, Ruiz-Ramos M, Munoz-Sanchez JL, Vargas-Guadarrama LA, Mendoza-Nunez VM. Efficient antioxidant capacity against lipid peroxide levels in healthy elderly of Mexico City. Environ Res 2005;97:322–329.

[265] Rossner P Jr, Svecova V, Milcova A, Lnenickova Z, Solansky I, Sram RJ. Seasonal variability of oxidative stress markers in city bus drivers. Part II. Oxidative damage to lipids and proteins. Mutat Res 2008;642:21–27.

[266] Sørensen M, Daneshvar B, Hansen M, Dragsted LO, Hertel O, Knudsen L, Loft S. Personal $PM_{2.5}$ exposure and markers of oxidative stress in blood. Environ Health Perspect 2003;111:161–166.

[267] Liu L, Ruddy TD, Dalipaj M, Szyszkowicz M, You H, Poon R, Wheeler A, Dales R. Influence of personal exposure to particulate air pollution on cardiovascular physiology and biomarkers of inflammation and oxidative stress in subjects with diabetes. J Occup Environ Med 2007;49: 258–265.

[268] Autrup H, Daneshvar B, Dragsted LO, Gamborg M, Hansen ÅM, Loft S, Okkels H, Nielsen F, Nielsen PS, Raffn E, Wallin H, Knudsen LE. Biomarkers for exposure to ambient air pollution—comparison of carcinogen-DNA adduct levels with other exposure markers and markers for oxidative stress. Environ Health Perspect 1999;107: 233–238.

[269] Svecova V, Rossner P Jr, Dostal M, Topinka J, Solansky I, Sram RJ. Urinary 8-oxodeoxyguanosine levels in children exposed to air pollutants. Mutat Res 2009;662:37–43.

[270] Romieu I, Barraza-Villarreal A, Escamilla-Nunez C, Almstrand AC, az-Sanchez D, Sly PD, Olin AC. Exhaled breath malondialdehyde as a marker of effect of exposure to air pollution in children with asthma. J Allergy Clin Immunol 2008;121:903–909.

[271] Barregard L, Sallsten G, Andersson L, Almstrand AC, Gustafson P, Andersson M, Olin AC. Experimental exposure to wood smoke: effects on airway inflammation and oxidative stress. Occup Environ Med 2008;65:319–324.

[272] Mills NL, Robinson SD, Fokkens PH, Leseman DL, Miller MR, Anderson D, Freney EJ, Heal MR, Donovan RJ, Blomberg A, Sandstrom T, MacNee W, Boon NA, Donaldson K, Newby DE, Cassee FR. Exposure to concentrated ambient particles does not affect vascular function in patients with coronary heart disease. Environ Health Perspect 2008;116:709–715.

[273] Sørensen M, Autrup H, Hertel O, Wallin H, Knudsen LE, Loft S. Personal exposure to $PM_{2.5}$ and biomarkers of DNA damage. Cancer Epidemiol Biomarkers Prev 2003; 12:191–196.

[274] Vinzents P, Møller P, Sørensen M, Knudsen LE, Hertel O, Palmgren F, Schibye B, Loft S. Personal exposure to ultrafine particles and oxidative DNA damage. Environ Health Perspect 2005;113:1485–1490.

[275] Bräuner EV, Forchhammer L, Møller P, Simonsen J, Glasius M, Wåhlin P, Raaschou-Nielsen O, Loft S. Exposure to ultrafine particles from ambient air and oxidative stress-induced DNA damage. Environ Health Perspect 2007;115: 1177–1182.

[276] Isik B, Isik RS, Akyildiz L, Topcu F. Does biomass exposure affect serum MDA levels in women? Inhal Toxicol 2005;17:695–697.

[277] Barregard L, Sallsten G, Andersson L, Almstrand AC, Gustafson P, Andersson M, Olin AC. Experimental exposure to wood smoke: effects on airway inflammation and oxidative stress. Occup Environ Med 2008;65:319–324.

[278] Danielsen PH, Bräuner EV, Barregard L, Sallsten G, Wallin M, Olinski R, Rozalski R, Møller P, Loft S. Oxidatively damaged DNA and its repair after experimental exposure to wood smoke in healthy humans. Mutat Res 2008;642: 37–42.

[279] Saber AT, Bornholdt J, Dybdahl M, Sharma AK, Loft S, Vogel U, Wallin H. Tumor necrosis factor is not required for particle-induced genotoxicity and pulmonary inflammation. Arch Toxicol 2005;79:177–182.

[280] Wang JJ, Sanderson BJ, Wang H. Cyto- and genotoxicity of ultrafine TiO_2 particles in cultured human lymphoblastoid cells. Mutat Res 2007;628:99–106.

[281] Gu ZW, Keane MJ, Ong TM, Wallace WE. Diesel exhaust particulate matter dispersed in a phospholipid surfactant induces chromosomal aberrations and micronuclei but not 6-thioguanine-resistant gene mutation in V79 cells. J Toxicol Environ Health A 2005;68:431–444.

[282] Bao L, Chen S, Wu L, Hei TK, Wu Y, Yu Z, Xu A. Mutagenicity of diesel exhaust particles mediated by cell-particle interaction in mammalian cells. Toxicology 2007; 229:91–100.

[283] Zhu L, Chang DW, Dai L, Hong Y. DNA damage induced by multiwalled carbon nanotubes in mouse embryonic stem cells. Nano Lett 2007;7:3592–3597.

[284] Xu DQ, Zhang WL. Monitoring of pollution of air fine particles (PM2.5) and study on their genetic toxicity. Biomed Environ Sci 2004;17:452–458.

[285] Nakagawa Y, Wakuri S, Sakamoto K, Tanaka N. The photogenotoxicity of titanium dioxide particles. Mutat Res 1997;394:125–132.

[286] Kang SJ, Kim BM, Lee YJ, Chung HW. Titanium dioxide nanoparticles trigger p53-mediated damage response in peripheral blood lymphocytes. Environ Mol Mutagen 2008;49:399–405.

[287] Mroz RM, Schins RP, Li H, Jimenez LA, Drost EM, Holownia A, MacNee W, Donaldson K. Nanoparticle-driven DNA damage mimics irradiation-related carcinogenesis pathways. Eur Respir J 2008;31:241–251.

[288] Don Porto Carero A, Hoet PHM, Verschaeve L, Schoeters G, Nemery B. Genotoxic effects of carbon black particles, diesel exhaust particles, and urban air particulates and their extracts on a human alveolar epithelial cell line (A549) and a human monocytic cell line (THP-1). Environ Health Perspect 2001;37:155–163.

[289] Karlsson HL, Nygren J, Moller L. Genotoxicity of airborne particulate matter: the role of cell-particle interaction and of substances with adduct-forming and oxidizing capacity. Mutat Res 2004;565:1–10.

[290] Karlsson HL, Ljungman AG, Lindbom J, Moller L. Comparison of genotoxic and inflammatory effects of particles generated by wood combustion, a road simulator and collected from street and subway. Toxicol Lett 2006; 165:203–211.

[291] Sharma AK, Jensen KA, Rank J, White PA, Lundstedt S, Gagne R, Jacobsen NR, Kristiansen J, Vogel U, Wallin H. Genotoxicity, inflammation and physico-chemical properties of fine particle samples from an incineration energy plant and urban air. Mutat Res 2007;633:95–111.

[292] Kisin ER, Murray AR, Keane MJ, Shi XC, Schwegler-Berry D, Gorelik O, Arepalli S, Castranova V, Wallace WE, Kagan VE, Shvedova AA. Single-walled carbon nanotubes: geno- and cytotoxic effects in lung fibroblast V79 cells. J Toxicol Environ Health A 2007;70:2071–2079.

[293] Lindberg HK, Falck GC, Suhonen S, Vippola M, Vanhala E, Catalan J, Savolainen K, Norppa H. Genotoxicity of

nanomaterials: DNA damage and micronuclei induced by carbon nanotubes and graphite nanofibres in human bronchial epithelial cells *in vitro*. Toxicol Lett 2009;186:166–173.

[294] Dhawan A, Taurozzi JS, Pandey AK, Shan W, Miller SM, Hashsham SA, Tarabara VV. Stable colloidal dispersions of C60 fullerenes in water: evidence for genotoxicity. Environ Sci Technol 2006;40:7394–7401.

[295] Møller P. Assessment of reference values for DNA damage detected by the comet assay in humans blood cell DNA. Mutat Res 2006;612:84–104.

This paper was first published online on Early Online on 22 October 2009.